AD_____

AWARD NUMBER: W81XWH-13-1-0395

TITLE: Prevention of the Post-traumatic Fibrotic Response in Joints

PRINCIPAL INVESTIGATOR: Pedro Beredjiklian, M.D.

RECIPIENT: Reconstructive Orthopaedic Associates II, PC
Philadelphia, PA 19107

REPORT DATE: December 2016

TYPE OF REPORT: Final

PREPARED FOR: U.S. Army Medical Research and Materiel Command
Fort Detrick, Maryland 21702-5012

REPORT DOCUMENTATION PAGE

Form Approved
OMB No. 0704-0188

1. REPORT DATE	2. REPORT TYPE	3. DATES COVERED
December 2016	Final	30 Sep 2013 - 29 Sep 2016

4. TITLE AND SUBTITLE

Prevention of the Posttraumatic Fibrotic Response in Joints

5a. CONTRACT NUMBER

5b. GRANT NUMBER
W81XWH-13-1-0395

5c. PROGRAM ELEMENT NUMBER

6. AUTHOR(S)

Dr. Pedro Beredjiklian

E-Mail: Pedro.Beredjiklian@rothmaninstitute.com

5d. PROJECT NUMBER

5e. TASK NUMBER

5f. WORK UNIT NUMBER

7. PERFORMING ORGANIZATION NAME(S) AND ADDRESS(ES)
Reconstructive Orthopaedic Associates II, PC
925 Chestnut Street, 5th Floor
Philadelphia, PA 19107-4206

8. PERFORMING ORGANIZATION REPORT NUMBER

9. SPONSORING / MONITORING AGENCY NAME(S) AND ADDRESS(ES)

U.S. Army Medical Research and Materiel Command
Fort Detrick, Maryland 21702-5012

10. SPONSOR/MONITOR'S ACRONYM(S)

11. SPONSOR/MONITOR'S REPORT NUMBER(S)

12. DISTRIBUTION / AVAILABILITY STATEMENT

Approved for Public Release; Distribution Unlimited

13. SUPPLEMENTARY NOTES

14. ABSTRACT

The ongoing study addresses the critical clinical problem of posttraumatic joint stiffness, a pathology that reduces the range of motion (ROM) of injured joints and contributes to the development of osteoarthritis. The fundamental hypothesis that drives the current study is that pathological fibrotic response of injured joint tissues may be limited by targeting the formation of collagen fibrils, a main component of the fibrotic mass. Key preliminary data indicate the following: (i) in comparison to the non-treated control, deposition of newly-formed collagen fibrils in posterior capsules from injured knees of rabbits treated with the anti-fibrotic antibody is reduced significantly, (ii) in comparison to the non-treated control, the correct collagen III/collagen I ratio in posterior capsules from injured knees of rabbits treated with anti-fibrotic antibody is maintained, (iii) in comparison to the non-treated control, the ROM of injured knees of rabbits treated with anti-fibrotic antibody is greater. Ongoing studies with additional groups of animals will determine the statistical significance of the differences observed in the measured parameters. Completion of these experiments will define the utility of the anti-collagen I antibody to block excessive fibrosis associated with joint injury.

15. SUBJECT TERMS

Post-traumatic joint stiffness, anti-fibrotic therapy, collagen, therapeutic antibody, fibrosis, knee joint, animal model, range of motion.

16. SECURITY CLASSIFICATION OF:			17. LIMITATION OF ABSTRACT	18. NUMBER OF PAGES	19a. NAME OF RESPONSIBLE PERSON
a. REPORT	b. ABSTRACT	c. THIS PAGE			USAMRMC
Unclassified	Unclassified	Unclassified	Unclassified	27	19b. TELEPHONE NUMBER *(include area code)*

Standard Form 298 (Rev. 8-98)
Prescribed by ANSI Std. Z39.18

ABSTRACT

The referenced project was funded through the Translational Research Partnership Award mechanism. This mechanism required research teams to conduct translational studies that would accelerate the movement of promising ideas in orthopaedic research into clinical applications to benefit soldiers with combat-relevant traumatic orthopaedic injuries. Moreover, this award mechanism required the formation of the multi-institutional and multi-disciplinary research partnership among orthopaedic surgeons and basic researchers. Our group has fulfilled both of these requirements.

Our group has been extremely successful in establishing a well-integrated partnership among orthopaedic surgeons and basic researchers focusing on research associated with post-traumatic joint stiffness. This team has grown from a group of three initial Principal Investigators into the Scientific Consortium for Arthrofibrotic Research (SCAR). At present, the scientists that form the SCAR focus on the scarring of elements of the musculoskeletal system, including tendons, joint capsules, peripheral nerves, and others.

Our key accomplishment of this project is proving the efficacy of our technology to reduce post-traumatic joint stiffness *in vivo.* The results of our study were then published in peer-reviewed journals and at major orthopaedic conferences.

In brief, posttraumatic joint contracture is a frequent orthopaedic complication that limits the movement of injured joints, thereby severely impairing affected patients. Non-surgical and surgical treatments often fail to improve the range of motion of stiff joints. The purpose of this study was to test a hypothesis that limiting the formation of collagen-rich tissue in the capsules of injured joints would reduce the consequences of the fibrotic response and improve joint mobility. To test this hypothesis, we targeted the formation of collagen fibrils, the main component of fibrotic deposits formed within the tissues of injured joints. We have employed a relevant rabbit model to test the utility of a custom-engineered antibody, delivered directly to the cavities of injured knees, to block the formation of collagen fibrils produced in response to injury. In comparison to the non-treated control, mechanical tests of the antibody-treated knees demonstrated a significant reduction of flexion contracture. Detailed microscopic and biochemical studies have verified that this reduction was a result of the antibody-mediated blocking of the assembly of collagen fibrils. The results of our study indicate that extracellular processes associated with excessive formation of fibrotic tissue represent a valid target for limiting model posttraumatic joint stiffness.

Table of Contents

INTRODUCTION

The original proposal was submitted in response to the announcement entitled “Peer Reviewed Orthopaedic Research Program: Translational Research Partnership Award” (W81XWH-12-PRORP-TRPA). By targeting the fibrotic process associated with joint stiffness, the main focus area of this project was: “Prevention or treatment of posttraumatic joint stiffness and contracture in the ankle, knee, and/or elbow, including physical therapy approaches".

By forming a partnership between basic researchers and orthopaedic surgeons, we proposed to implement the bench-to-bed translation of a novel approach to reduce or eliminate posttraumatic joint stiffness and contractures. Although the pathology of stiff joints and contractures is complex and may involve such processes as ectopic bone formation and activation of fibroblasts, its common feature is the formation of fibrotic tissue consisting primarily of collagen fibrils. In the referenced study, we employed an antibody with the potential to inhibit or reduce posttraumatic joint stiffness and contracture [1-6].

The central hypothesis was that by inhibiting the process of collagen fibril formation, it is possible to block or reduce excessive formation of collagen-rich fibrotic deposits in joint tissues, thereby limiting the chance of developing posttraumatic joint stiffness. We also postulated that blocking posttraumatic fibrosis in joints can be achieved by applying monoclonal chimeric antibody (chIgG) developed to target collagen fibril formation [1-6]. The chief objective of this study was to move the proposed concept from bench to bed through testing the above hypotheses in a relevant animal model. The formation of the Translational Research Partnership ensured reaching the stated objective.

Two Specific Aims were defined to test the fundamental hypothesis that antibody-mediated reduction of fibrosis will prevent or minimize posttraumatic joint stiffness:

(1) "To block the fibrotic process after joint injury in a rabbit-based model"

(2) "To analyze long-term effects of the antibody-based inhibitor of fibrosis at the biochemical, cellular, and biomechanical levels".

The proposed study was carried out in a relevant rabbit-based animal model. In brief, rabbit joints underwent a surgical procedure of which the consequences mimic the stiffness of a posttraumatic joint. The treated group of animals received the therapeutic antibody to minimize the formation of excessive fibrotic deposits. Evaluation of the efficacy of the proposed approach was achieved by biochemical assays of collagen content and composition, then by the amount of cross-links in collagen deposits, by histological assays of involved tissues, and by biomechanical evaluation of the flexion contracture. Appropriate controls were also included [5,6].

Note, that this is a comprehensive report that combines research activities of all PIs, *i.e.* Drs. Fertala, Abboud, and Beredjiklian. Specific tasks assigned to each PI in the original SOW are clearly marked.

Keywords: arthrofibrosis; posttraumatic joint stiffness; joint injury; joint contracture; fibrosis; scarring; collagen; therapeutic antibody; biologics; range of motion

OVERALL PROJECT SUMMARY

For Specific Aim 1: To block the fibrotic process after joint injury in a rabbit-based model.

Major Task 1. Production and purification of therapeutic antibodies.

Site and Involved PIs: Dr. Fertala (TJU).

In this task performed on a continuous basis for both specific aims, we will employ CHO cells that produce the monoclonal antibody (chIgG), which will be applied to reduce the fibrotic response of the injured knees of experimental rabbits. As a result, the critical chIgG variant will be available throughout the entire study."

Subtask 1. High-density cell culture to produce preparative-scale amounts of therapeutic chIgG.

In this subtask, cell cultures will be carried out in a laboratory-scale bioreactor.

Site and Involved PIs: Dr. Fertala (TJU).

Subtask 2. Purification of the chIgG.

chIgG secreted by CHO cells will be purified by salt precipitation and chromatography. If necessary, variable fragments of the chIgG, F(ab')2, will be prepared by pepsin digestion.

Site and Involved PIs: Dr. Fertala (TJU).

Subtask 3. Quality control of purify chIgG.

The structural integrity and purity of purified chIgG will be monitored by polyacrylamide gel electrophoresis done in reducing and non-reducing conditions. The specific activity of the chIgG will be monitored by its ability to interact with the targeted epitope.

Site and Involved PIs: Dr. Fertala (TJU).

Rationale

The main goal of Task 1 was to establish a robust and cost-effective method for production of the anti-collagen therapeutic monoclonal antibody (chIgG) tested in this study as an inhibitor of fibrosis associated with posttraumatic joint stiffness [3]. In this task we employed the BioFlo/CelliGen 115 bioreactor to culture CHO cells we engineered to produce the chIgG. Initially, we tested two cell culture media types to determine optimal conditions for production of the chIgG. Based on outcomes we selected CD-CHO cell culture media as optimal for our needs.

In this task we also developed methods for purification and quality control of the chIgG.

Please note that for consistency with our publications from now on we will refer to the chIgG as the anti-collagen antibody (ACA).

Methods

Bioreactor runs and assays of glucose and lactate. Two experimental runs of the CelliGen BLU 5 L Packed-Bed bioreactor (working volume of 3L; Eppendorf) were performed employing the New Brunswick BioFlo/CelliGen 115 Benchtop Fermenter & Bioreactor (Eppendorf). CHO cells producing the ACA pre-

conditioned to serum-free CD-CHO (Gibco) or Ham's F-12 (Corning) were grown initially in suspension to obtain 2 x 10^9 cells, which is the initial inoculum needed to seed the bioreactor. These cells were seeded into the bioreactor via a sample port.

Prior to seeding, both the pH and dissolved oxygen (DO) probe were calibrated according to the manufacturer's instructions. Each bioreactor run was performed under identical physiochemical conditions for up to three months of continuous culture. These conditions included a pH set point of 7.1 that was controlled by the addition of CO_2 or 10% NaOH; a dissolved oxygen set point of 40% that was controlled by the addition of O_2; and a constant temperature of 37°C that was controlled by an external heating blanket.

A picture of the bioreactor vessel and control cabinet is seen in Fig. 1 and a schematic representation of the vessel is depicted in Fig. 2. Bioreactor runs were performed using a modified control-fed perfusion format in which media was completely removed from the vessel every two days, and 3 L of fresh media was added via inlet and outlet ports on the bioreactor. Based on tests we found that CHO cells needed a dissolved oxygen content of 40% in order to ensure maximum cell viability and protein production.

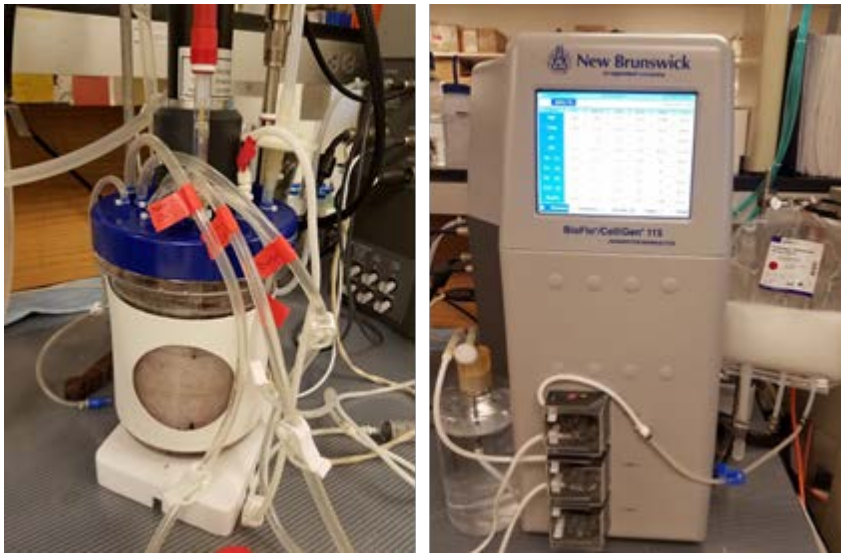

Figure 1. 5 L CelliGen BLU bioreactor and control cabinet. The vessel contains media inlet and outlet ports, a gas inlet, and a sample port. There is also a pH probe, DO probe, and a heating blanket. The control cabinet monitors and modulates all important parameters.

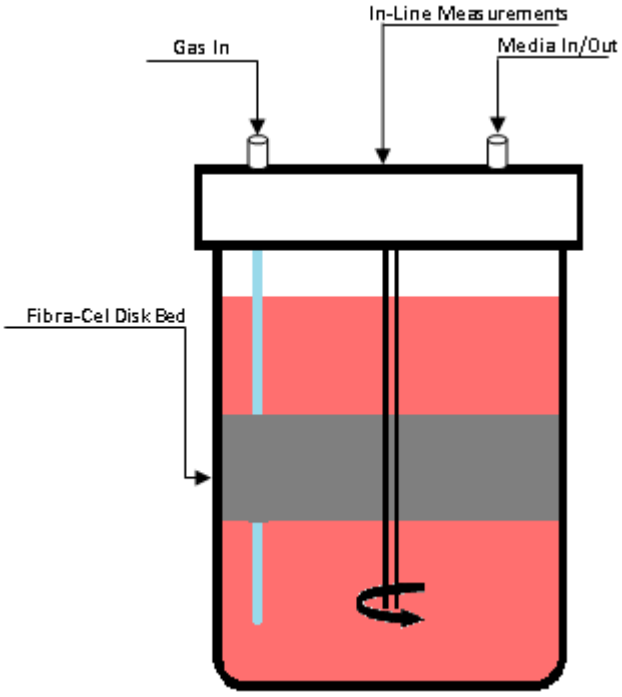

Figure 2. Schematic representation of PBR. The working volume of the vessel is 3.75 L and the packed-bed contains 150 g Fibra-Cel disks. The vessel contains an impellor to circulate media throughout the vessel. Ports located at the top of the vessel provide for feed and harvest, as well as all in-line measurements such as dissolved oxygen, pH, and temperature.

Glucose and lactate concentrations in cell culture media were monitored daily with the use of an Eton Biosciences glucose and lactate assay kit (Eton Biosciences). Following glucose concentration assays, a 45% glucose stock solution (Corning) was added up to the final concentration set for each media type on days when fresh media was not added to the vessel. Media was collected in 3-L batches into a sterile 10-L carboy stored in a refrigerator. Although the direct microscopic assessment of cell density and viability was not possible, the glucose consumption rate (GCR) and oxygen consumption rate (OCR) were sufficient indicators of the biological activity of the culture.

Purity, integrity, and yields of the ACA. After three media-change cycles (*i.e.* 9 total liters collected), media was processed by filtration through a 0.2 µm filter to remove cell debris. Sodium azide (Acros Organics) was added to 0.02% to prevent bacterial growth and then the media was run over a Protein-L affinity column (Fig. 3). Protein-L agarose (Genscript Inc.) is an affinity resin that binds specifically to the light kappa chain of human IgG.

The column-bound ACA was eluted with 0.1 M Glycine (pH=3.0). Gel electrophoresis (SDS-PAGE) was performed on samples reduced using 2-mercaptoethanol and the gels were stained with Coomassie blue (Bio-Rad) to assess the purity and structural integrity of eluted ACA. Protein yields were determined by a Bradford protein concentration assay (Bio-Rad). Finally, samples were concentrated using ultrafiltration on a 30 kDa-cut off filter (Millipore).

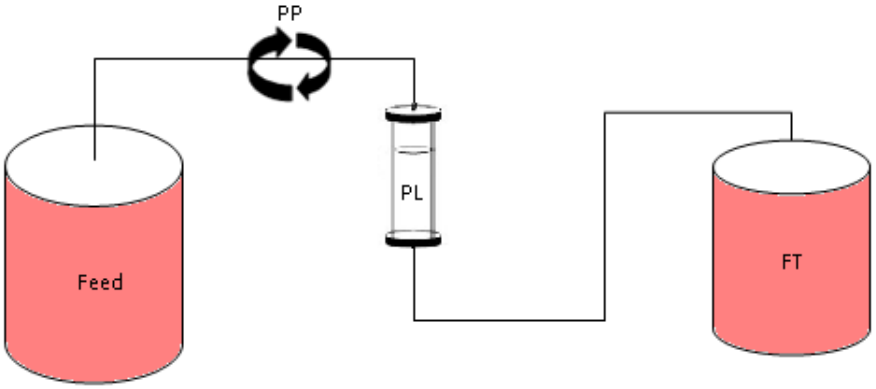

Figure 3. Schematic representation of protein-L agarose column. Collected media was processed before being pumped over a resin bed containing 5 mL of Protein-L agarose (PL) using a peristaltic pump (PP). Flow through media (FT) was also collected and analyzed to ensure all protein bound to the resin.

Size Exclusion Chromatography. The purified ACA from each run were tested using size exclusion chromatography HPLC (SEC-HPLC) in order to ensure that the protein does not form aggregates during either the bioreactor run or after collection. A 15-µL purified sample of the ACA from each bioreactor run at 2 mg/mL was run over a BioBasic SEC-300 size exclusion column (Thermo Scientific) using a Varian Prostar Model 210 HPLC system and the elution profiles were compared to a known molecular mass γ-globulin standard (Bio-Rad).

ACA-antigen binding assays. The binding kinetics of the combined pool of the ACA batches collected from each bioreactor run were evaluated by analyzing the binding affinity of the purified antibody to procollagen I standard that contains the ACA-specific epitope. Binding assays were done using the Pioneer Biosensor (Sensiq Technologies).

Briefly, human procollagen I was bound to a COOH5 biosensor chip (Sensiq Technologies), and the ACA solubilized in HEPES buffer (pH=7.4) supplemented with 0.005% Tween-20 was run over the chip. In subsequent cycles that included association and dissociation events, the ACA was added at concentrations of 200 nM, 100 nM, 50 nM, 25 nM, 12.5 nM, 6.25 nM, and 3.125 nM. Binding kinetics were analyzed using the Qdat software (Sensiq Technologies). Consequently, association rate constants (k_{on}), dissociation rate constants (k_{off}), and equilibrium dissociation constants (K_D) were determined from the data collected for each tested chIgG batch.

Polyethylene glycol (PEG)-modified ACA. The PEGylated variant (P-ACA) was generated by binding a 12-mer polyethylene glycol chains (PEG; ThermoFisher Sci.) via random lysine residues present in the ACA. Since binding the PEG molecules increases the mass of the ACA chains, we monitored the outcomes of the PEGylation by gel electrophoresis.

Long-term stability of antibodies. Prior to employing the antibodies for their pump-controlled delivery into the injured knees (see below for description of a rabbit-based model), we analyzed whether their stability, solubility, and the binding characteristics remained unchanged despite the antibody-filled pumps being kept constantly under the skin of the rabbits.

In brief, the 2-mg/ml antibody samples were stored for 4 weeks in a cell culture incubator set to 37°C. During this time antibody aliquots were collected weekly. The structural integrity of the γ and κ chains of collected antibodies was analyzed by gel electrophoresis. Moreover, the binding specificity of these antibodies was analyzed by Western blot with human collagen I as a target, as described [2,3]. Also, the affinity of the antibody-collagen I binding was measured with the use of a biosensor [2,3].

Employing SEC-HPLC, we also analyzed whether antibodies would aggregate during the 4-week incubation at 37°C. For these assays we employed the BioBasic SEC-300 column (ThermoFisher Sci.), as we described elsewhere [2,3]. In addition to testing the antibodies stored in an incubator, similar tests were run on a portion of antibodies that remained in pumps retrieved from beneath the skin of rabbits at the end of the 8-week treatment period (see below for description of a rabbit-based model).

Results

Bioreactor runs and assays of glucose and lactate. The bioreactor run using Ham's F-12 media was maintained for a total of 25 days. The average glucose consumption rate was found to be 3.22 g/L/day. This represented 71.6% of initial glucose present (4.5 g/L) in Ham's F-12 media. The average lactate production rate was 2.81 g/L/day. The average daily glucose consumed and lactate produced per week is shown in Fig. 4.

The bioreactor run using CD-CHO media was carried out for a total of 83 days. The average glucose consumption rate was found to be 4.28 g/L/day (65.8% of initial glucose present (6.5 g/L) in CD-CHO media) and the average lactate production rate was 3.80 g/L/day. The average daily glucose consumed and lactate produced per week is shown in Fig. 4. During each culture, oxygen consumption was closely monitored.

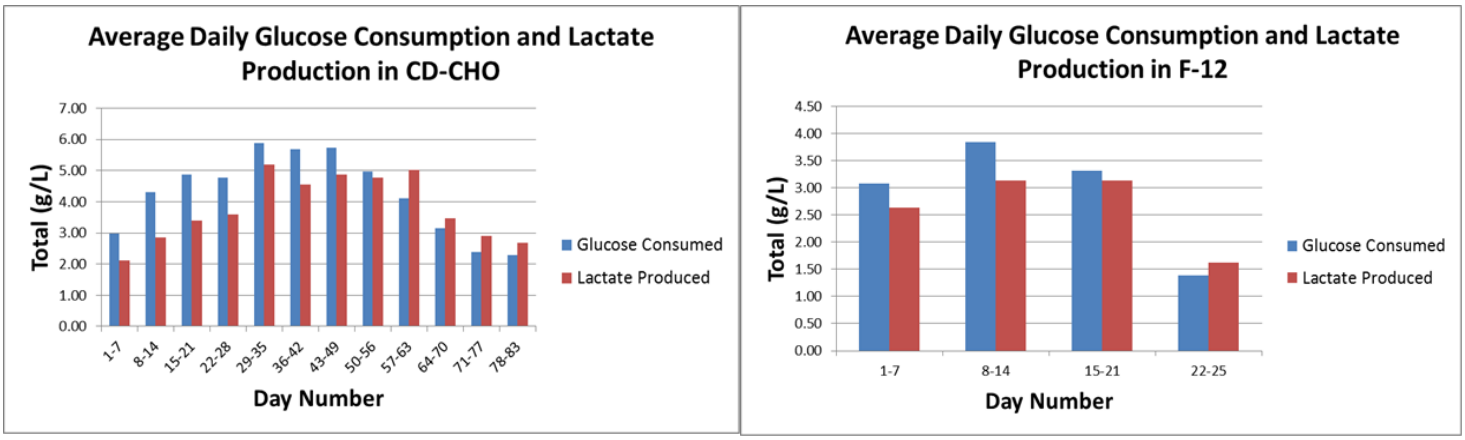

Figure 4. Average daily lactate produced and glucose consumed by CHO cells in CD-CHO and F-12 media in a 5 L BLU bioreactor.

Purity, structural integrity, and yields of ACA. After purification of the ACA, Coomassie-stained gels were analyzed to determine the purity of eluted antibody. Electrophoretic separation of reduced ACA

chains demonstrated the presence of expected γ and κ chains; no contaminating proteins were apparent, thereby indicating high purity of the ACA preparations (Fig. 5). Moreover, the absence of degraded γ and κ chains indicates proper structural integrity of the ACA preparations.

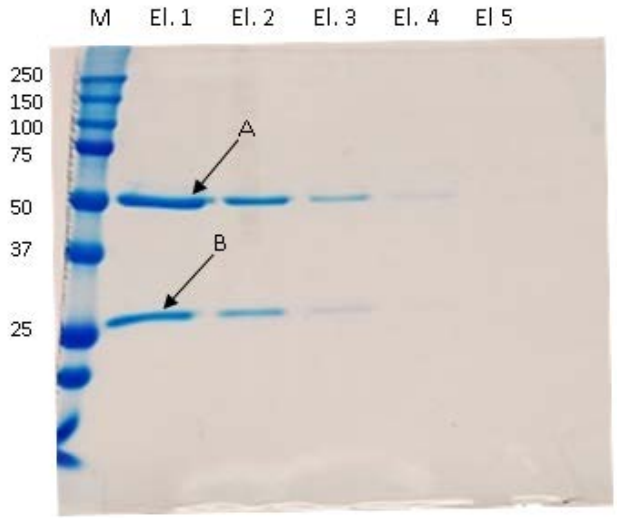

Figure 5. Coomassie stained SDS-PAGE gel depicting 5 elutions (El) from protein L-agarose. The gamma heavy chain (A) and kappa light chain (B) of the chimeric antibody are indicated. Lane 1: Molecular mass marker (kDa). Lanes El.1 to El.5 represent the ACA eluted from protein L-agarose in five elution steps.

The peak of the weekly-protein-yield in F-12 media was 21.73 mg in week 2 of the bioreactor run and the total protein yield was 69.43 mg. The peak of the weekly-protein-yield in CD-CHO media was 37.15 mg during week 7 of the bioreactor run and the total protein yield was 184.04 mg (Fig. 6).

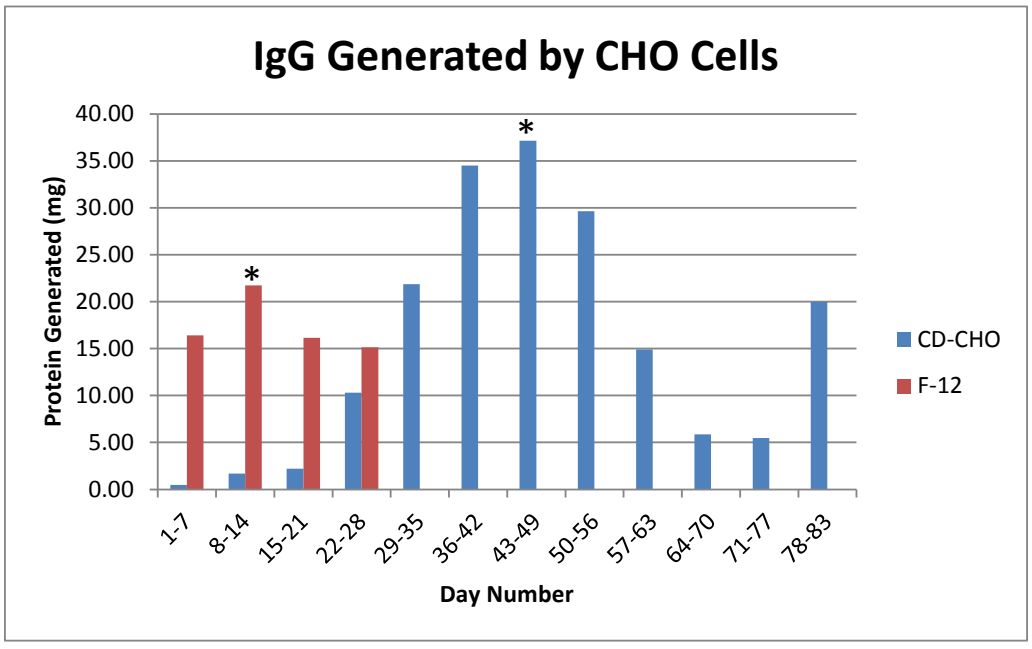

Figure 6. Weekly yields of the ACA generated by CHO cells cultured in CD-CHO and F-12 media. Peak weekly yields (*) of 37.15 mg and 21.73 mg, respectively.

Size exclusion chromatography. Each ACA sample eluted as one peak of expected mass with no apparent aggregate formation. Retention profiles for the peaks were similar to that of a known 158-kDa bovine γ-globulin standard (Bio-Rad) (Fig. 7).

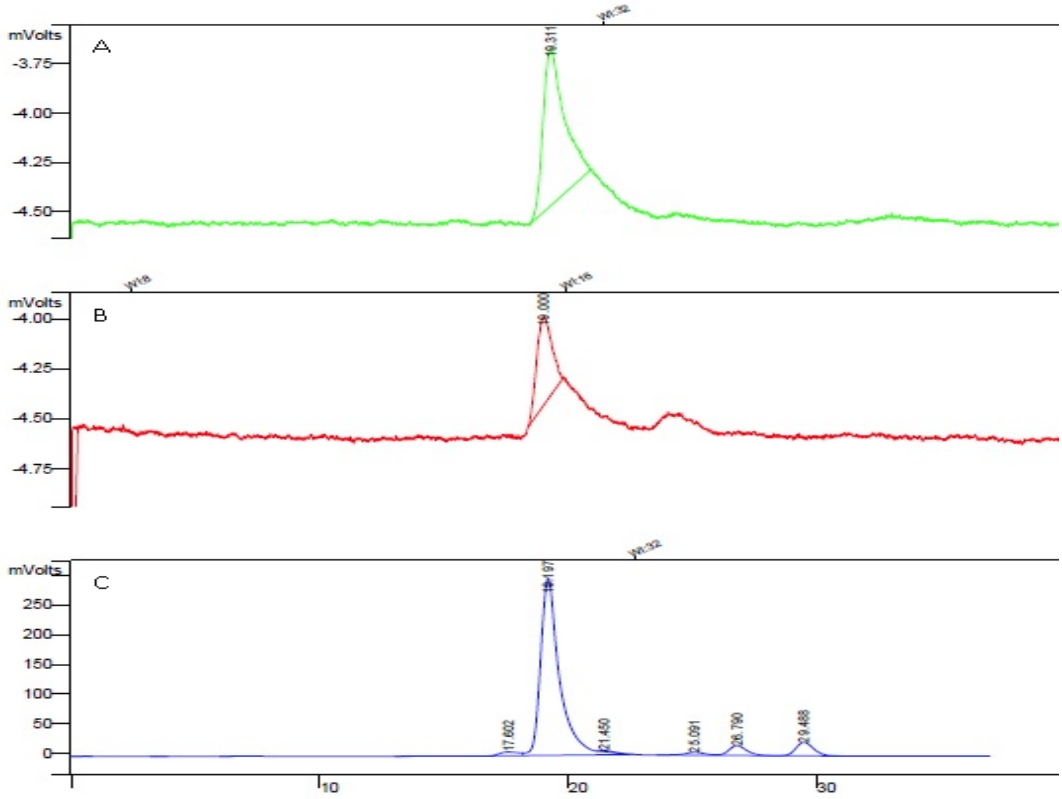

Figure 7. Size exclusion chromatography peaks of the ACA produced in (A) F-12 and (B) CD-CHO compared to (C) a known 158 kDa γ-globulin standard.

ACA-antigen binding assays. ACA samples purified from each media type were run over a COOH5 chip with immobilized procollagen I target. Table 1 and Fig. 8 summarize key results.

Table 1: Kinetics of binding of chIgG produced in CD-CHO and F-12 media

Media Type	k_{on} **($M^{-1}s^{-1}$)**	k_{off} **(s^{-1})**	K_D **(nM)**
CD-CHO	2.081×10^{4}	2.82×10^{-4}	13.53
F-12	1.894×10^{4}	4.67×10^{-4}	24.65

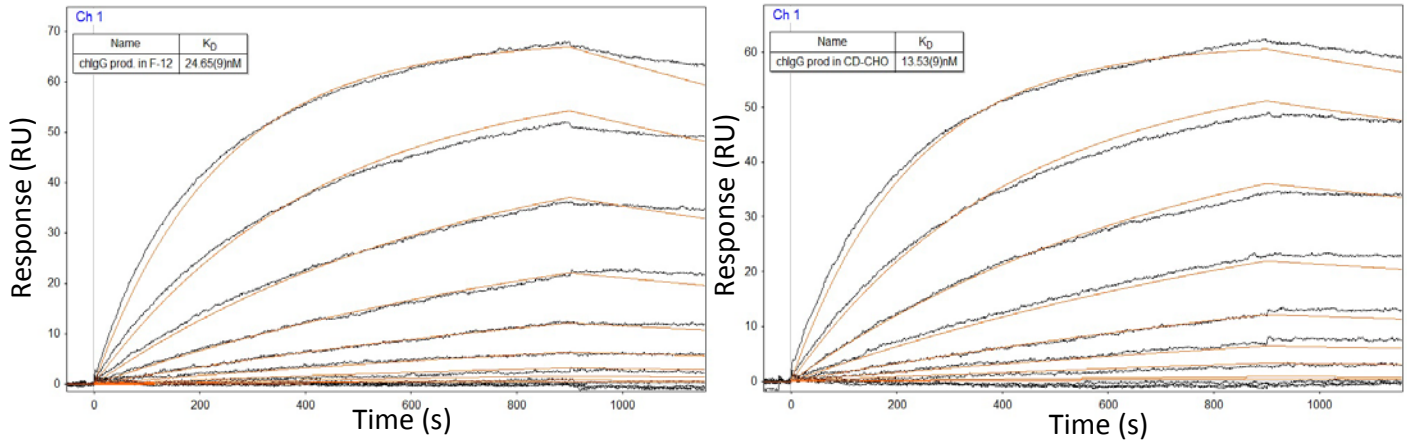

Figure 8. Association/dissociation curves for the ACA produced in F-12 (left panel) and CD-CHO media (right panel). Each curve shows data points and their fit to curves representing a theoretical simple bimolecular binding model.

Assays of P-ACA. The P-ACA variant we generated for this study represents a PEGylated version of the ACA. Since PEGylation increases the mass of a protein, the efficiency of the PEGylation process can be readily analyzed by electrophoresis. As indicated by the absence of unmodified chains of the original ACA, the PEGylation process was quite effective (Fig. 9 A). The P-ACA protein bands with slow electrophoretic mobility represent, most likely, partially reduced P-ACA molecules (Fig. 9 A).

Employing Western blot (Fig. 9 C) and biosensor-based (not shown) assays we investigated key binding characteristics of the P-ACA. As indicated in Fig. 9 C, the Western blot-based positive signal for the P-ACA-α2(I) binding indicates proper binding interactions.

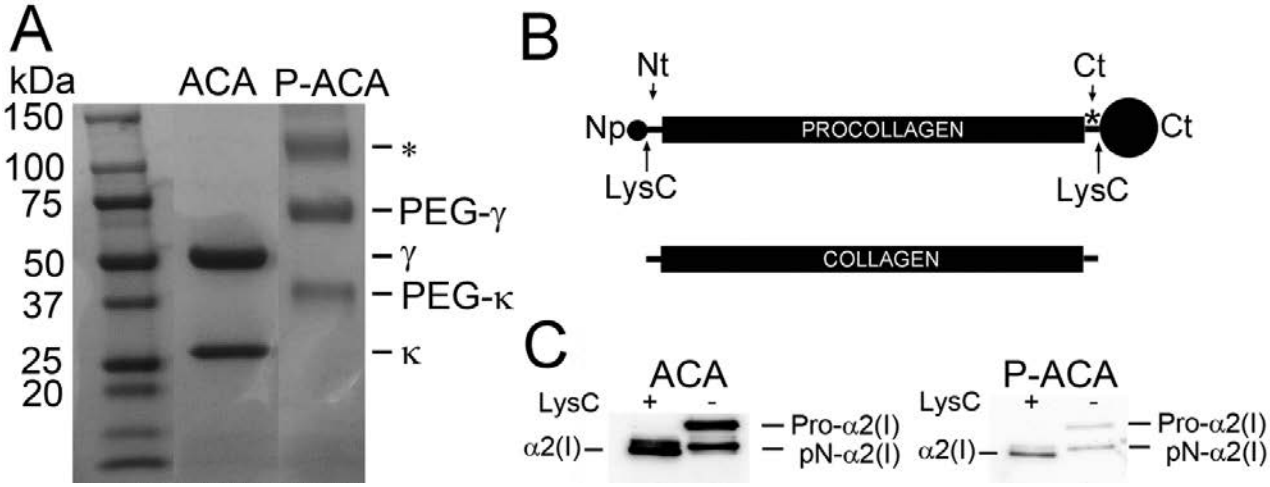

Figure 9. Assays of the ACA and P-ACA. A, An electrophoretic separation of the γ and κ chains of the ACA and P-ACA. An asterisk indicates partially-reduced chains of the P-ACA. B, A schematic of key procollagen I domains: Np, Cp; procollagen N-terminal and C-terminal globular propeptides. Nt, Ct; procollagen N-terminal and C-terminal telopeptides. Note that LysC cleavage of procollagen I preserves the telopeptide regions recognized by the ACA and P-ACA. Asterisk indicates the antibody-binding site. A pN collagen variant represents a procollagen form in which the C-terminal propeptides have been processed by enzymatic digestion. This form is frequently present in procollagen preparations. C, Western blot assays of the binding of the ACA and P-ACA variants to procollagen I and collagen I. Both variants recognize procollagen and collagen forms. Symbols: γ, κ, PEG-γ, PEG-κ; heavy and light chains of the ACA and P-ACA, respectively, LysC;

endopeptidase LysC, Pro-α2(I), pN-α2(I), and α2(I); pro-α2 chain of intact procollagen I, partially processed pro-α2 chain of procollagen I in which the C-terminal propeptides have been removed, α2 chain of collagen I, respectively.

Long-term stability of antibodies. Assays of antibodies stored at 37° C in an incubator and those recovered from pumps implanted for 8 weeks in the rabbits indicated that long-term incubation changed neither's structural integrity (Fig. 10). Analysis of the size exclusion chromatography (SEC) elution profiles of the antibody variants did not show formation of antibody aggregates (not shown). Moreover, long-term storage of the antibodies did not change their epitope-specific association/dissociation profiles (Fig. 11).

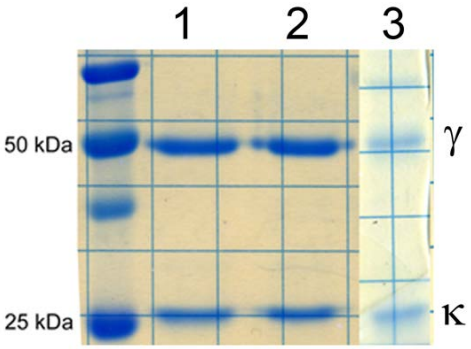

Figure 10. Electrophoresis of the γ and κ chains of the ACA: (1), control ACA stored at 4°C; (2) ACA incubated 4 weeks at 37°C-incubator; (3) ACA retrieved from a pump implanted in a rabbit for 8 weeks. As indicated by intact γ and κ chains, all samples retain their structural integrity.

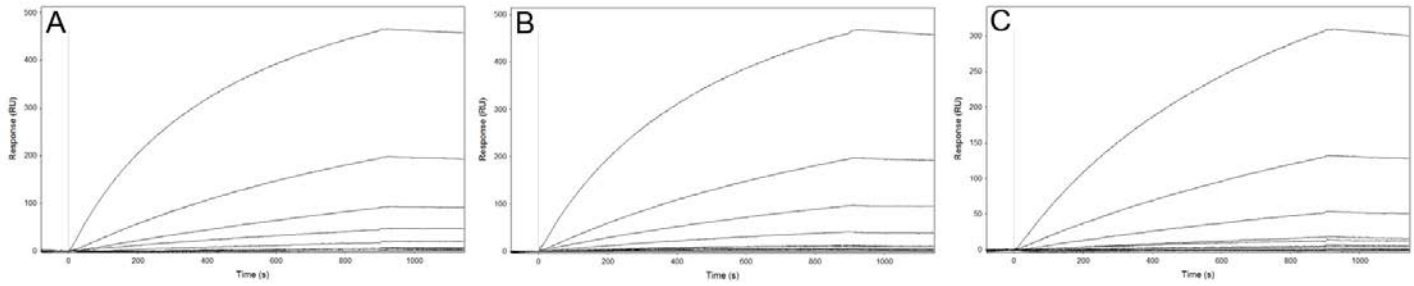

Figure 11. Association and dissociation profiles of the ACA after its long-term storage. A, Control ACA stored at 4°C. B, ACA stored for 4 weeks at 37°C. C, ACA stored for 8 weeks in the reservoir of a pump implanted under the skin of a rabbit. Note that the different curves seen in each panel represent association/dissociation profiles of the ACA added at varying concentrations.

Summary

Selecting optimal conditions for ACA production. In this task, we evaluated CD-CHO and F-12 media to establish the most efficient and cost effective method to produce the ACA. We chose commercially available media types that are formulated for serum-free culture of CHO cells.

The duration of cell cultures maintained in each media type varied greatly. The culture performed in F-12 lasted for only 28 days and the CD-CHO culture lasted 83 days. Because of the disparity in length of the cultures, the overall antibody yield in CD-CHO was significantly higher than in F-12. We hypothesize that cultures in F-12 media are more metabolically active, as shown in the higher lactate production as well as higher ACA production early in the culture, leading to greater nutrient demand. This may have led to diminishing the viability of culture relatively quickly due to exhausting its set biological potential.

Considering the same initial cost of starting bioreactor cultures, regardless of the type of cell culture media, the ability of CD-CHO media to support long-term cultures was an important factor for reducing the overall cost of the ACA production. Consequently, we utilized this cell culture medium to produce the ACA for animal-based studies.

Milestones Achieved

In the Major Task 1 we successfully developed a robust method for production of the ACA.

Major Changes

No major changes were introduced.

Technical Problems

No major technical problems were encountered.

Major Task 2. Testing procedures for generating a rabbit-based model of joint stiffness.

Site and Involved PIs: Dr. Fertala (TJU), Dr. Abboud (RI), Dr. Beredjiklian (RI).

In the initial phase of the proposed study, participating clinical PIs, together with supporting personnel, will prepare a pilot group of animals to test procedures needed to create the required animal model. As a result, not only will surgical methods and procedures be perfected, but a pilot set of data will also be obtained. This data set will be critical for generating the animal groups needed for Specific Aim 2.

Subtask 1. Performing surgeries and immobilization of joints.

The participating surgeons will establish detailed procedures for the critical joint-contracture model.

Site and Involved PIs: Dr. Fertala (TJU), Dr. Abboud (RI), Dr. Beredjiklian (RI).

Subtask 2. Establishing the effective range of chIgG concentrations for limiting the posttraumatic fibrotic response of injured joint.

Groups of rabbits will be treated with various concentrations of the inhibitory chIgG. As a result, effective and safe ranges of concentration of therapeutic chIgG will be established.

Site and Involved PIs: Dr. Fertala (TJU), Dr. Abboud (RI), Dr. Beredjiklian (RI).

Subtask 3. Microscopic, biochemical and biomechanical tests of the pilot group of animals.

A pilot group of rabbits will be sacrificed and knee joints from treated and control groups will be analyzed. Specifically, light and electron microscopy will be employed to analyze changes in the content of bundles of collagen fibrils present in the joints' tendons and capsules. Changes in the total collagen content in the analyzed elements of injured knee joints will be analyzed by measuring hydroxyproline, a residue prevalent in collagenous proteins. The relevant content of collagen cross-links, an important indicator of fibrotic changes, will be determined by gel electrophoresis. A mechanical test of the analyzed joints will finally establish the efficacy of the applied inhibitory chIgG to sustain the mobility of joints after traumatic injury.

Site and Involved PIs: Dr. Fertala (TJU), Dr. Abboud (RI), Dr. Beredjiklian (RI).

Rationale

The major aim of Task 2 was to establish a rabbit-based model of posttraumatic joint stiffness. This model was a major tool for testing the efficacy of the ACA to limit posttraumatic joint stiffness. Moreover, in this task we developed a set of methods needed to determine the outcomes of treatment with the ACA.

Methods

Animals. We employed female New Zealand White rabbits, 8- to 12-months old (Covance, Inc., Princeton, NJ). All animal studies were approved by the TJU IACUC and by the ACURO.

Surgical procedures. Posttraumatic contracture was generated by simulating an intra-articular fracture (using drill holes) and a capsular injury (with a hyperextension injury) in the right knee and maintaining it in a flexed position using Kirschner (K)-wires for 8 weeks [6]. The contralateral uninjured limb served as the uninjured control. During surgery a refillable pump was installed subcutaneously to deliver the ACA, P-ACA, or PBS directly into the articular cavity of the injured knee joints (see below). In brief, an incision in the middle of the right knee was made starting 5 mm proximal to the patella, and extending distally to the tibial tubercle and down the tibia. Subsequently, a lateral parapatellar arthrotomy was made and then the patella was dislocated medially. Following flexing the knee, the fat pad was released and retracted medially (Fig. 12). Next, the anterior (ACL) and posterior (PCL) crucial ligaments were transected and the knee was hyperextended to 45° to disrupt the posterior capsule.

Employing a 2-mm drill, a hole was made in the medial femoral condyle in non-articulating bone. Beginning as far posteriorly in the notch as possible, and exiting out through the lateral condyle, a second 2-mm whole was made. Starting from the notch, a custom-made silicone catheter (0.6 mm ID/1.2 mm OD, Access Technologies, Skokie, IL) with a fixed retention bead at one end was passed through the hole (Fig. 13). While the retention bead secured the catheter inside the operated knee, the opposite end was connected with a pump (see below).

The injured knee was fixed in a flexed position by employing a K-wire. In brief, a drill was driven in the anterior-posterior direction to create a 2-mm bicortical drill hole in the tibia. Subsequently, a 1.6-mm K-wire (Modern Grinding, Port Washington, WI) was passed through the hole in the tibia (Figs. 12 & 14). Flexing the knee, the K-wire was maneuvered to exit through the incision made on the lateral side of the femur. Two 90° bends, approximately 1 cm apart, were made to form a hook at the end of the K-wire. Next, the hook was positioned around the femur (Fig. 14). Finally, the knee was fixed in the flexed position by tightening a nut placed on the opposite, threaded end of the K-wire (Fig. 12).

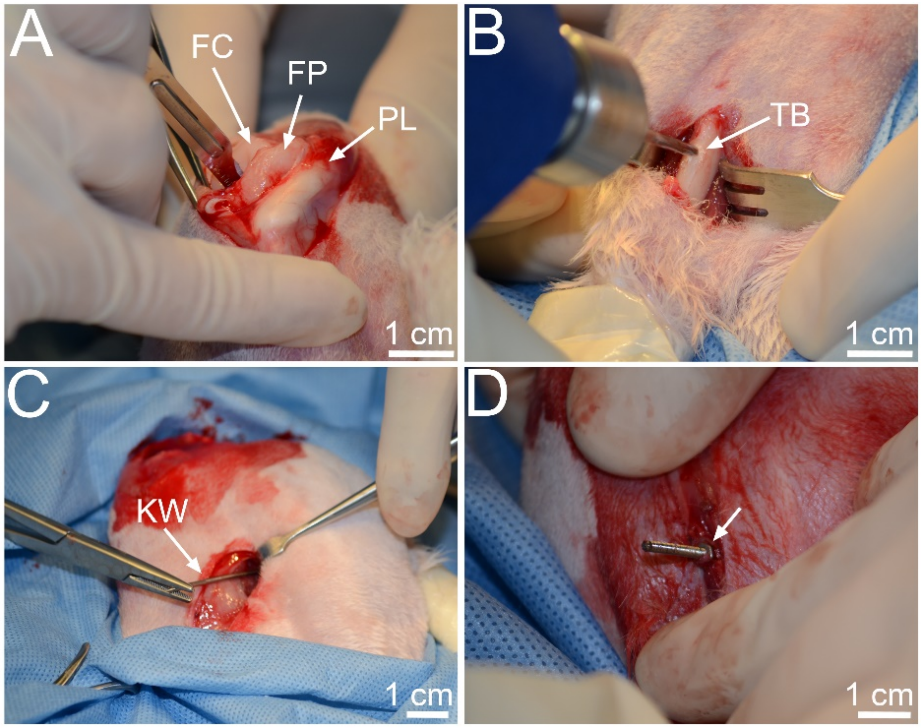

Figure 12. Key steps in surgical procedures to create posttraumatic joint contracture. A, Exposing the articular cavity of the knee joint; transecting the ACL and the PCL. B, Drilling the tibia to install a K-wire. C, A K-wire maneuvered to exit through the incision made on the lateral side of the femur. Subsequently, two 90° bends, approximately 1 cm apart, are made to form a hook that is then positioned around the femur. D, After

positioning around the femur, the K-wire is secured with a nut (arrow). Symbols: FC; femoral condyles, FP; fat pad, PL; patellar ligament, TB; tibia, KW; K-wire

Pump installation. Employing a stainless steel tube-connector (Access Technologies) the free end of the catheter (see above) was connected to a silicon tube attached directly to the iPrecio SMP-200 refillable pump (Primetech, Corp., Tokyo, Japan) filled with 0.9 ml of PBS or with antibodies. Nylon sutures (Ethicon Inc. Somerville, NJ) were tied around the silicon tubes at their juncture to ensure the stability of the connection site. A pump was then inserted into a subdermal pocket developed in the lateral area of the thigh. Finally, the incisions were closed with 4-0 absorbable sutures (Redisorb, MYCO Medical, Cary, NC). Following the surgery, the rabbits were allowed unrestricted cage activity. Figs. 13 & 14 depict installation and typical pump position.

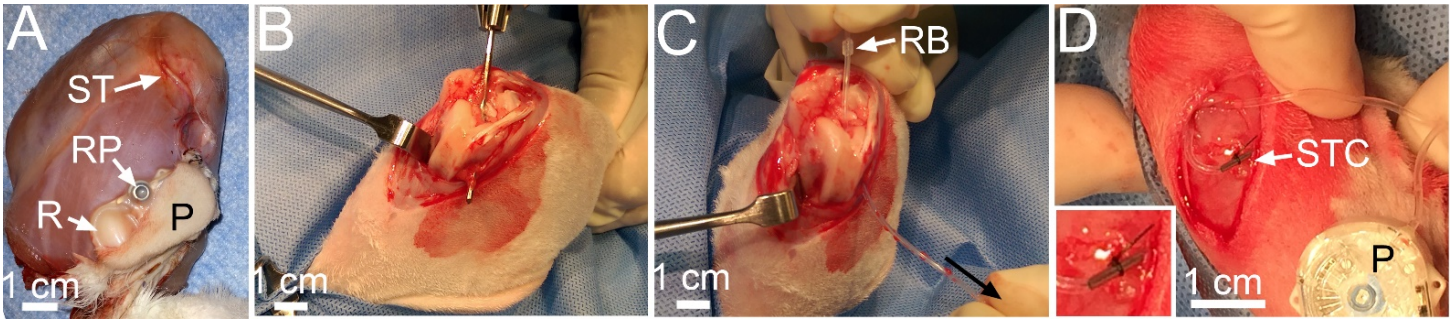

Figure 13. Depiction of a typical position of pump installed under the skin of an operated rabbit and key steps performed during pump installation. A, A typical position of an installed pump (P). B, Drilling a channel through the lateral condyle. C, Starting from the notch, a custom-made silicone catheter with a fixed retention bead at one end is passed through the hole in the direction indicated by the black arrow. While the retention bead secures the catheter inside the operated knee, the opposite end is connected with a pump. D, Checking the integrity of connection between the cannula seen in C and a silicon tube of a pump 8 weeks after pump installation. The silicon tubes remain connected via a stainless steel tube. The insert depicts this connection secured with nylon sutures. Symbols: ST; silicon tube, RP; refill port of a pump, R; reservoir of a pump, RB; fixed retention bead, STC; stainless steel connector.

K-wire and pump removal. After 8 weeks of immobilization the rabbits underwent a second surgery to remove the K-wires and the pumps. Bridging heterotopic ossification was manually disrupted. Subsequently, the rabbits were allowed 2 weeks or 16 weeks of unrestricted cage time, after which the rabbits were euthanized.

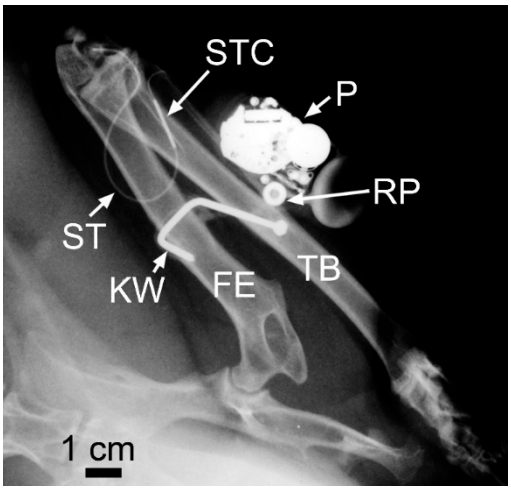

Figure 14. An X-ray depicting the uninterrupted flow path of a contrast agent from the pump to the knee cavity at the end of the 8-week delivery period. Symbols: STC; stainless steel connector, P; pump, RP; refill port, TB; tibia, FE; femur, KW; K-wire, ST; silicone tube.

Before removing the pump, we confirmed the integrity of the connection site created during pump installation (Fig. 13). After disconnecting the pumps, they were kept in the laboratory to confirm their continuous operation. This was done by observing the outflow of the solution that still remained in a pump's reservoir at the end of the treatment period.

Antibody delivery. A contrast agent (Hexabrix) was injected into the pump 8 weeks after the initial surgery, 24 h before the K-wire removal surgery. Subsequently, just before the K-wire removal, anesthetized rabbits were X-rayed to visualize the flow path of the contrast agent. This confirmed unobstructed flow from the pump to the operated knee (Fig. 14).

Utilizing rabbits that were sacrificed within the 8-week antibody-delivery period, we analyzed the presence of the antibodies within the collagen-rich structure of the posterior capsules (PC) of treated knees. Since the engineered antibodies employed here were a human-IgG type, it is possible to specifically detect them in the context of rabbit tissues. To achieve this, we employed a monoclonal mouse anti-human IgG antibody (ThermoFisher Sci.) able to bind the ACA and the P-ACA present within the collagen-rich architecture of PCs. Subsequently, utilizing a highly sensitive detection method (CSAII Biotin-free Tyramide Signal Amplification System, Dako North America, Inc., Carpinteria, CA) we visualized the monoclonal anti-human IgG antibody bound via the ACA or P-ACA (Fig. 15). Negative controls in which the anti-human IgG antibody was not applied were also prepared.

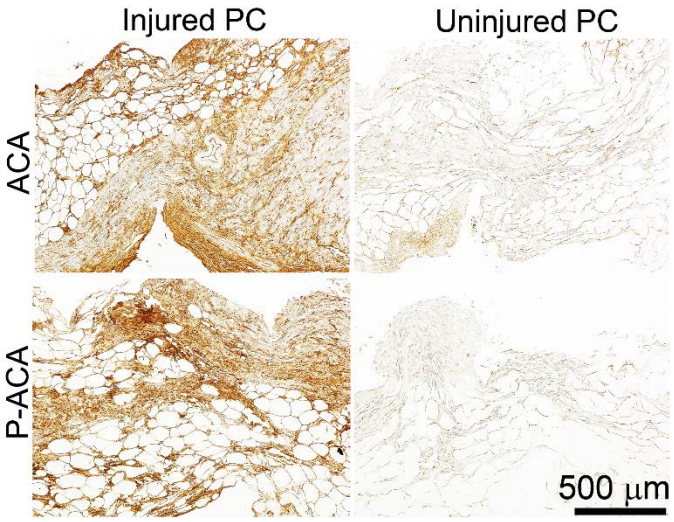

Figure 15. Immunodetection of the ACA and P-ACA in the PCs of rabbits that had to be sacrificed during the 8-week treatment period. The strong antibody-positive staining of the injured PCs treated with the ACA or the P-ACA is readily visible. This indicates proper delivery of the ACA into target sites.

Selecting antibody concentration. During initial planning of this experiment we took under a consideration the possibility of side effects associated with ACA treatment. Thus, the pilot group of rabbits received varying ACA concentrations. Since no apparent negative effects were noticed in any of the analyzed groups, we decided on applying the ACA and P-ACA at the rate of 0.5 mg/week/injured knee. This was the highest concentration of the ACA tested in the pilot group.

Joint angle measurements. Following euthanasia, the legs of the rabbits were processed to remove the bulk of skin and muscle tissue. Then, the tibia and the femur were transected about 6 cm from the knee joint. Subsequently, the ends of the bones were potted in polycarbonate cylinders with the use of polymethyl methacrylate and acrylic copolymer (PMMA, Flexbar Machine Corp., Islandia, NY) (Fig. 16). Such processing ensured the secure placement of bones in the grips of a custom-made flexion-measuring device (Test Resources, Inc., Shakopee, MN). This instrument included a torsional actuator/motor, a torque cell, and an angular displacement transducer (Fig. 16). After securing the analyzed limb in the grips, the femur and tibia were positioned at a right angle, and then the instrument was set to 0°. Subsequently, applying the rate of loading set to 40°/min, the extension torque was applied to 0.2 Nm, and the joint extension was recorded. Values near 90° indicated maximum extension, while angles larger than 90° represented hyperextension. Flexion contracture was expressed as the difference between the angles of the control limb and the injured limb recorded at 0.2 Nm. Thus, the larger difference between the maximum extension angles of control and operated limbs indicates a more severe joint contracture.

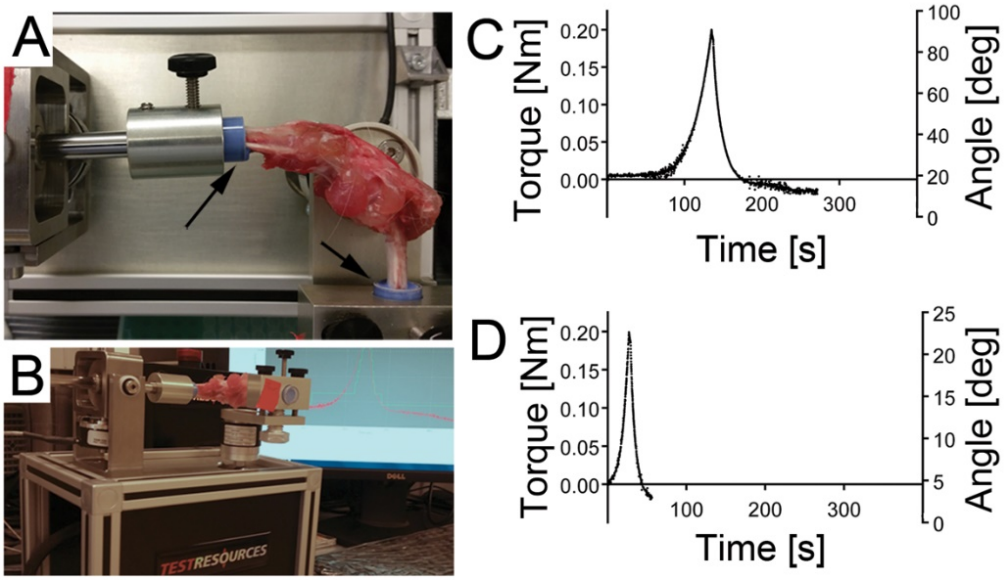

Figure 16. A system employed to measure the flexion contractures of analyzed knees. In A, arrows indicate femur and tibia whose ends are potted into tubes with the use of a PMMA. C, D, Representative data from measurements of the flexion contractures of the healthy (C) and the contracted (D) knees at 0.2 Nm torque. Ascending and descending parts of the depicted graphs represent extension and flexion behavior of the analyzed knees.

Tissue collection. As the fibrosis of the posterior joint capsule (PC) is the main cause of contracture in the rabbit model employed here, following the flexion contracture measurements, the PCs were dissected from the limbs [7,8].

Total collagen content. Tissue samples were frozen in liquid nitrogen and then pulverized in a stainless steel mortar. The samples were treated with a 3:1 mixture of chloroform and methanol to extract lipids and then lyophilized and weighed. Next, a collagen-specific hydroxyproline assay was used to determine the collagen content per unit of dry mass [5,6].

Collagen III:collagen I ratio. First, the acid-soluble collagen fraction was extracted from collected tissues with the use of 0.5 M acetic acid. Subsequently, the pepsin-soluble fraction was obtained with the use of pepsin (Sigma-Aldrich, St Louis, MO) prepared in 0.5 M acetic acid at a final concentration of 1 mg/ml. Employing the Sircol Collagen Assay Kit (Biocolor Ltd., Carrickfergus, UK), the concentration of extracted collagen was determined, and then the samples were prepared for electrophoresis. To separate the monomeric forms of collagen I chains from collagen III monomers, we employed an interrupted electrophoresis method that takes advantage of the fact that, unlike the collagen I α-chains, the collagen III α-chains are bound together via reducible disulfide bonds. In brief, heat-denatured collagen samples were initially run in a 6% polyacrylamide gel in non-reducing conditions. After 15 minutes, a 10-μl aliquot of 0.5 M DTT was added to each well and then electrophoresis continued. Recombinant collagen III served as a marker (Fibrogen Inc., San Francisco, CA). Pixel intensities of protein bands corresponding to the α1(III) and the α2(I) chains were measured by densitometry (EZQuant Ltd., Tel-Aviv, Israel), and then collagen III:collagen I ratios were calculated [5,6].

The ratios of cross-linked α-chains forming the β and the γ oligomers to the monomeric α-chains of the collagen pool extracted from PCs were also analyzed with the use of densitometry [5,6].

Microscopy of collagen fibrils. 3-μm thick sections of paraffin-embedded PCs were stained with H&E and with collagen-specific picrosirius red (Polysciences, Inc., Warrington, PA). The latter staining technique combined with polarized-light microscopy makes it possible to describe the thickness, the organization, and to a

certain degree, the collagen type-specific composition of the fibrils. As the thickness of fibers increases, their birefringence color changes from green to yellow to orange to red, *i.e.*, from shorter to longer wavelengths.

Employing a polarizing microscope (Eclipse LV100POL, Nikon Inc., Melville, NY) and the NIS Elements software (Nikon Inc., Melville, NY), we determined the percentages of differently colored collagen fibrils. Applying the built-in settings of the NIS Elements software, three main groups of colors were defined: (i) green, (ii) yellow, and (iii) orange-red. The entire image was analyzed, and then the areas occupied by pixels corresponding to the defined colors were determined. Considering the sum of all pixels to be 100%, the percentage of each color group in the analyzed samples was calculated. A minimum of three histological sections for control and for injured PCs were analyzed per each rabbit. The organization of collagen fibrils, expressed as theoretical anisotropy score, was evaluated by employing the ImageJ software that included the FibrilTool plug-in [5,6].

Results

In this task, we successfully developed and tested all methods needed to determine the utility of the ACA to limit posttraumatic joint contracture. Specific results obtained employing these methods are presented below when reporting outcomes for Specific Aim 2.

Summary

Milestones Achieved

In Major Task 2 we successfully developed and tested the complex methodology for the referenced project.

Major Changes

No major changes were introduced.

Technical Problems

At the initial phase of implementing the animal model, a few unexpected technical problems had to be solved. The first problem was a result of employing K-wires that were too short to form the correct hook needed to keep it firmly positioned over the femur (Fig. 14). As a result, two K-wires slipped from the femora where they were positioned during the surgical operation. To prevent this problem, we designed longer K-wires, so the critical hooks could be readily formed with the use of a K-wire bender tool (Fig. 17). Since implementing this change, no K-wire slippage has occurred.

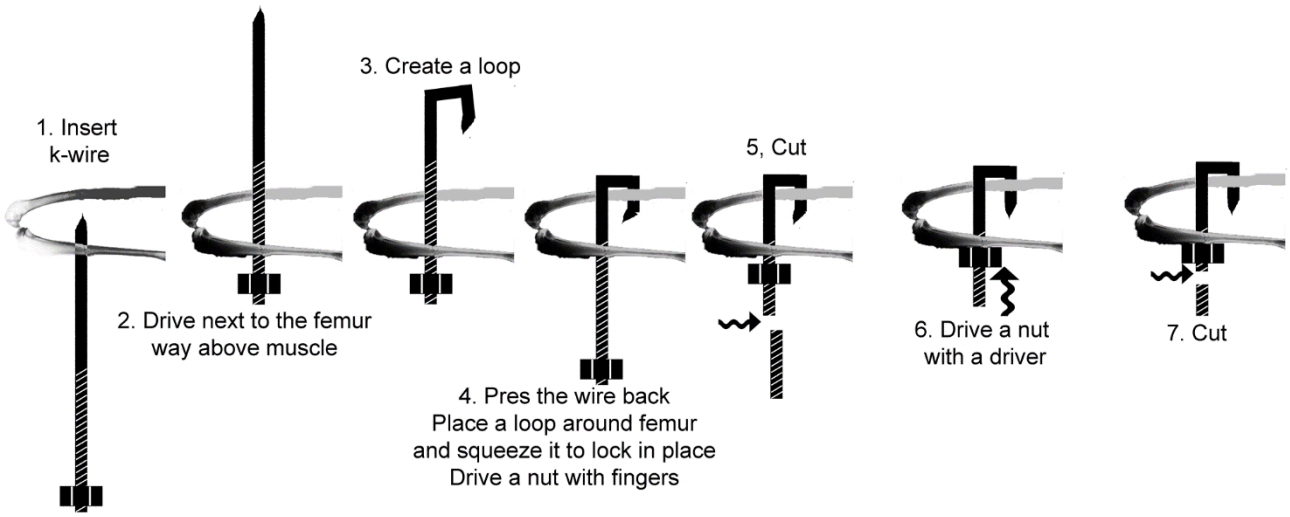

Figure 17. A schematic depicting the technique to immobilize the rabbits' knees.

The second technical problem was associated with immobilization of a silicon tube that delivers the antibody from the pump to the injured joint. As this tube runs through a femoral condyle, it was difficult to secure it with sutures. To eliminate this problem, we designed a tube whose one end includes a retention bead. This bead, whose diameter is slightly larger than that of the actual tube, prevents the tube from sliding out from its position within the knee cavity (Figs. 13 & 18). Following this modification, all tubes remained securely positioned throughout the entire experimental period.

Figure 18. Processing of a rabbit's leg to harvest the anterior and posterior knee capsule. The insert indicates a retention bead (arrow) that keeps the tube used to deliver the anti-collagen I antibody in the correct position.

For Specific Aim 2: To analyze long-term effects of the antibody-based inhibitor of fibrosis at the biochemical, cellular, and biomechanical levels.

Major Task 3. Creating an animal model for joint-contracture - A model representing posttraumatic joint contracture will be created.

Site and Involved PIs: Dr. Fertala (TJU), Dr. Abboud (RI), Dr. Beredjiklian (RI).

This model will be used to test the central hypothesis that by blocking posttraumatic fibrosis, it is possible to prevent or significantly reduce joint stiffness.

Subtask 1. Preparing critical animal groups.

Site and Involved PIs: Dr. Fertala (TJU), Dr. Abboud (RI), Dr. Beredjiklian (RI).

Animal groups will include the following: (i) a control group in which the injured knee joint will be treated with an anti-inflammatory agent, (ii) a chIgG-treated group in which the injured knee joint will be treated with the therapeutic chIgG variant, (iii) a control IgG-treated group in which the injured knee joint will be treated with an inactive IgG variant, and (iv) a non-treated control group in which the injured knee joint will not be treated with any therapeutic agents.

Subtask 2. Applying inhibitory chIgG and control agents into injured joints.

Site and Involved PIs: Dr. Fertala (TJU), Dr. Abboud (RI), Dr. Beredjiklian (RI).

Animals from the groups identified in Subtask 1 (see above) will receive the inhibitory chIgG and control agents. Techniques that ensure stability of antibodies will be applied according to the suggestions of Dr. Shoyele, an expert in the field of therapeutic biologics (see letter of support in original application).

Methods

Antibodies. Although we determined that the ACA is stable when incubated at 37°C for at least 4 to 8 weeks, our initial concern was the stability of this antibody in a tissue environment. A standard procedure to increase the stability of biologics, including antibodies, is their modification with PEG. Binding of PEG to antibodies may increase their resistance to proteolysis improve solubility and retention time in target sites. Downsize of this modification, however, may be lower binding affinity of the PEGylated form [9,10].

With the set time frame to complete this study (~2.5 years for animal studies), we felt we did not have enough time to run long-term pilot experiments, prior to running large-group experiments, that would help us to determine which antibody variant apply *in vivo*. Thus, to increase the likelihood of finding an appropriate antibody form with adequate stability and persistence in the injury sites, we tested in parallel the ACA and its modified form, P-ACA. This strategy increased our chances for success. At the end, we determined that both forms are effective with the P-ACA showing somewhat greater effects [6].

Experimental groups. As indicated above, our experimental system followed the following plan: (i) right knees of rabbits were injured and immobilized with K-wires for 8 weeks; (ii) during 8-week immobilization period the antibodies or control compounds were administered; (iii) after 8 weeks K-wires were removed and the rabbits were allowed to recover for 2 or 16 weeks.

We created the following experimental groups: (i) 2-week and 16-week recovery control groups treated in the injured knees with phosphate buffered saline (PBS) only (PBS-2, PBS-16); (ii) 2-week and 16-week recovery groups treated in the injured knees with a 2-mg/ml solution of the ACA (ACA-2, ACA-16); (iii) 2-week and 16-week recovery groups treated in the injured knees with a 2-mg/ml solution of the P-ACA (P-ACA-

2, P-ACA-16); and (iv) 2-week and 16-week recovery groups treated with anti-inflammatory agent Depo-Medrol (Depo, methylprednisolone acetate) (Depo-2, Depo-16).

Surgical procedures. We employed the rabbit model of posttraumatic joint contracture we describe above [6].

Delivery of tested compounds. The delivery of the ACA and P-ACA started right after surgery and continued for 8 weeks. This 8-week time frame is referred to as the treatment period. At the mid-point of this period, *i.e.* 4 weeks after surgery, the pumps' reservoirs were refilled through a subdermal port (Figs. 13 & 14). Starting at time "zero" of the treatment period, the flow rates were controlled by a pump's on-board computer according to the following fluid-delivery sequence: 1μl/h for 120h; 30 μl/h for 6h; 1 μl/h for 666h; 30 μl/h for 6h; 1 μl/h for 520h; 30 μl/h for 26h. In the Depo-2 and Depo-16 groups Depo-Medrol was delivered weekly for 8 weeks via intramuscular injection.

Major Task 4. Evaluating the efficacy of inhibitory chIgG to reduce the consequences of traumatic joint injury.

Site and Involved PIs: Dr. Fertala (TJU), Dr. Abboud (RI), Dr. Beredjiklian (RI).

In this task, microscopic, biochemical, and biomechanical assays will be employed to determine the efficacy of the proposed treatment of injured joints. These tests (see below) will provide the ultimate evidence to determine to what extent inhibiting excessive formation of collagen-rich deposits by blocking collagen fibril formation reduces the posttraumatic contractures of affected joints. At the same time, these tests will demonstrate how our novel approach differs in its effectiveness when compared to methods currently applied (application of steroids) in joint contractures.

Subtask 1. Microscopic testing of analyzed joints.

Site and Involved PIs: Dr. Fertala (TJU), Dr. Abboud (RI), Dr. Beredjiklian (RI).

Electron and light microscopy techniques such as polarized-light microscopy will be employed to analyze the morphology and quantity of fibrous deposits. Electron microscopy will be performed in a specialized facility available for us on the TJU campus. Light microscopy will be done in Dr. Fertala's laboratory equipped with state-of-the art imaging hardware and software.

Subtask 2. Biochemical assays of the content of fibrotic tissue.

Site and Involved PIs: Dr. Fertala (TJU).

Biochemical assays of the content of collagenous deposits will be done by assaying the content of hydroxyproline residues. Analyses of collagen cross-links, an indicator of the degree of fibrosis, will be done electrophoretically.

Subtask 3. Biomechanical assays. Biomechanical measurements of joint stiffness will be done by measuring a defined set of biomechanical parameters. These assays directed by Dr. J. Abboud will be done with the assistance of Dr. Soslowsky, an expert in the field (see letter of support).

Site and Involved PIs: Dr. Fertala (TJU), Dr. Abboud (RI).

Major Task 5. Data analysis and statistical evaluation of results.

Site and Involved PIs: Dr. Fertala (TJU), Dr. Abboud (RI), Dr. Beredjiklian (RI).

Subtask 1. Continuous data collection and analysis.

Data will be collected throughout the duration of animal-based experiments. Critical analysis of data will be done with the assistance of Biostatistics Shared Resources available at TJU.

Site and Involved PIs: Dr. Fertala (TJU), Dr. Abboud (RI), Dr. Beredjiklian (RI).

Methods

We described all applied methods in the "Major Task 2" section above.

Results

Body mass changes. Compared to their pre-surgery body mass, rabbits from all groups lost their initial mass at the end of the 8-week antibody-treatment period (Fig. 19). Rabbits in the PBS-treated group lost less than 10% of their initial mass and rabbits in the Depo-treated group lost almost 20% of their initial mass, a statistically significant difference ($p = 0.004$). Although the mass loses in the ACA-treated or the P-ACA-treated groups trended higher than that seen in the PBS-treated control, these differences were not statistically significant; $p = 0.8$ and $p = 0.08$, respectively. When compared to the ACA-treated or to the P-ACA-treated groups, the loss of body mass in the Depo-treated group was significantly higher; $p = 0.02$ and $p = 0.04$, respectively.

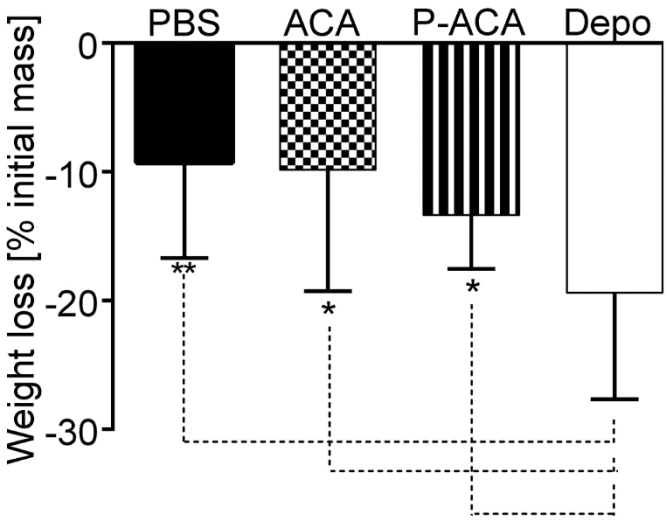

Figure 19. Changes in the body weight of rabbits during the initial 8 weeks of the experimental study. During this time the rabbits were treated with tested and control substances.

Drug delivery system. Examinations of the rabbits during the K-wire removal surgery have shown no adverse reaction to the 8-week presence of the pumps. All the pumps have operated, as programmed, and none of them has failed or was disconnected from the cannulas whose ends were fixed in the articular cavities of the operated knee joints (Fig. 13).

Employing a contrast agent at the end of the 8-week treatment period, we determined the unobstructed flow path from the pump to the injured knee (Fig. 14). Moreover, immunohistology assays done on the PCs of rabbits that had to be sacrificed during the treatment period have shown ACA-positive and P-ACA-positive staining in antibody-treated knees (Fig. 15). In contrast, the antibody-specific staining was seen neither in the PCs isolated from untreated healthy joints nor in the PCs derived from Depo-treated rabbits (not shown).

Morphology of joint tissues. In agreement with earlier reports, all surgically operated knees were characterized by joint contracture [5-7,11-13]. Microscopic examinations of transverse sections of uninjured PCs demonstrated that they consist of the layer of a fibrous, compact connective tissue (Fig. 20 A&B) and the adjoining net-like layer of fatty subintima of the synovial membrane (Fig. 20 A&B). Compared to the uninjured PCs, the fibrous layers of the PCs from the injured knees are noticeably thicker with a markedly increased number of cells (Fig. 20 B). Moreover, accumulation of atypical tissue deposits within subintima was also clearly apparent in the PCs isolated from the injured knees (Fig. 20 B). We did not observe any changes to the surface of articular cartilage isolated from the injured knees treated with PBS (not shown) or injured knees treated with antibodies (Fig. 20 C).

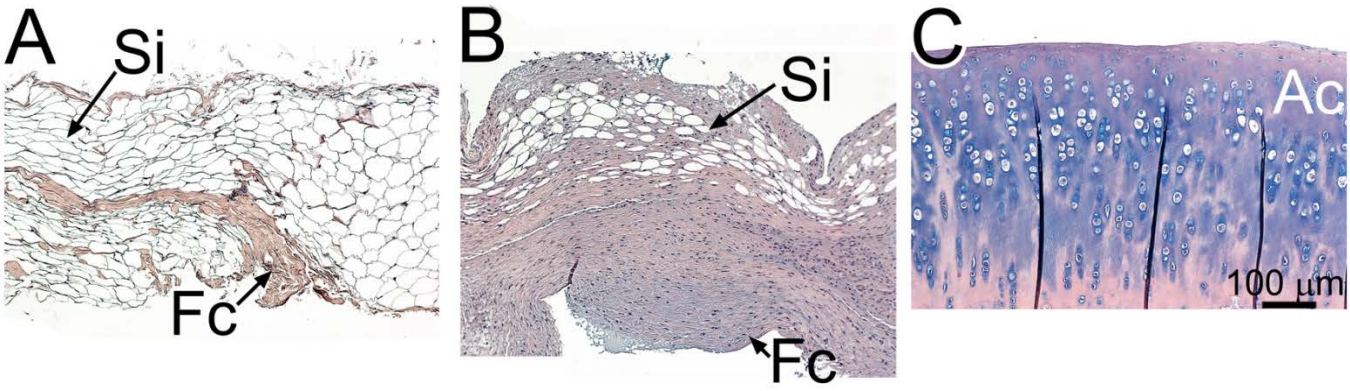

Figure 20. Microscopic assays of PCs from control and injured knees. A, B, H&E staining of cross-sections of uninjured (A) and injured (B) PCs isolated from the PBS-2 group. Fibrous capsules (Fc) and subintima regions (Si) are indicated. Note rich fibrotic deposits in the Fc and the Si regions of the injured PC seen in B. C, A microscopic image of the surface of articular cartilage (Ac) from the injured knee treated for 8 weeks with the ACA; no pathological changes are observed.

Effects of ACA and P-ACA on joint contracture-We measured the flexion contracture of injured knees to determine the effects of the agents applied during the 8-week treatment period on developing the posttraumatic joint stiffness. Fig. 21 presents the results of these measurements in the 2-week and the 16-week recovery groups. Comparison of the PBS-2 control group with the ACA-2 group or with the P-ACA-2 group indicates a statistically significant reduction of the flexion contracture in the groups treated with both antibody variants; $p = 0.05$ and $p = 0.003$, respectively (Fig. 21). Comparison of the ACA-2 and the P-ACA-2 groups indicates that treating the rabbits with the P-ACA trends toward greater reduction of the flexion contracture; $p = 0.1$. Compared to the PBS-2 group, the Depo-2 group was characterized by a statistically significant reduction of the flexion contracture; $p = 0.0007$ (Fig. 21). Compared to the ACA-treated rabbits in the 2-week recovery group, the Depo-treated rabbits showed a significantly greater reduction of the flexion contracture ($p = 0.009$). Compared to the P-ACA-treated rabbits in the 2-week recovery group the Depo-treated rabbits trended toward greater reduction of the flexion contracture ($p = 0.06$)

In the 16-week recovery groups, we observed a statistically significant difference in the flexion contractures between the PBS-16 and Depo-16 groups ($p = 0.006$). While the flexion contractures for the PBS-16 and ACA-16 groups were similar ($p = 0.7$) in the P-ACA-treated rabbits, the flection contracture trended toward lower values compared to the PBS-16 or ACA-16 groups; $p = 0.2$ and $p = 0.1$, respectively (Fig. X).

When comparing the flexion contractures between corresponding groups of rabbits from the 2-week and 16-week recovery groups (Fig. 21) (*i.e.*, PBS-2 vs. PBS-16, ACA-2 vs. ACA-16, and P-ACA-2 vs. P-ACA-16), we observed a statistically significant reduction of the flexion contracture had occurred in the PBS-16 group ($p = 0.005$). Although the flexion contractures in the ACA-16 and P-ACA-16 groups trended toward lower values

compared to the 2-week recovery counterparts (Fig. 21), these changes were not statistically significant; p = 0.2 and p = 0.1, respectively [6].

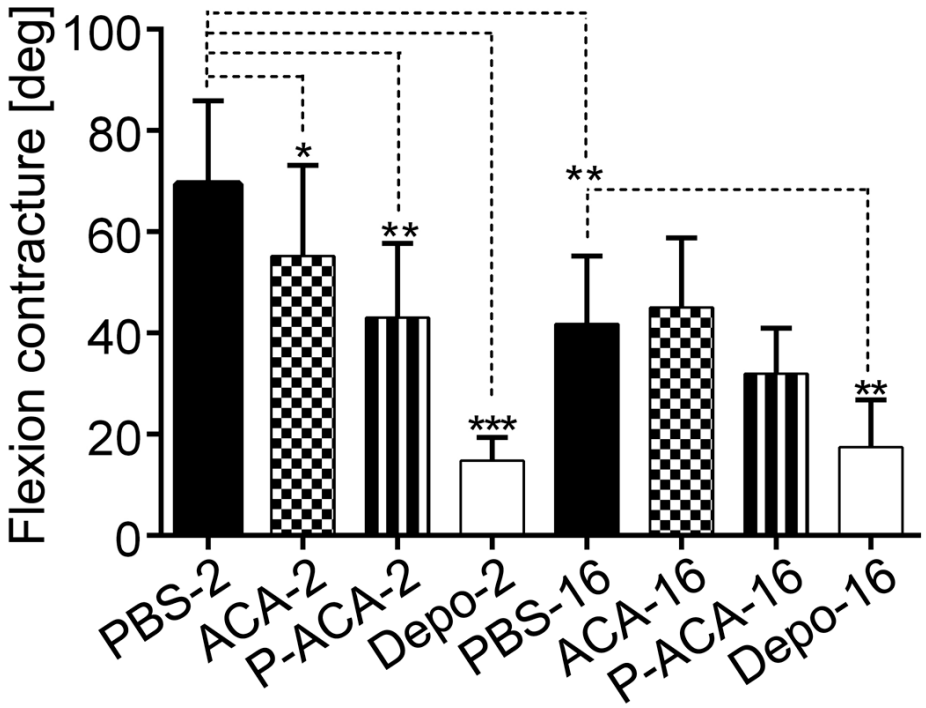

Figure 21. A graphic representation of the measurements of the flexion contracture of the injured knees. The flexion contracture was calculated as the difference between the flexion contracture of the non-injured leg and the flexion contracture of the injured leg. Note that a larger difference between the maximum extension angles of control and operated limbs indicates a more severe joint contracture. Asterisks indicate statistically significant differences between analyzed groups: *P < 0.05, **P < 0.01, ***P < 0.001.

Assays of collagen fibrils deposited in the PCs – Since we targeted collagen fibril formation as a method to reduce the posttraumatic contracture, we analyzed the relative content of various subpopulations of collagen fibrils present in dissected PCs. As described earlier, the red/orange-birefringence fibrils represent thick, mature collagen fibrils and the green-birefringence fibrils indicate the presence of thin collagen fibrils. Yellow-birefringence structures represent intermediate-diameter fibrils. Studies demonstrated that in fibrotic tissue with the active formation of new collagen fibrils, the relative content (injured PC/uninjured PC) of green-birefringence structures increases. Fig. 22 indicates that in the PBS-2 group the relative content of green-colored thin fibrils has increased in the injured knees in the PBS-2 group, calculated as the injured PC/uninjured PC ratio. Compared to the PBS-2 group, the increase in the content of thin fibrils was significantly smaller in the ACA-2 and P-ACA-2 groups; p = 0.01 and p = 0.04, respectively. In the Depo-2 group the relative content of green-colored fibrils seen in the injured PC was comparable to that calculated for the PBS-2 group (p = 0.8) [6].

A similar trend was observed in the 16-week recovery groups group, but the differences were not statistically significant between the PBS-16 and ACA-16, the PBS-16 and P-ACA-16, and the PBS-16 and Depo-16 groups; p = 0.3, p = 0.4, and p = 0.4, respectively (Fig. 22 B). Fig. 23 depicts representative images of collagen fibrils analyzed in the PCs as described above.

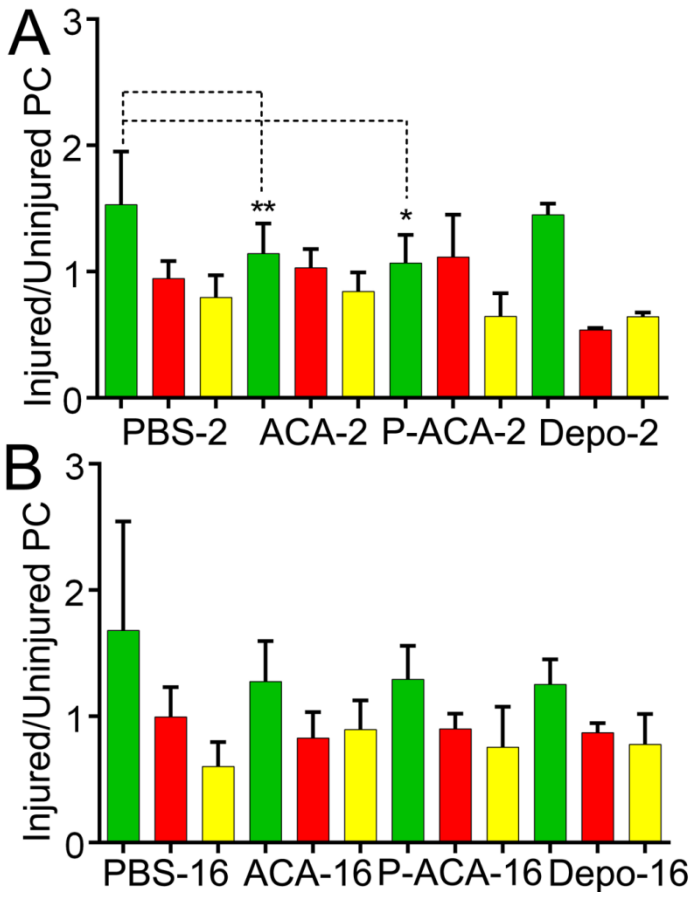

Figure 22. Graphic representations of results from microscopic assays of changes in subpopulations of collagen fibrils present in the PCs from injured vs. uninjured knees. A, B, 2-week and 16-week recovery groups. Bars represent the ratios of percent areas occupied by corresponding birefringence colors seen in injured and uninjured PCs. Asterisks indicate statistically significant differences between analyzed groups: *P < 0.05, **P < 0.01.

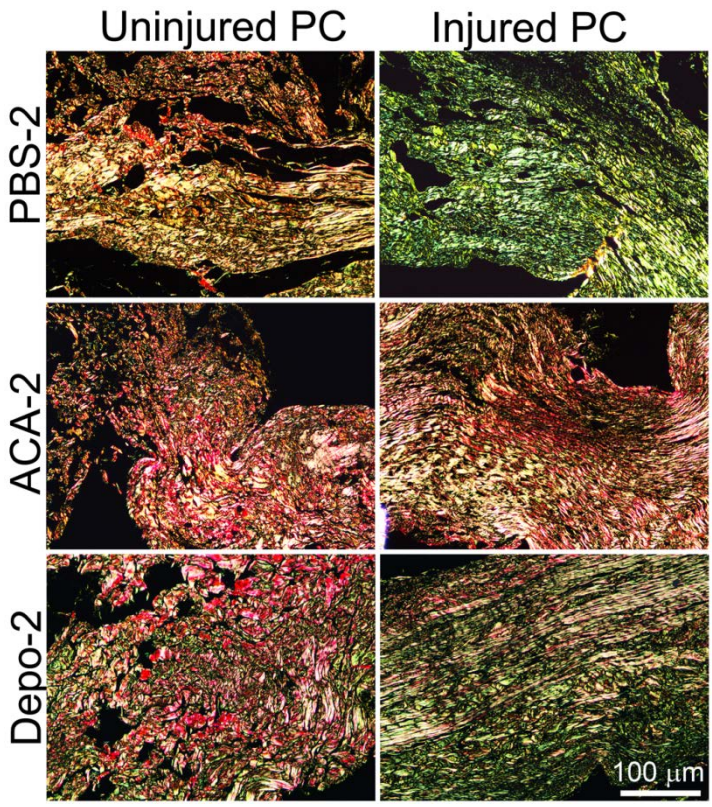

Figure 23. Representative images of collagen fibrils observed in the PCs with the use of a polarizing microscope. Note that thin green-colored fibrils dominate in the PBS-treated injured knees and Depo-treated injured knees. In contrast, the green-colored fibrils are not readily apparent in the ACA-treated PCs.

Fibril organization- While the anisotropy score was relatively high in the uninjured knees of all groups, thus indicating the preferred orientation of fibrils (Fig. 24 A & B), it was relatively low in the injured knees of the PBS-2 and the Depo-2 groups (Fig. 24 B). This low anisotropy score suggests non-preferential or more random organization of the fibrillar structures. Antibody-treated injured PCs in the 2-week groups showed the anisotropy score values similar to those of uninjured counterparts (Fig. 24 B). As represented by the PBS-16 group (Fig. 24 B), the anisotropy score values were comparable for the injured and uninjured PCs from the 16-week recovery groups [6].

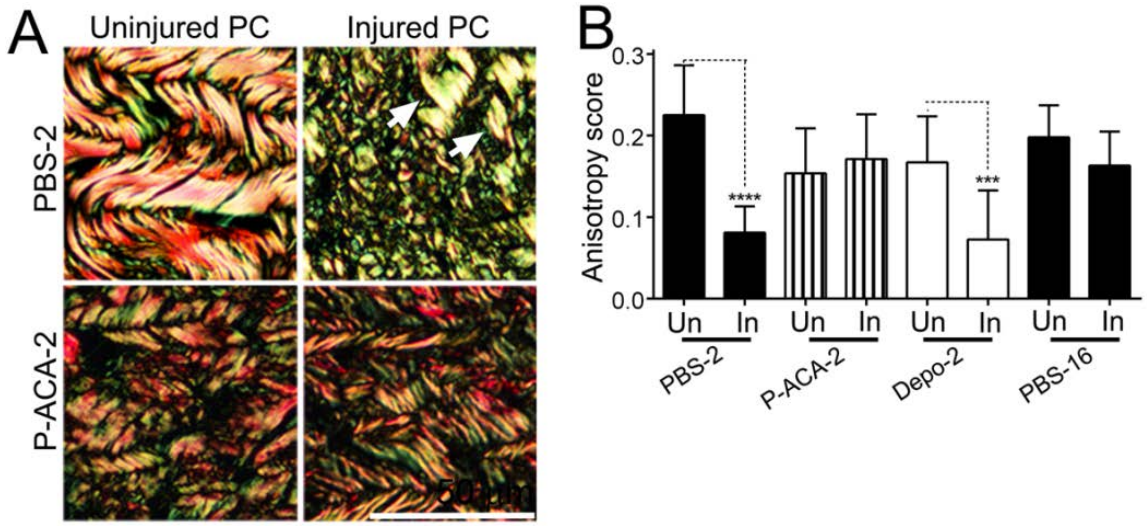

Figure 24. Analysis of the organization of collagen fibrils in the longitudinal sections of the PCs. A, Representative images of collagen fibrils seen in selected PCs. Arrows indicates fibrils in an injured PC whose alignment resembles that in uninjured counterpart. B, A graphic representation of measurements of the anisotropy scores. Asterisks indicate statistically significant differences between analyzed groups: ***P < 0.001, **** P < 0.0001.

Total collagen content. Assays of the hydroxyproline concentration in the PC samples indicate a relatively high percentage of collagenous proteins in the PCs isolated from the healthy and contracted knees (Fig. 25). Compared to the content of collagen in uninjured PCs from the PBS-2, ACA-2, or the P-ACA-2 groups, the collagen content in both uninjured and injured capsules was significantly reduced in the Depo-treated group (Fig. 25).

Comparison of the collagen content in uninjured PCs and injured PCs within the PBS-2, ACA-2, and P-ACA-2 groups indicates a statistically significant decrease of the collagen content in the injured PCs of the P-ACA-treated capsules ($p = 0.04$, Fig. 25).

There were no statistically significant differences between the collagen content in the PCs from injured and uninjured knees in rabbits from the 16-week recovery groups. Moreover, no statistically significant differences were observed in collagen content between the PBS-16 and ACA-16 groups, the PBS-16 and P-ACA-16 groups, or the PBS-16 group and Depo-16 groups (Fig. 25).

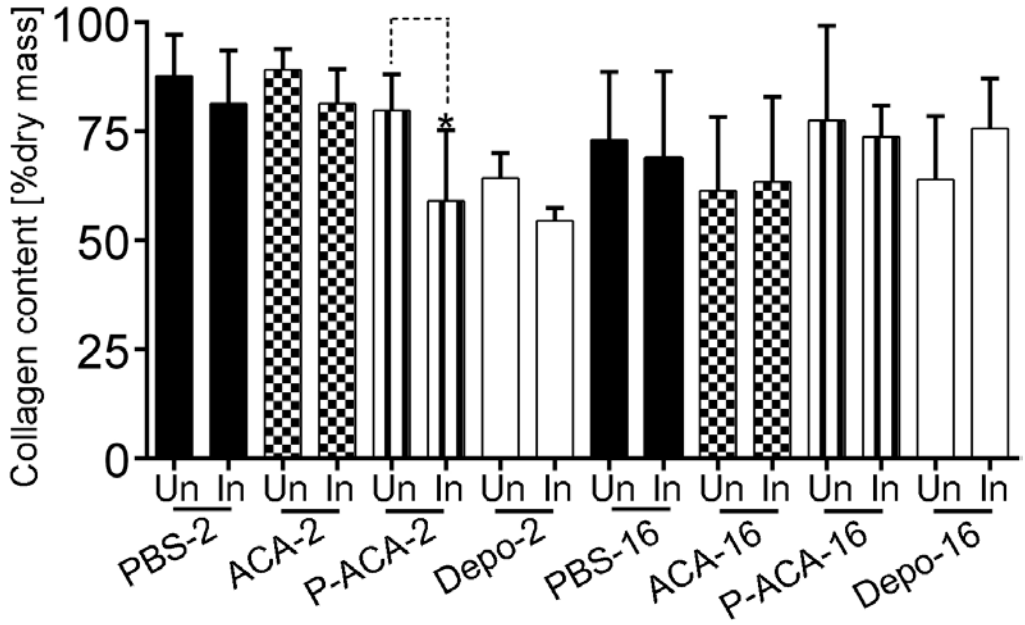

Figure 25. A graphic representation of the collagen content in the PCs. Asterisk indicates statistically significant differences between analyzed groups: *P < 0.05.

Collagen III content. Comparison of the relative contents of collagen III in the uninjured and injured PCs indicates 1.35-fold (± 0.4 SD) increase in the PBS-2 group. In the ACA-2, P-ACA-2, and Depo-2 groups, the relative content of collagen III in injured PCs increased 1.06-fold (± 0.2 SD), 1.10-fold (± 0.3 SD), and 1.18-fold (± 0.2 SD), respectively (Fig. 26 B).

Comparison of the relative content of collagen III in the uninjured and injured PCs indicates 1.12-fold (± 0.3 SD) increase in the PBS-16 group. In the ACA-16, P-ACA-16, and Depo-16 groups, the relative content of collagen III in injured PCs changed 0.91-fold (± 0.2 SD), 0.96-fold (± 0.3 SD), and 1.13-fold (± 0.2 SD), respectively (Fig. 26 B). Analyses of the statistical significances of the differences between changes in collagen III content in injured capsules from the PBS-treated groups and the ACA-treated, P-ACA-treated, or Depo-treated groups are presented in Fig. 26.

Relative amount of cross-linked collagen chains. Analyses of the relative content of the cross-linked collagen chains in the uninjured PCs and in injured PCs indicate no changes across all analyzed groups (Fig. 26 C)

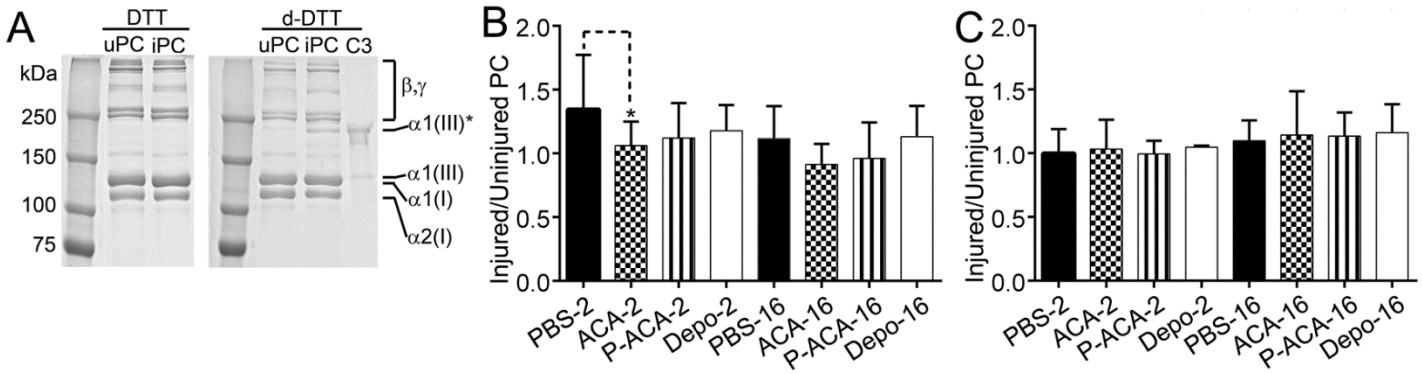

Figure 26. A graphic representation of the results from electrophoretic assays of collagenous proteins extracted from the PCs. A, Patterns of migration of collagen I and collagen III chains separated in standard reducing conditions (DTT) and in delayed-reduction conditions (d-DTT) of electrophoresis. B, A graphic representation of the proportions of the collagen III:collagen I ratios calculated for the injured and uninjured PCs (*P < 0.05). C, A graphic depiction of the results of measurements of the proportions of the βγ:α ratios; no statistically

significant difference was observed. Symbols: uPC, iPC; uninjured and injured PC, C3; collagen III marker, α1(I), α2(I), α1(III); specific chains of collagen I and collagen III, respectively; α1(III)*; collagen III chains separated with the use of delayed-reduction conditions; β, γ; β and the γ oligomers consisting of cross-linked collagen α chains.

Conclusions and Discussion

We analyzed the utility of applying the ACA after knee injury to reduce posttraumatic joint contracture. Mechanical tests demonstrated that the flexion contractures in the ACA-2 and P-ACA-2 groups were significantly reduced compared to the PBS-2 control [6]. Consistent with earlier studies, similar reduction of the flexion contracture was also observed in the Depo-2 group. Although the flexion contractures decreased further in the ACA-16 and P-ACA-16 rabbits compared to the corresponding 2-week recovery groups, this decrease was not statistically significant. In contrast, the decrease in the flexion contracture in the PBS-16 group compared to the PBS-2 group was statistically significant. A spontaneous reduction of the flexion contracture in non-treated PBS-16 group is consistent with earlier reports indicating that the flexion contracture of the rabbits knees had decreased about 50% 16 weeks after removing K-wires compared to the shortly after K-wire removal [7]. Considering that the reduction of the flexion contracture in the ACA-2 and the P-ACA-2 groups was similar to that observed 4 months later in the PBS-16 group, we hypothesize that the application of ACA and P-ACA limits the development of full fibrotic changes rather than accelerates spontaneous recovery.

Since rabbit-based studies demonstrated that applying non-specific human IgG to the cavities of injured knees does not change the flexion contracture of the injured joints, we propose that the changes observed in the ACA-2 and P-ACA-2 groups are ACA and P-ACA-related [14].

We analyzed the PCs to learn what caused the reduced flexion contracture in the ACA-treated, P-ACA-treated, and Depo-treated groups. Since the main target of the ACA and P-ACA is collagen fibril formation, we first studied the fibrillar architecture of the treated PCs. In earlier studies, we had determined that an increase in green-birefringence thin collagen fibrils reflects an active process of collagen fibrillogenesis in injured PCs in response to injury [6]. Consequently, we postulate that the observed reduction in the relative amount of the thin fibrils in the injured PCs treated with the ACA or P-ACA results from inhibition of the collagen fibril formation process.

The similar anisotropy scores in the injured and uninjured PCs from the antibody-treated groups may have resulted from the reduced formation of new fibrils by the ACA and P-ACA. Thus, we suspect that these relatively high anisotropy scores seen in injured PCs reflect the organization of mature fibrils that existed before joint injury rather that improved organization of new fibrils formed *de novo* in response to joint trauma. Supporting this hypothesis of persistence of the original fibrils in the injured PCs from the ACA and P-ACA groups is our observation that the organization of clusters of fibrils in the injured PCs of the PBS-2 group resembles that of the uninjured control. In the injured PCs from the PBS-2 group, however, the general pattern of organization of the original fibrils is markedly disrupted by newly formed fibrillar assemblies. We expect that limiting the formation of new fibrils in the PCs of the ACA and P-ACA groups preserved the correct fibrillar architecture, thereby reducing the flexion contracture of injured knees.

It is important to note that the anisotropy score for the fibrils in the injured PCs from the Depo-2 group was significantly smaller than that of uninjured control. Considering that the flexion contracture was significantly reduced in this group compared to the PBS-2 group, we cannot associate this reduction with preservation of correct fibril arrangement, as proposed above for the antibody treated groups.

To further elucidate the mechanisms that reduced flexion contracture in the ACA-treated and the P-ACA-treated groups, we analyzed the total collagen content in the PCs. We propose that the approximately 20% reduction of the collagen content in the injured PCs from the P-ACA-2 group resulted from blocking the incorporation of newly produced collagen molecules into fibrils. Researchers demonstrated that the triple-helical structure of individual collagen molecules is quite unstable at body temperature, allowing degradation of

collagen molecules by proteolytic enzymes. In contrast, the stability of collagen molecules increases upon their incorporation into fibrils, thereby rendering them more resistant to enzymatic degradation.

We also postulate that the significant decrease in the relative collagen content observed in the PCs from the Depo-2 group resulted from reduced expression of collagens. The negative impact of glucocorticoids on the expression of collagen genes is a well-recognized phenomenon that occurs in many connective tissues. Examples of how glucocorticoid-mediated reduction in collagen content weakens connective tissue include: atrophy of skin, weakening of tendons, degeneration of intervertebral discs, and avascular necrosis of bones [15-18]. Thus, we postulate that reduced flexion contracture in the Depo-2 group resulted from the negative global impact of Depo Medrol on the production of collagenous proteins needed to maintain the mechanical strength of the PCs. We predict that despite relatively poor organization of collagen fibrils in the Depo-2 group described above, the overall low collagen content was a main reason that the flexion characteristics of the injured knees remained largely unchanged.

We have also analyzed potential effects of applied treatments on the collagen III:collagen I ratio in the injured PCs and on the relative amount of cross-links present in the pepsin-extracted fraction of collagenous proteins. Consistent with our earlier studies, the relative amount of collagen III increased in the injured PCs from the PBS-2 group [19]. Although the collagen III:collagen I ratio trended lower in the antibody-treated and Depo-treated groups, a statistically significant difference was observed only in the PBS-2 and ACA-2 groups. We speculate that blocking the formation of collagen I fibrils could reduce the amount of collagen III that accumulates *in vivo* on the surface of pre-existing collagen I assemblies [20].

By studying the cross-linked versus non-cross-linked collagen α chains, we determined that the relative amounts of the cross-linked fractions in the injured and healthy capsules were similar in all analyzed groups. Since we employed the pepsin-soluble fraction of the collagen pool, we cannot exclude the possibility of changes in the quality and the quantity of cross-links present in the non-soluble collagen pool. Considering the similar quantities of the cross-links, we postulate that the aberrant orientation of the collagen fibrils formed *de novo* in response to injury contributed to joint stiffness. In a study of muscle fibrosis that supports this postulation, Chapman *et al*. suggested that a change in collagen fibril orientation, rather than increased cross-linking, was a decisive factor in developing muscle stiffness [21].

Our results showed that the P-ACA causes stronger effects compared to the ACA despite some steric hindrance caused by the presence of the PEG 12-mers. We speculate that these stronger effects were likely due to greater stability of the PEG-modified antibody and perhaps to its prolonged residence in the injury sites. These qualities of PEG-modified molecules are the main reason behind the PEGylation of a number of therapeutic biologics, such as peptides and monoclonal antibodies [9,10].

The results of our study demonstrated that collagen fibril formation is a valid target to reduce post-traumatic joint contracture. Unlike anti-fibrotic approaches that target broad intracellular processes associated with inflammation and cell proliferation, the anti-fibrotic approach tested here targets a well-defined extracellular process, thereby reducing the chance for unwanted side effects. In this sense, our technique to limit the consequences of the fibrotic process in injured joints is similar to the anti-fibrotic approaches that target extracellular lysyl oxidase (LOX), which catalyzes collagen-cross linking, or $\alpha v\beta 6$ integrin, which participates in TGF-β1 activation [22,23].

There are a few limitations in the presented study. First, although the rabbit model of posttraumatic joint stiffness represents the key biological processes occurring in human patients, due to anatomical differences, this model cannot replicate all characteristics of human knee joints. Second, unlike in human patients, the post-K-wire-removal activity of the rabbits is limited, thereby altering improvement of knee motion. Third, due to the specific delivery system, the antibodies cannot reach all joint structure sites within which fibrotic changes occur. Consequently, the effectiveness of the applied antibodies is limited. We postulate that systemic or biomaterial-based delivery of the ACA and P-ACA could offer an alternative and perhaps more effective delivery routes.

Considering that the mechanism of posttraumatic fibrosis is similar in all connective tissues regardless of the nature of initial trauma, we believe the results presented here provide a blueprint for designing anti-fibrotic approaches targeting collagen fibril formation in other tissues of the musculoskeletal system.

Summary

Milestones Achieved

In the Major Tasks 4&5 we successfully demonstrated the utility of the ACA and P-ACA to reduce posttraumatic joint contracture.

Moreover, we build an active research group consisting of basic researchers and orthopaedic surgeons. Specifically, as indicated above, our project was funded through the Translational Research Partnership Award mechanism. This mechanism required research teams to conduct translational studies that would accelerate the movement of promising ideas in orthopaedic research into clinical applications to benefit soldiers with combat-relevant traumatic orthopaedic injuries. Moreover, this award mechanism required the formation of the multi-institutional and multi-disciplinary research partnership among orthopaedic surgeons and basic researchers. Our group has fulfilled both of these requirements.

Our team has been extremely successful in establishing a well-integrated partnership among orthopaedic surgeons and basic researchers focusing on research associated with posttraumatic joint stiffness. This team has grown from a group of three initial Principal Investigators into the Scientific Consortium for Arthrofibrotic Research (SCAR). At present, the scientists that form the SCAR focus on the scarring of elements of the musculoskeletal system, including tendons, joint capsules, peripheral nerves, and others. Moreover, integration of our group is strengthened by the university-wide initiative entitled: “The Link between Wound Repair, Inflammation, Fibrosis and Cancer”.

Major Changes

No major changes were introduced.

Technical Problems

No major technical problems were encountered.

KEY RESEARCH ACCOMPLISHMENTS

The referenced project was funded through the Translational Research Partnership Award mechanism. This mechanism required research teams to fulfill the following key requirements:

1. To conduct translational studies that would accelerate the movement of promising ideas in orthopaedic research into clinical applications to benefit soldiers with combat-relevant traumatic orthopaedic injuries.

2. To form the multi-institutional and multi-disciplinary research partnership among orthopaedic surgeons and basic researchers.

Our group has fulfilled both of these requirements.

Key accomplishments of this project include:

- Proving the efficacy of our technology to reduce posttraumatic joint stiffness *in vivo.* Specifically, we demonstrated that applying the ACA to injured joints significantly limits the development of posttraumatic joint contracture. We also demonstrated that this technology, in comparison to applying anti-inflammatory steroids, is safe and it does not cause any apparent side effects.

- Establishing key parameters for applying therapeutic ACA to limit posttraumatic joint contracture. Specifically, we determined that applying the ACA right after joint injury provides an effective strategy to limit joint contracture.

- Determining the utility of ACA modifications on therapeutic efficacy of this antibody. Specifically, in addition to the ACA we tested its PEGylated form, P-ACA. We demonstrated that this variant offers great stability, retention time, and is active in reducing posttraumatic joint contracture.

- Discovering that posttraumatic joint stiffness is not only caused by excessive production of collagen-rich fibrotic tissue but also by aberrant organization of collagen fibrils. This discovery defines collagen fibril organization as a new target to limit posttraumatic joint stiffness. We contemplate novel technologies to improve the organization of fibrillar structure of healing joint capsules that could preserve their proper mechanical characteristics.

- Creating multi-disciplinary research partnership. Our group has been extremely successful in establishing a well-integrated partnership among orthopaedic surgeons and basic researchers focusing on research associated with posttraumatic joint stiffness. This team has grown from a group of three initial Principal Investigators into the Scientific Consortium for Arthrofibrotic Research (SCAR).

At present, the scientists that form the SCAR focus on the scarring of elements of the musculoskeletal system, including tendons, joint capsules, peripheral nerves, and others. Moreover, integration of our group is strengthened by the university-wide initiative entitled: “The Link between Wound Repair, Inflammation, Fibrosis and Cancer”.

CONCLUSION

Military benefits and significance. Arthrofibrosis, or joint stiffness due to scar tissue, is a common problem after military service members and/or veterans sustain traumatic injuries, and it may affect multiple joints of the body, including the shoulder, elbow, wrist, hand, hip, knee, ankle, and foot. Early on, joint injury can lead to pain, hemarthrosis, and the need for a period of joint immobilization. As a result, patients commonly develop joint contractures and adhesions that can result in persistent pain and limit long-term function. If surgery is indicated, stiffness can worsen after interventions have been performed. Because of this, arthrofibrosis is perhaps the single most common complication following both nonoperatively and operatively treated joint injuries.

The presence of arthrofibrosis can lead to significant functional limitations, as specific ranges of motion are necessary to perform basic activities of daily living. For example, functional knee flexion is necessary for the swing through phase of ambulation (67°), to ascend an 8-inch stair (83°), to descend stairs (90-100°), to rise from a standing chair (93°), to rise from a low chair (105°), and to kneel (125°). In the military setting, posttraumatic stiffness following injury or surgery may result in further loss of function, potentially limiting the ability to work, to serve, and to perform activities of daily living. Thus, there is a direct healthcare need for decreasing the incidence of arthrofibrosis after orthopaedic injuries and surgical interventions in military service members and/or veterans.

Currently, there are limited methods for treating arthrofibrosis, regardless of the affected joint. Oral non-steroidal anti-inflammatory drugs (NSAIDs) have been used with limited utility to decrease the inflammation that accompanies arthrofibrosis. Similarly, cryotherapy has been utilized in patients to decrease inflammation and is often used as an adjunct to other therapies. Intraarticular or intravenous corticosteroids have been demonstrated to improve range of motion in patients with arthrofibrosis, but there are significant potential side effects associated with both treatment regimens, including infection, immunosuppression, decreased wound healing, insomnia, and weight gain. Active physical manipulation of the arthrofibrotic joint through physical therapy or passive manipulation through devices, such as continuous passive motion machines, can potentially increase range of motion. However, this increase in range of motion is often achieved with the trade-off of increased pain and inflammation from the intervention.

Once arthrofibrosis has set in, surgical interventions are often necessary, including open surgical treatment and arthroscopy. For open surgical management, an incision is made into the arthrofibrotic joint, and scar tissue is manually removed to improve motion. Additional manipulation of the joint is often performed under anesthesia to further break up scar tissue and restore range of motion. For arthroscopy, adhesions are lysed and scars are removed using a shaving tool. In these cases, the joint must be large enough to accommodate a camera and a shaving tool. In both surgical scenarios, the outcomes are unpredictable because surgical interventions to remove scar tissue also result in increased bleeding and inflammation that may result in the formation of additional scar tissue.

From a clinical perspective, these options for treating arthrofibrosis are suboptimal. Non-surgical methods only provide incremental benefit in functional improvement. Surgical methods are invasive and the results are unpredictable. Patients who sustain arthrofibrosis and receive standard of care treatments may not return to work and may not regain their functional abilities. Military personnel who have arthrofibrosis may lose time from work and from duty to undergo surgical interventions and perform intense physical therapy without any guarantee that their stiffness will improve.

The most ideal method for treating arthrofibrosis is to prevent the occurrence of stiffness in the first place. The goal of this study was to develop a novel approach to treat military service members and/or veterans at the time of musculoskeletal injury with a paradigm-changing targeted antibody (ACA) that would reduce the potential for future arthrofibrosis. By utilizing this novel ACA-based method to prevent arthrofibrosis after

injury, patient care would change after injury, as further non-surgical and surgical interventions may not be necessary and functional restoration may occur at a faster rate.

In the short-term, implementing this method of arthrofibrosis prevention after injury should allow for earlier return to functional activities. Military personnel may return to duty or work sooner after sustaining an injury, may not need to change duties to accommodate a stiffened joint, and may demonstrate earlier return to duty and unit readiness after sustaining a musculoskeletal injury.

In the long-term, individuals recovering from traumatic orthopaedic injuries may have higher patient satisfaction and increased work longevity if arthrofibrosis is prevented at the time of injury.

Future plans. Our group plans to expand research on blocking posttraumatic joint contracture by developing clinically-relevant methods for intra-articular delivery of the ACA. If successful, this research would bring our novel therapeutic approach closer to clinical application.

To achieve this, we attracted a group of scientist who are experts in biomaterial-based delivery of therapeutic biologics, including antibodies, into joints. By determining an optimal method of drug delivery, without adverse wound healing, the use of our therapeutic antibody may become the standard of care in patients who sustain orthopaedic injuries or who undergo orthopaedic surgical procedures that may result in post-operative arthrofibrosis. Once utilized in patients, new evidence-based policy changes may be made and may revolutionize the way that arthrofibrosis is managed after combat-related orthopaedic injuries.

PUBLICATIONS, ABSTRACTS, AND PRESENTATIONS

Considering the 3-year duration of this complex project and the need to maintain certain groups of rabbits for 6 months, our group has made significant progress. The following list summarizes key publications:

Peer-Reviewed Scientific Journals

1. Auxiliary proteins that facilitate formation of collagen-rich deposits in the posterior knee capsule in a rabbit-based joint contracture model. Steplewski A, Fertala J, Beredjiklian PK, Abboud JA, Wang ML, Namdari S, Barlow J, Rivlin M, Arnold WV, Kostas J, Hou C, Fertala A (2016). J Orthop Res 34:489-501. PMID: 26241613

2. Blocking collagen fibril formation in injured knees reduces flexion contracture in a rabbit model. Steplewski A, Fertala J, Beredjiklian PK, Abboud JA, Wang ML, Namdari S, Barlow J, Rivlin M, Arnold WV, Kostas J, Hou C, Fertala A (2016). J Orthop Res. [Epub ahead of print] PMID: 27419365

Abstracts (* indicates presentations leading to publication).

*1. Testing the Utility of Engineered Anti-Collagen I Antibody to Limit the Formation of Collagen-Rich Fibrotic Deposits in a Rabbit Model of Posttraumatic Joint Stiffness. Steplewski, A., Fertala, J., Barlow, J., Beredjiklian, Pedro., Abboud, J., Wang, M., Namdari, S., Arnold, W., Kostas, J., Hou., C., and Fertala, A.

Orthopaedic Research Society Conference, 2015

Invited Presentations

1. Inhibition of Fibrosis. Synageva, Inc., Lexington, MA, 2014

2. Novel Targets to Limit Organ Fibrosis. Bristol-Myers Squibb, Hopewell, NJ; 2015

3. Prevention of the Posttraumatic Fibrotic Response in Joints. Center for Musculoskeletal Disorders, University of Pennsylvania, PA, 2016

Presentations made during the last year (* indicates presentations leading to publication)

*1. Local Administration of Anti-Collagen I Antibody Limits the Formation of Collagen-Rich Fibrotic Deposits in a Rabbit Model of Posttraumatic Joint Contracture. Steplewski, A., Fertala, J., Barlow, J., Beredjiklian, Pedro., Abboud, J., Wang, M., Namdari, S., Arnold, W., Michael R., Kostas, J., Hou, C., and Fertala, A.

Fibrosis: From Basic Mechanisms to Targeted Therapies; Keystone Symposia, 2016

INVENTIONS, PATENTS AND LICENSES

None.

REPORTABLE OUTCOMES

● Determining the *in vivo* utility of the antibody (ACA) we developed as an inhibitor of collagen fibril formation. As collagen fibril formation is the key step in posttraumatic fibrosis, blocking this process offers a therapeutic method to limit the consequences of the excessive formation of fibrotic scars. Since mechanisms of fibrotic scarring are similar in all tissues and organs, the method developed in this study to block posttraumatic joint contracture may be applicable in other fibrotic diseases.

● Our research demonstrated that intraarticular ACA application is a proper delivery method to limit joint contracture. This is important information that will lead to developing site-specific therapies with minimal off-target effects.

● We laid the foundation for the dosage regime of the ACA. Specifically, we demonstrated that applying this antibody earlier in the healing process limits the formation of excessive fibrotic tissue in joint capsules, thus improving joint function. This is important for designing therapies to limit posttraumatic joint stiffness.

● Development of PEG-modified ACA (P-ACA). We demonstrated that P-ACA may offer a prolonged dwelling time at the site of injury, thereby increasing the therapeutic activity of this variant.

● We demonstrated that poor organization of collagen-rich matrices formed in response to injury is a critical factor in developing posttraumatic joint stiffness. This observation defines the organization of collagen fibrils as a novel target to limit joint contracture.

● Our research demonstrated the presence of morphologically-unique collagen fibrils in fibrotic tissues formed in joints in response to injury. Unique characteristics of these fibrils seen under a polarizing microscope offer a powerful diagnostic tool to determine the extent, progress, or regress of arthrofibrosis.

OTHER ACHIEVEMENTS

This list may include degrees obtained that are supported by this award, development of cell lines, tissue or serum repositories, funding applied for based on work supported by this award, and employment or research opportunities applied for and/or received based on experience/training supported by this award.

Degrees Obtained

As a result of this study the following graduate degrees were obtained:

Bradley Snyder, M.S. "Investigation of the Long-Term Stability of a Chimeric Antibody (chIgG) that Binds the Terminal Telopeptide of the α2-chain of Human Collagen I", Thomas Jefferson University, 2016.

James Kostas, M.S. "Comaprison of the Efficiency of CHO Cell Culture Producing a Chimeric Antibody to the α-2 Telopeptide of Collagen I in a 5 L Packed-Bed Bioreactor Using CD-CHO and Ham's F-12 Media", Thomas Jefferson University, 2016.

Funding Applied for Based on Work Supported by This Award, and Employment or Research Opportunities Applied for and/or Received Based on Experience/Training Supported by this Award

As indicated earlier, according to the spirit of this study funded through the Translational Research Partnership Award mechanism, the PIs of this project have established the Scientific Consortium for

Arthrofibrotic Research (SCAR). First, we attracted junior orthopaedic surgeons interested in fibrotic diseases of musculoskeletal tissues to participate in the SCAR. Their involvement in this project included animal-based experiments, data analysis, preparation of manuscripts, *etc.* Subsequently, the participating surgeons applied for pilot grants to expand their interest in posttraumatic joint stiffness and other fibrotic diseases associated with their orthopaedic practice. All selected subjects are relevant to military and civilian populations.

The following list presents awards received within the last two years by surgeons directly participating in this project and as a result of collaboration within the SCAR:

Dr. Mark Wang. Dr. Wang is a practicing hand surgeon with research interest in arthrofibrosis, osteoporosis, and tendon repair. He received grants from the American Foundation for Surgery of the Hand and from the Orthopaedic Research and Education Foundation.

Dr. Antonia Chen. Dr. Chen is an active orthopaedic surgeon specializing in hip and knee replacements. Dr. Chen is funded by the Orthopaedic Research and Education Foundation to study remodeling of 3D architecture of scar tissue as a potential method to improve the range of motion of stiff joints.

Dr. Surena Namdari. Dr. Namdari is a practicing orthopaedic surgeon specializing in shoulder and elbow. His research interest involves arthrofibrosis of the shoulder. He received a grant from the Orthopaedic Research and Education Foundation.

Dr. Michael Rivlin. Dr. Rivlin is a hand surgeon with an interest in peripheral nerve injuries. His research includes studies on posttraumatic neural scarring and arthrofibrosis. With support of a grant from the American Foundation for Surgery of the Hand, he studied novel approaches to limit neural scarring and improve axonal growth.

REFERENCES

1. Chung HJ, Steplewski A, Chung KY, Uitto J, Fertala A (2008) Collagen fibril formation. A new target to limit fibrosis. J Biol Chem 283: 25879-25886.
2. Fertala J, Kostas J, Hou C, Steplewski A, Beredjiklian P, et al. (2014) Testing the anti-fibrotic potential of the single-chain Fv antibody against the alpha2 C-terminal telopeptide of collagen I. Connect Tissue Res 55: 115-122.
3. Fertala J, Steplewski A, Kostas J, Beredjiklian P, Williams G, et al. (2013) Engineering and characterization of the chimeric antibody that targets the C-terminal telopeptide of the alpha2 chain of human collagen I: a next step in the quest to reduce localized fibrosis. Connect Tissue Res 54: 187-196.
4. Steplewski A, Fertala A (2012) Inhibition of collagen fibril formation. Fibrogenesis Tissue Repair 5 Suppl 1: S29.
5. Steplewski A, Fertala J, Beredjiklian PK, Abboud JA, Wang ML, et al. (2016) Auxiliary proteins that facilitate formation of collagen-rich deposits in the posterior knee capsule in a rabbit-based joint contracture model. J Orthop Res 34: 489-501.
6. Steplewski A, Fertala J, Beredjiklian PK, Abboud JA, Wang ML, et al. (2016) Blocking collagen fibril formation in injured knees reduces flexion contracture in a rabbit model. J Orthop Res.
7. Hildebrand KA, Sutherland C, Zhang M (2004) Rabbit knee model of posttraumatic joint contractures: the long-term natural history of motion loss and myofibroblasts. J Orthop Res 22: 313-320.
8. Hildebrand KA, Zhang M, Germscheid NM, Wang C, Hart DA (2008) Cellular, matrix, and growth factor components of the joint capsule are modified early in the process of posttraumatic contracture formation in a rabbit model. Acta Orthop 79: 116-125.
9. Pasut G (2014) Pegylation of biological molecules and potential benefits: pharmacological properties of certolizumab pegol. BioDrugs 28 Suppl 1: S15-23.
10. Koussoroplis SJ, Paulissen G, Tyteca D, Goldansaz H, Todoroff J, et al. (2014) PEGylation of antibody fragments greatly increases their local residence time following delivery to the respiratory tract. J Control Release 187: 91-100.
11. Hildebrand KA, Holmberg M, Shrive N (2003) A new method to measure posttraumatic joint contractures in the rabbit knee. J Biomech Eng 125: 887-892.
12. Hildebrand KA, Holmberg M, Sutherland C, Shrive N. Posttraumaticjoint contractures: development of rabbit model; 2002 February 10; Dallas, TX. pp. 0068.
13. Monument MJ, Hart DA, Befus AD, Salo PT, Zhang M, et al. (2012) The mast cell stabilizer ketotifen reduces joint capsule fibrosis in a rabbit model of posttraumatic joint contractures. Inflamm Res 61: 285-292.
14. Fukui N, Tashiro T, Hiraoka H, Oda H, Nakamura K (2000) Adhesion formation can be reduced by the suppression of transforming growth factor-beta1 activity. J Orthop Res 18: 212-219.
15. Oikarinen A, Haapasaari KM, Sutinen M, Tasanen K (1998) The molecular basis of glucocorticoid-induced skin atrophy: topical glucocorticoid apparently decreases both collagen synthesis and the corresponding collagen mRNA level in human skin in vivo. Br J Dermatol 139: 1106-1110.
16. Taguchi T, Kubota M, Saito M, Hattori H, Kimura T, et al. (2015) Quantitative and Qualitative Change of Collagen of Achilles Tendons in Rats With Systemic Administration of Glucocorticoids. Foot Ankle Int.
17. Aoki M, Kato F, Mimatsu K, Iwata H (1997) Histologic changes in the intervertebral disc after intradiscal injections of methylprednisolone acetate in rabbits. Spine (Phila Pa 1976) 22: 127-131; discussion 132.
18. Gold EW, Fox OD, Weissfeld S, Curtiss PH (1978) Corticosteroid-induced avascular necrosis: an experimental study in rabbits. Clin Orthop Relat Res: 272-280.
19. Steplewski A, Fertala J, Beredjiklian PK, Abboud JA, Wang ML, et al. (2015) Auxiliary proteins that facilitate formation of collagen-rich deposits in the posterior knee capsule in a rabbit-based joint contracture model. J Orthop Res.
20. Keene DR, Sakai LY, Bachinger HP, Burgeson RE (1987) Type III collagen can be present on banded collagen fibrils regardless of fibril diameter. J Cell Biol 105: 2393-2402.

21. Chapman MA, Pichika R, Lieber RL (2015) Collagen crosslinking does not dictate stiffness in a transgenic mouse model of skeletal muscle fibrosis. J Biomech 48: 375-378.
22. Katsumoto TR, Violette SM, Sheppard D (2011) Blocking TGFbeta via Inhibition of the alphavbeta6 Integrin: A Possible Therapy for Systemic Sclerosis Interstitial Lung Disease. Int J Rheumatol 2011: 208219.
23. Rodriguez HM, Vaysberg M, Mikels A, McCauley S, Velayo AC, et al. (2010) Modulation of lysyl oxidase-like 2 enzymatic activity by an allosteric antibody inhibitor. J Biol Chem 285: 20964-20974.

APPENDICES

1. Auxiliary proteins that facilitate formation of collagen-rich deposits in the posterior knee capsule in a rabbit-based joint contracture model. Steplewski A, Fertala J, Beredjiklian PK, Abboud JA, Wang ML, Namdari S, Barlow J, Rivlin M, Arnold WV, Kostas J, Hou C, Fertala A (2016). J Orthop Res 34:489-501. PMID: 26241613

2. Blocking collagen fibril formation in injured knees reduces flexion contracture in a rabbit model. Steplewski A, Fertala J, Beredjiklian PK, Abboud JA, Wang ML, Namdari S, Barlow J, Rivlin M, Arnold WV, Kostas J, Hou C, Fertala A (2016). J Orthop Res. [Epub ahead of print] PMID: 27419365

3. Original SOW with a brief synopsis of outcomes.

Auxiliary Proteins That Facilitate Formation of Collagen-Rich Deposits in the Posterior Knee Capsule in a Rabbit-Based Joint Contracture Model

Andrzej Steplewski,[1] Jolanta Fertala,[1] Pedro K. Beredjiklian,[1,2] Joseph A. Abboud,[1,2] Mark L. Y. Wang,[1,2] Surena Namdari,[1,2] Jonathan Barlow,[1,2] Michael Rivlin,[1,2] William V. Arnold,[1,2] James Kostas,[1] Cheryl Hou,[1] Andrzej Fertala[1]

[1]Department of Orthopaedic Surgery, Sidney Kimmel Medical College, Thomas Jefferson University, Philadelphia, Pennsylvania, [2]Rothman Institute of Orthopaedics, Thomas Jefferson University Hospital, Philadelphia, Pennsylvania

Received 12 April 2015; accepted 31 July 2015
Published online 18 August 2015 in Wiley Online Library (wileyonlinelibrary.com). DOI 10.1002/jor.23007

ABSTRACT: Post-traumatic joint contracture is a debilitating consequence of trauma or surgical procedures. It is associated with fibrosis that develops regardless of the nature of initial trauma and results from complex biological processes associated with inflammation and cell activation. These processes accelerate production of structural elements of the extracellular matrix, particularly collagen fibrils. Although the increased production of collagenous proteins has been demonstrated in tissues of contracted joints, researchers have not yet determined the complex protein machinery needed for the biosynthesis of collagen molecules and for their assembly into fibrils. Consequently, the purpose of our study was to investigate key enzymes and protein chaperones needed to produce collagen-rich deposits. Using a rabbit model of joint contracture, our biochemical and histological assays indicated changes in the expression patterns of heat shock protein 47 and the α-subunit of prolyl 4-hydroxylase, key proteins in processing nascent collagen chains. Moreover, our study shows that the abnormal organization of collagen fibrils in the posterior capsules of injured knees, rather than excessive formation of fibril-stabilizing cross-links, may be a key reason for observed changes in the mechanical characteristics of injured joints. This result sheds new light on pathomechanisms of joint contraction, and identifies potentially attractive anti-fibrotic targets. © 2015 Orthopaedic Research Society. Published by Wiley Periodicals, Inc. J Orthop Res 34:489–501, 2016.

Keywords: joint contracture; posterior capsule; collagen; collagen fibrils; arthrofibrosis; knee

Post-traumatic joint contracture is a common orthopaedic complication manifested by reduced range of motion.[1] Regardless of the nature of the initial injury, development of joint contracture includes: (i) inflammation, (ii) proliferation of activated cells, and (iii) enhanced production of extracellular matrix macromolecules that form collagen-rich fibrotic tissue that may be deposited in the intraarticular and periarticular areas.[2,3] These deposits are created by complex intracellular processes of biosynthesis of individual collagen molecules and their extracellular self-assembly.[4]

Upregulation of collagen production in the capsules of injured joints has been associated with joint contracture.[5–8] In spite of the critical role that collagen plays in fibrosis, the accompanying changes in key auxiliary proteins needed for posttranslational processing of collagen chains in fibrosis are poorly understood.

Each collagen molecule is composed of three collagen α-chains that associate in the endoplasmic reticulum (ER) into a triple-helical structure.[9] In the fibril-forming collagens, each chain consists of approximately 300 uninterrupted repeats of –Gly–X–Y– triplets. These collagens are produced as procollagens in which the triple-helical domains are flanked by globular N-terminal and C-terminal propeptides (Fig. 1). Relatively short telopeptides separate the propeptides and the triple-helical domain. Post-translational modification of selected proline and lysine residues of nascent collagen α-chains is a key step in procollagen biosynthesis. In particular, proline and lysine residues present in the –Y– positions of the –Gly–X–Y– triplets are hydroxylated by prolyl-4-hydroxylase (P4H) and lysyl hydroxylase (LH), respectively.[9] P4H is a tetramer consisting of two catalytic α units (P4Hα) and two non-catalytic β units (P4Hβ). P4Hβ also serves as protein disulfide isomerase (PDI). In addition to catalyzing the formation of disulfide bonds in procollagens and other proteins, PDI also functions as a protein chaperone that prevents premature aggregation of procollagen chains.[4,10] 3-hydroxyproline residues have also been found in the –X– and –Y– positions of the –Gly–X–Y– triplets, and the extent of 3-hydroxylation varies among different collagen types.[11] In procollagen I, however, only one proline residue of the α1(I) chains is 3-hydroxylated.[12]

Mature procollagen chains fold into a triple-helical structure in a zipper-like fashion.[13] By transiently binding to the procollagen chains, chaperone proteins stabilize them and prevent their nonspecific aggregation. Three key chaperone proteins are involved in procollagen folding: (i) heat-shock protein 47 (HSP47), (ii) heat-shock 70 kDa-related luminal binding protein (BiP), and (iii) P4Hβ/PDI.[14]

Upon secretion to the extracellular space, enzymatic cleavage of propeptides triggers collagen fibril formation.[15] A group of enzymes cleaves the N-terminal propeptides, including a disintegrin and metallopro-

Conflict of interest: None.
Current address of Jonathan Barlow is Department of Orthopaedics, Ohio State University, Columbus, Ohio.
Grant sponsor: Department of Defense; Grant number: W81XWH-13-1-0393.
Correspondence to: Andrzej Fertala (T: +1-215-503-0113; F: 215-955-9159; E-mail: andrzej.fertala@jefferson.edu)

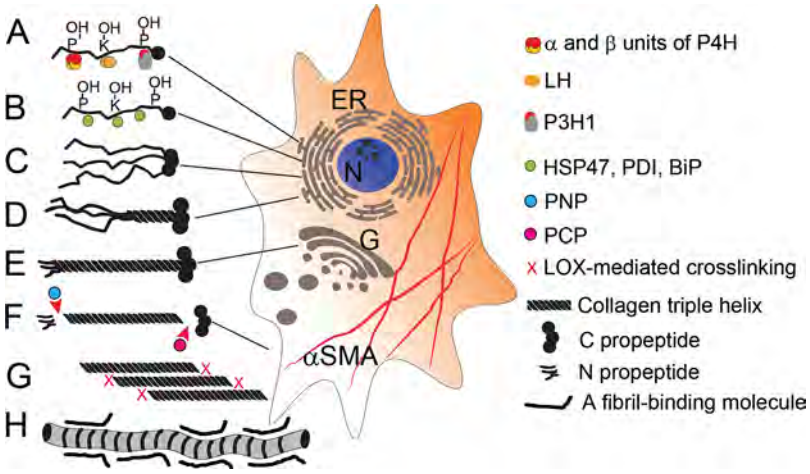

Figure 1. An illustration depicting intracellular and extracellular molecules and processes involved in the formation of collagen-rich deposits by fibrosis-associated cells. (A) Biosynthesis and post-translational modifications of individual procollagen α chains; during this process, selected proline and lysine residues are hydroxylated. Moreover, selected hydroxylysine residues may be further glycosylated. (B) The interaction of nascent procollagen chains with protein chaperones prevents nonspecific aggregation of individual chains. (C and D) Site-specific interaction of the C-terminal propeptides drives the selection of procollagen chains and initiates their folding into a triple-helical structure. (E) Intracellular translocation and secretion of procollagen molecules into the extracellular space. (F) Cleavage of the N and C propeptides by PNP and PCP, respectively. (G and H) Assembly of collagen molecules into fibrils in which formation of covalent cross-links stabilizes their structural integrity. ER, endoplasmic reticulum; G, Golgi apparatus; N, nucleus; αSMA, α smooth muscle actin.

tease with thrombospondin motifs (ADAMTS)-2, -3, and -14.[16] Enzymes belonging to the tolloid family of zinc metalloproteinases cleave the C-terminal propeptides of fibrillar procollagens, of which procollagen C proteinase (PCP) plays a pivotal role.[17] Procollagen propeptides may also be processed by meprins and mast cells chymase, enzymes whose activity increases during inflammation and fibrosis.[18,19]

Collagen fibrils form the main architecture of all elements of the musculoskeletal system. They self-assemble in a process driven by site-specific interactions among individual collagen molecules.[20] The covalent intramolecular and intermolecular cross-links stabilize the collagen fibrils. The hydroxylation of selected lysine residues and the catalytic activity of lysyl oxidase (LOX) facilitate the formation of collagen cross-links[4]

Collagen III co-assembles with collagen I to form heterotypic fibrils.[21] Studies indicate that collagen III regulates the diameter of the fibrils.[21] Researchers also showed that alterations of the collagen III:collagen I ratio may be responsible for changes in the morphology of collagen fibrils seen, for example, in Achilles tendinopathies and in the fibrotic skin of lipodermatosclerosis.[22,23]

In order to learn more about collagen formation after joint trauma, we analyzed the formation of collagen-rich deposits in the posterior knee capsules in a rabbit-based knee injury model. Since the role of the auxiliary protein machinery in the excessive production of collagen molecules is not well understood, we focused our efforts on characterizing contracture-associated profiles of its key elements.

MATERIALS AND METHODS

Joint Contracture Model

Animal studies were approved by our Institutional Animal Care and Use Committee (IACUC). We employed 10 female New Zealand White rabbits, 8- to 12-months old (Covance, Inc., Princeton, NJ) to study key aspects of the formation of collagen-rich deposits in a model of posttraumatic joint contracture. The clinical relevance of the model we selected is well established and its core design has been adapted by a number of independent research groups.[2,7,24–32] This model was employed as a part of an ongoing study that utilizes subcutaneous pumps to deliver compounds of interest to an injured rabbit. Here, we focused on the fibrotic processes in a group of untreated rabbits in which only phosphate buffered saline (PBS) was applied. Post-traumatic contracture was generated, as described, by simulating an intra-articular fracture (using drill holes) and a capsular injury (with a hyperextension injury) in the right knee and maintaining it in a flexed position using Kirschner (K)-wires for 8 weeks.[26,27] The contralateral uninjured limb served as control. Following the surgery, the rabbits were allowed unrestricted cage activity. After 8 weeks of immobilization, the K-wires were removed, and the rabbits were allowed an additional 2 weeks of unrestricted cage activity. After a 2-week recovery period the rabbits were euthanized.

Joint Angle Measurements

Following euthanasia, the legs of the rabbits were processed to remove the bulk of skin and muscle tissue.[6] Then, the tibia and the femur were transected about 6 cm from the knee joint. Subsequently, the ends of the bones were potted in polycarbonate cylinders with the use of polymethyl methacrylate and acrylic copolymer (PMMA, Flexbar Machine Corp., Islandia, NY) (Fig. 2). Such processing ensured the secure placement of bones in the grips of a custom-made flexion-measuring device (Test Resources, Inc., Shakopee, MN); the device was designed with key technical parameters described by Hildebrand et al.[6,27] Apart from the gripping mechanism, this instrument included a torsional actuator/motor, a torque cell, and an angular displacement transducer (Fig. 2). After securing the analyzed limb in the grips, the femur and tibia were positioned at a right angle, and then the instrument was set to 0°.[6,27] Subsequently, applying the rate of loading set to 40°/min, an extension torque was applied to 0.2 Nm, and the joint extension was recorded.[6,27] Values near 90° indicated maximum extension, while angles larger than 90° represented hyperextension. Flexion contracture was expressed as the difference between the angles of the control limb and the injured limb recorded at 0.2 Nm.[6,27] Thus, a larger difference between the maximum extension angles of control and operated limbs indicates a more severe joint contracture.

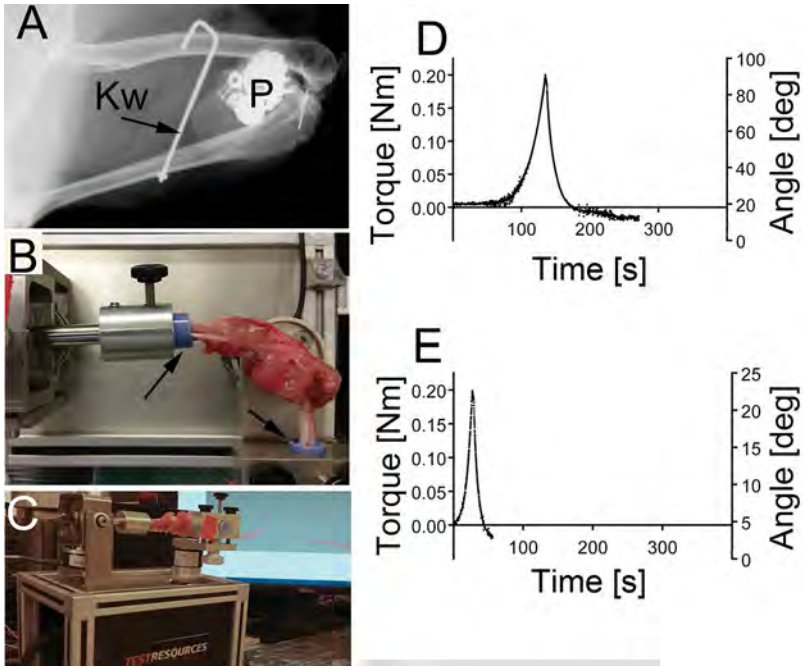

Figure 2. A rabbit-based model of joint contracture. (A) An X-ray image of the operated knee. A k-wire (Kw) and a pump (P) delivering PBS are depicted. (B and C) Views of a system employed to measure the flexion contractures of analyzed knees. In B, arrows indicate femur and tibia whose ends are potted into tubes with the use of a PMMA. (D and E) Representative data from measurements of the flexion contractures of the healthy (D) and the contracted (E) knees at 0.2 Nm torque. Ascending and descending parts of the depicted graphs represent extension and flexion behavior of the analyzed knees.

Tissue Collection

As the fibrosis of the posterior joint capsule (PC) is the main cause of contracture in the rabbit model employed here, following the flexion contracture measurements, the PCs were dissected from the limbs, as described (Fig. 3).[6,29,33]

Total Collagen Content

Tissue samples were frozen in liquid nitrogen and then pulverized in a stainless steel mortar. The samples were treated with a 3:1 mixture of chloroform and methanol to extract lipids and then lyophilized and weighed. Next, a hydroxyproline assay was used to determine the collagen content per unit of dry mass.[34]

Collagen III: Collagen I Ratio

First, the acid-soluble collagen fraction was extracted from collected tissues with the use of 0.5 M acetic acid. Subsequently, the pepsin-soluble fraction was obtained with the use of pepsin (Sigma–Aldrich, St Louis, MO) prepared in 0.5 M acetic acid at a final concentration of 1 mg/ml. Employing the Sircol Collagen Assay Kit (Biocolor Ltd., Carrickfergus, UK), the concentration of extracted collagen was determined, and then the samples were prepared for electrophoresis. To separate the monomeric forms of collagen I chains from collagen III monomers, we employed an interrupted electrophoresis method that takes advantage of the fact that, unlike the collagen I α-chains, the collagen III α-chains are bound together via reducible disulfide bonds.[35] In brief, heat-denatured collagen samples were initially run in a 6% polyacrylamide gel in non-reducing conditions. After 15 min, a 10-μl aliquot of 0.5 M DTT was added to each well and then electrophoresis continued. Recombinant collagen III served as a marker (Fibrogen, Inc., San Francisco, CA). Pixel intensities of protein bands corresponding to the α1(III) and the α2(I) chains were measured by densitometry (EZQuant Ltd., Tel-Aviv, Israel), and then collagen III:

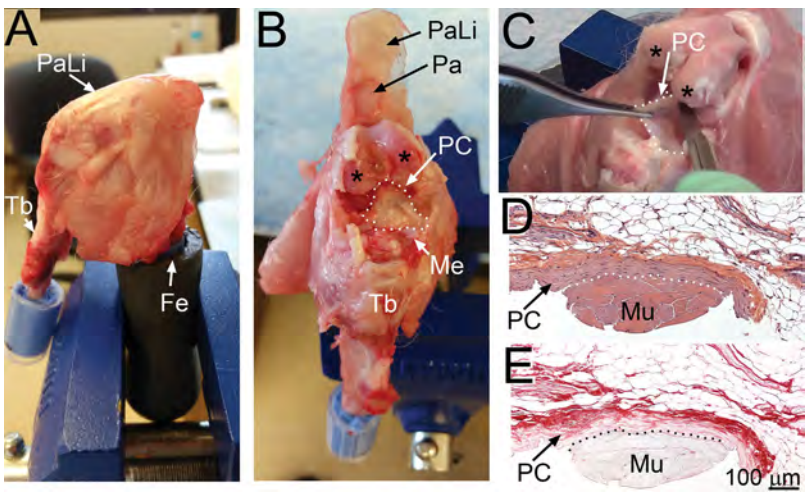

Figure 3. Dissecting the PC from a rabbit's knee. (A) A medial aspect of the intact right knee. (B) Anterior femoropatellar compartment of the analyzed knee. In panel B the anterior portion of periarticular tissues has been dissected to expose the PC, delineated by the dotted line. (C) Dissecting the exposed PC, delineated by the dotted line; patellar ligament has been removed. (D and E) Histological staining of the consecutive cross-sections of dissected PC; in these panels the underlying muscle tissue has been purposely preserved to indicate the position of the PC. (D) H&E; staining of the cross section of the PC. (E) Collagen-specific picrosirius staining of the PC observed in non-polarized light; in this panel the collagen-rich PC is clearly indicated by red staining. In D and E, the net-like layer of fatty subintima of the synovial membrane is clearly apparent. The dotted lines in D and E mark the border between the PC and underlying muscle tissue. PaLi; patellar ligament, Tb; tibia, Fe; femur, Pa; patella, Me; meniscus, Mu; muscle tissue. Asterisks indicate the femoral condyles.

collagen I ratios were calculated. The ratios of cross-linked α-chains forming the β and the γ oligomers to the monomeric α-chains of the collagen pool extracted from PCs were also analyzed with the use of densitometry.

Microscopy of Collagen Fibrils

Three-micrometer thick sections of paraffin-embedded PCs were stained with H&E and with collagen-specific picrosirius red (Polysciences, Inc., Warrington, PA). The latter staining technique combined with polarized-light microscopy makes it possible to describe the thickness, the organization, and to a certain degree, the collagen type-specific composition of the fibrils.[36] As the thickness of fibers increases, their birefringence color changes from green to yellow to orange to red, that is, from shorter to longer wavelengths.[36–38] Employing a polarizing microscope (Eclipse LV100POL, Nikon Inc., Melville, NY) and the NIS Elements software (Nikon Inc., Melville, NY), we determined the percentages of differently colored collagen fibrils, as described.[39] Applying the built-in settings of the NIS Elements software, three main groups of colors were defined: (i) green, (ii) yellow, and (iii) orange-red. The entire image was analyzed, and then the areas occupied by pixels corresponding to the defined colors were determined. Considering the sum of all pixels to be 100%, the percentage of each color group in the analyzed samples was calculated. A minimum of three histological sections for control and for injured PCs were analyzed per each rabbit. The organization of collagen fibrils, expressed as theoretical anisotropy score, was evaluated by employing the ImageJ software that included the FibrilTool plug-in.[40,41]

Immunohistology

The main focus of the quantitative immunohistological assays done with paraffin-embedded samples was to analyze the changes in key proteins associated with the biosynthesis of collagen deposits formed in analyzed PCs. Immunohistology was also employed to visualize selected markers of the fibrotic process. Table 1 lists all antibodies employed in our study and indicates the experimental conditions applied. In addition, all samples were exposed to 4′,6-diamidino-2-phenylindole (DAPI) to visualize the nuclei.

In all assays, the specimens from injured and healthy PCs were processed simultaneously to ensure identical conditions for immunostaining. A fluorescence microscope (Eclipse E600, Nikon, Inc.) equipped with a digital camera (DS-Qi1Mc, Nikon, Inc.) was employed. Adopting a strict protocol for the quantitation of the pixel intensity, values assured the accuracy of measurements of the immunostained specimens.[42] For quantitative assays, a minimum of three sections of the PCs isolated from the injured and control knees were employed to measure each parameter. The mean pixel intensity values derived from measurements of immunostained cells observed in separate viewing areas of analyzed samples were calculated and presented individually as scatter plots. These values were compared to control set at 100%.

Statistical Analyses

For each parameter analyzed in a PC isolated from an injured knee ($n = 10$), a corresponding parameter for the contralateral PC ($n = 10$) served as control. For histology-based assays, data from multiple sections of a capsule were analyzed. The statistical significance of differences between the control group mean and the experimental group mean has been evaluated with the use of the Student's *t*-test (GraphPad Prism v. 5.03, GraphPad Software, Inc., La Jolla, CA).

RESULTS

Joint Contracture Model

Consistent with earlier reports, all surgically operated knees developed flexion contracture.[6,27] The mean value for the flexion contracture, defined as the difference between the flexion angles at 0.2 Nm measured for control (92.3°, ± 10.4 SD) and for operated limbs (22.4°, ± 7.7 SD), was 69.9° (± 7.5 SD) (Fig. 2D and E).

Observations of transverse sections of uninjured PCs indicate that this structure is built by the layer of a fibrous, compact connective tissue (Fig. 4A) and the adjoining net-like layer of fatty subintima of the synovial membrane (Fig. 4B). Compared to the control, the fibrous layers of the capsules isolated from the injured knees were noticeably thicker and their apparent cellularity has increased (Fig. 4A and C). In addition to the fibrous layer of the capsule, accumulation of atypical tissue deposits within subintima was also clearly apparent in the specimens from the injured knees (Fig. 4B and D).

Microscopic Assays of Collagen Fibrils

Picrosirius red staining (Fig. 4E, F, H, and I) revealed changes in the percentages of green, yellow, and orange-red sub-populations of fibrils. Specifically, in comparison to 22.1% (± 7.4 SD) of green-colored fibrils seen in the control, the percentage of corresponding fibrils increased to 32.5% (± 9.4 SD) in injured PCs. This increase was accompanied by a decrease in the percentages of the yellow-colored and the orange-red-colored fibrils (Fig. 4G). We also demonstrated changes in the organization of collagen fibrils. Specifically, observations of longitudinal sections of the PCs revealed a defined, fishbone-like pattern, a result of crimps in parallely-organized fibrils (Fig. 4H). In contrast, such an arrangement was not readily apparent in the fibrotic capsules (Fig. 4I). Instead, the fibrils were distributed more randomly through the entire area of the analyzed PCs. The mean value for the theoretical anisotropy score calculated for the fibrils seen in the healthy capsules was 0.26 (± 0.07 SD) while the corresponding value for the injured capsules was 0.09 (± 0.04 SD).

Total Collagen Content

Assays of hydroxyproline content indicate a relatively high amount of collagen in the PCs isolated from the healthy and contracted knees. In the healthy knees, the total collagen contributed 0.92 (± 0.14 SD) mg per 1 mg of dry mass of the PC. Similarly, in the capsule from the contracted knee, collagenous proteins contributed 0.88 (± 0.15 SD) mg per 1 mg of dry mass. There was no statistically significant difference between these two values ($p = 0.4$).

Table 1. Primary and Secondary Antibodies Used to Detect Selected Targets

Target	Antigen Recovery: Buffer Incubation Conditions	Primary Antibody: Manufacturer Catalog Number Dilution; Incubation Conditions	Secondary Antibody: Manufacturer Catalog Number Dilution; Incubation Time; Temperature
CTGF	Citrate buffer 70°C; 2 h	Santa Cruz Biotechnology, Dallas, TX sc-14939 1:200; 2 h; RT	Thermo Fisher Scientific, Rockford, IL anti-Goat-Alexa Fluor© 594; A11058 1:1,000; 1 h; RT
P4Hα	Citrate buffer 70°C; 2 h	LifeSpan Biosciences, Inc., Seattle, WA LS-B3291 1:200, 1 h; RT	Molecular Probes anti-Goat-Alexa Fluor© 594; A11058 1:1,000; 1 h; RT
P4Hβ	Citrate buffer 70°C; 2 h	LifeSpan Biosciences, Inc., Seattle, WA LS-B3137 1:200; 1 h; RT	Thermo Fisher Scientific, Rockford, IL anti-Mouse-Alexa Fluor© 594; A11032 1:1,000; 1 h; RT
HSP47	Citrate buffer 70°C; 2 h	Santa Cruz Biotechnology, Dallas, TX sc-5293 1:200; 2 h; RT	Thermo Fisher Scientific, Rockford, IL anti-Mouse-Alexa Fluor© 594; A11032 1:1,000; 1 h; RT
BiP	Citrate buffer 70°C; 2 h	LifeSpan Biosciences, Inc., Seattle, WA LS-B4157 1:200; 1 h; RT	Thermo Fisher Scientific, Rockford, IL anti-Mouse-Alexa Fluor© 594; A11032 1:1,000; 1 h; RT
Mast cells chymase	No antigen retrieval step	Acris Antibodies, Inc., San Diego, CA SM1536P 1:2,000, 1 h; RT	Thermo Fisher Scientific, Rockford, IL anti-Mouse-Alexa Fluor© 594; A11032 1:1,000, 1 h; RT
LOX	Citrate buffer 70°C; 2 h	Santa Cruz Biotechnology, Dallas, TX sc-48723 1:500; 1 h; RT	Thermo Fisher Scientific, Rockford, IL anti-Goat-Alexa Fluor© 594; A11058 1:1,000; 1 h; RT
LH1	Citrate buffer 70°C; 2 h	Santa Cruz Biotechnology, Dallas, TX sc-271640 1:500; 1 h; RT	Thermo Fisher Scientific, Rockford, IL anti-Mouse-Alexa Fluor© 594, A11032 1:1,000; 1 h; RT
α-SMA	0.1% trypsin in 5 mM $CaCl_2$, 37°C; 30 min	Abcam, Cambridge, MA ab-7817 1:200; 2 h; RT	Thermo Fisher Scientific, Rockford, IL anti-Mouse-Alexa Fluor© 594; A11032 1:1,000; 1 h; RT
Laminin β2	0.1% trypsin in 5 mM $CaCl_2$, 37°C; 30 min	EMD Millipore, Billerica, MA 05-206 1:200; 2 h; RT	Thermo Fisher Scientific, Rockford, IL anti-Rat-Alexa Fluor© 488; A11006 1:1,000; 1 h; RT

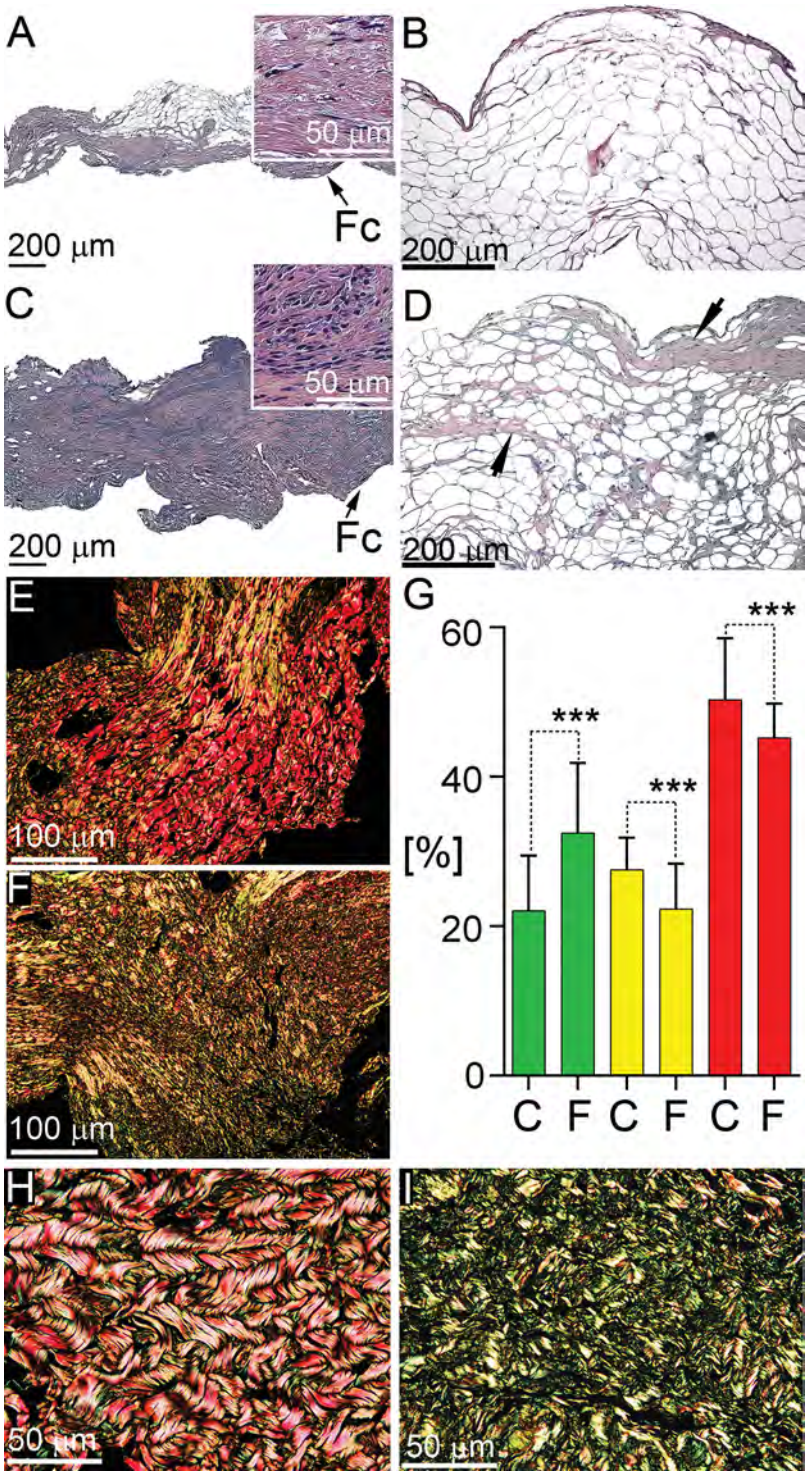

Figure 4. Microscopic assays of PCs from control and injured knees. (A and B) H&E staining of cross-sections of a fibrous capsule (Fc) (A) and subintima (B) of control PC. (C and D) H&E staining of cross-sections a fibrous capsule (C) and subintima (D) of injured PC. The inserts presented in A and C indicate the apparent difference in the overall cellularity of the capsules. In D, arrows indicate fibrotic deposits within subintima. (E and F) Birefringence of picrosirius-stained cross-sections of control (E) and injured (F) PCs. (G) Graphic representation of results of measurements of percent areas occupied by defined birefringence colors seen in control (C) and fibrotic (F) PCs ($^{***}p < 0.001$). (H and I) longitudinal sections of the control (H) and injured (I) PCs stained with picrosirius. In H, the fishbone-like pattern of the organization of collagen fibrils is clearly apparent. In contrast, collagen fibrils seen in I are randomly distributed.

Electrophoretic Assays of Collagen

Densitometry assays show that the mean collagen III:collagen I ratio for control knee capsules is 0.78 (± 0.18 SD), while the corresponding value for the injured capsules is 0.98 (± 0.21 SD), a statistically significant difference ($p = 0.01$) (Fig. 5B). In contrast, as indicated by a similar $\beta\gamma/\alpha-$chains ratios, there was no difference between the relative amounts of the cross-linked chains present in the pools of the pepsin-extracted collagens from control and experimental groups ($p = 0.7$) (Fig. 5C). As the amount of acid-extracted collagen was low (not shown), this collagen fraction was not further analyzed. Moreover, as collagen chains from control and fibrotic PCs co-migrated in the electrophoretic field, no overmodification, that is, overhydroxylation and overglycosylation, of collagen chains from fibrotic tissues was present.

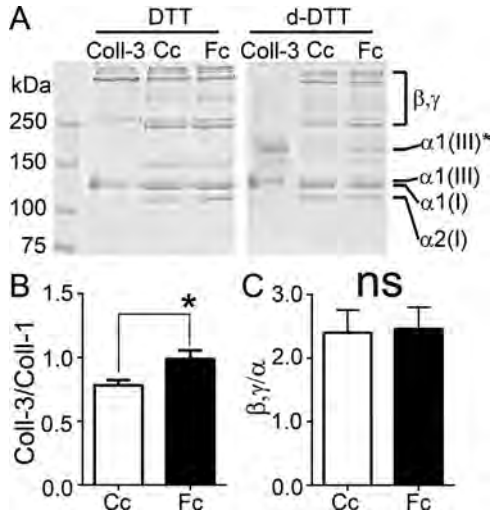

Figure 5. Electrophoretic assays of collagenous proteins extracted from control capsule (Cc) and fibrotic capsule (Fc). (A) Patterns of migration of collagen I and collagen III chains separated in standard reducing conditions (DTT) and in delayed-reduction conditions (d-DTT) of electrophoresis. (B and A) Graphic representation of the results of assays of collagen III: collagen I ratios ($^*p < 0.05$). (C and A) Graphic depiction of the results of measurements of βγ:α ratios; no statistically significant difference was observed. Coll-3; collagen III marker, α1(I), α2(I), α1(III); specific chains of collagen I and collagen III, respectively; α1(III)*; collagen III chains separated with the use of delayed-reduction conditions; β, γ; β and the γ oligomers formed consisting of cross-linked collagen α chains.

Selected Markers of Fibrosis

In addition to the changes seen in the collagen-rich extracellular matrix, the fibrotic process in the injured PCs was demonstrated by qualitative immunohistological assays (Fig. 6). First, the α smooth muscle actin (αSMA)-positive staining in fibroblastic cells seen in the fibrous (Fig. 6A) layer of fibrotic PCs was clearly apparent. These cells were readily distinguishable from the αSMA-positive and laminin β2-positive smooth muscle cells present in blood vessels (Fig. 6B). Control capsules were largely negative for the αSMA-specific staining (not shown). Second, we demonstrated that, unlike in the control, cells present in the injured capsules stain positively for connective tissue growth factor (CTGF) (Fig. 6C and D). Third, the chymase-specific staining demonstrated the presence of mast cells in the injured but not the control PCs (Fig. 6E and F). No immunostaining was detected in the negative controls in which the primary antibodies were omitted (not shown).

Proteins Associated With Collagen Production

Measurements of the pixel intensities of fluorescence signals associated with the analyzed proteins revealed their expression profiles in cells present in the injured PCs (Figs. 7–9). Specifically, a threefold increase was observed for the catalytic P4Hα subunit and for HSP47 (Figs. 7, 8, and 9). The increase in the P4Hβ/PDI subunit was 1.5-fold, while relative to the control, the amount of the LOX and BiP increased 1.8-fold and 1.2-fold, respectively (Figs. 7, 8, and 9). There was no statistically significant change in the relative amount of LH1 in the analyzed cells (Figs. 7 and 9). Background-levels of fluorescence signals in the negative controls validate the specificity of immunostaining in the positively-stained cells (not shown).

DISCUSSION

In this study, we focused on fibrotic changes taking place in the PC of rabbits' knees. Although intraarticular fibrotic adhesions may be formed as a result of trauma, Hildebrand et al. have demonstrated that fibrosis of the PC is the main cause of joint contracture in the rabbit model employed here.[6,29] Since the biosynthesis of extracellular collagen-rich deposits requires the involvement of auxiliary protein chaperones and collagen-modifying enzymes, the increase in collagen content seen in the fibrotic joint capsules cannot be explained simply by the increased production of collagen chains. Consequently, we studied critical elements of a biological system that allow efficient processing of collagen molecules produced in response to joint injury. The development of severe flexion contracture, increased cellularity, and the presence of fibrosis-specific αSMA-positive, CTGF-positive, and chymase-positive cells in the injured PCs validate the biological relevance of the employed model.[2,7,43,44] Our assays of the total collagen content indicate that the healthy and fibrotic PCs are collagen-rich tissues. Assays of the injured capsules demonstrated that at the end of a 2-week recovery period, there was a significant increase in the content of green-colored fibrils. This result suggests that the population of new fibrotic tissue formed in the injured capsules includes relatively thin fibrils. These collagen fibrils could represent a pool of fibrils undergoing lateral aggregation into large-diameter fibers similar to those seen in the control. These fibrils, however, could also be the end-product of the fibril formation process. Considering such a possibility, we propose that collagen III may act as the fibril diameter-limiting factor. This notion is supported by earlier observations that collagen III limits fibril growth through co-polymerization with collagen I.[21] Moreover, researchers studying the decrease in the diameter of fibrils seen in tendinopathies have suggested that an increased collagen III:collagen I ratio contributed to such a change.[23] A similar increase in the collagen III: collagen I ratio was also associated with a decrease in the diameter of collagen fibrils observed in the fibrotic skin of lipodermatosclerosis.[22]

To further elucidate mechanisms that enable efficient processing of the increased amount of collagen in fibrotic capsules, we analyzed collagen-modifying enzymes and protein chaperones. In the first category of molecules, the most prominent increase was noticed in catalytic P4Hα and non-catalytic P4Hβ/PDI subunits of P4H. Although the P4Hβ unit does not directly participate in the catalytic activity of P4H, its

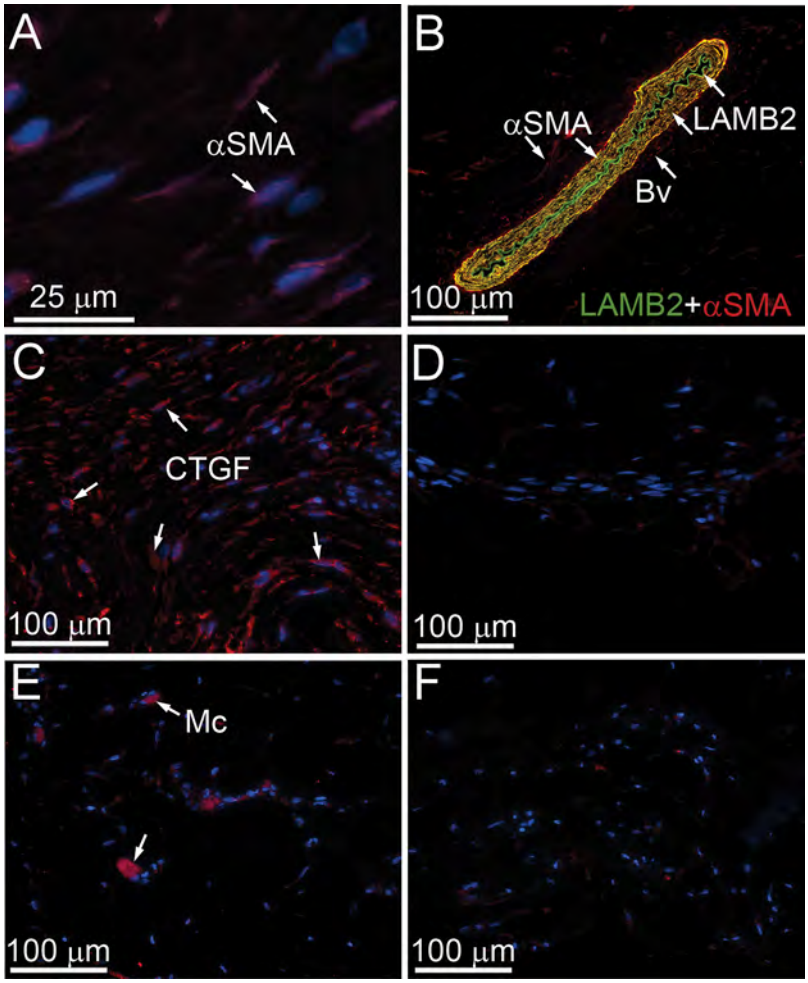

Figure 6. Immunostaining assays of selected markers of fibrosis in the cross-sections of analyzed PCs. (A)Visualization of αSMA (arrows) in cells present in the injured PC. (B) Depiction of a blood vessel (Bv) that stains positively for αSMA and β2 chain of laminin (LAMB2). This picture clearly distinguishes αSMA-positive fibroblastic cells from the αSMA-staining seen in Bv (arrows). (C and D) Staining of fibrotic (C) and control (D) PCs for CTGF. (E and F) Staining of fibrotic (E) and control (F) PCs for mast cells (Mc) chymase. Arrows indicate the chymase-positive cells clearly apparent in panel E.

presence is needed to anchor this enzyme in the ER and to maintain the catalytically active structure of its P4Hα subunit. As the presence of nascent collagen chains is a prerequisite for the assembly of stable αα/ββ tetramers, we believe that increased production of collagen chains promotes the association of individual subunits into active P4H.[45] Such a system provides an effective regulatory mechanism for P4H, thereby ensuring proper post-translational modifications of collagen chains and their folding into thermostable molecules.

In contrast to the increased expression of P4H in fibrotic PCs, the expression of LH1, an enzyme that catalyzes the hydroxylation of certain lysine residues in the triple-helical domain of collagens, did not change in comparison to the control. This result is consistent with a study of the keloid-derived fibroblasts in which researchers demonstrated that expression of the LH1 variant at the mRNA level was similar to that in control cells.[46] Moreover, no statistically significant LH1 expression changes were seen in fibroblasts derived from Dupuytren's lesions.[46] Normal expression of LH1 was also consistent with the lack of apparent overmodification of collagen chains, a process dependent on the overhydroxylation of lysine residues. These results are also consistent with studies reported by Akeson et al. who reported no changes in the hydroxylysine/lysine ratio in periarticular tissues surrounding contracted rabbits' joints.[24] Based on our studies, however, we cannot exclude the possibility of an increased production of LH2, a telopeptide lysyl hydroxylase variant whose expression changes in certain fibrotic tissues.[46]

In this study, a steady amount of LH1 was accompanied by a 1.8-fold increase in LOX production. LOX plays a critical role in maintaining the integrity of collagen-rich tissues as the enzyme catalyzing the formation of allysine and hydroxyallysine. Allysine and hydroxyallysine formation are key steps in the formation of the covalent cross-links between fibril-incorporated collagen molecules.[47] The expression of LOX, however, varies in different fibrotic tissues. For instance, mRNA-based studies of the expression of LOX in cells derived from keloids, hypertrophic scars, hepatic stellate cells, and fibroblasts derived from Dupuytren's lesions have demonstrated that a significant, twofold increase of LOX expression was seen only in the last group of cells.[46] Based on the electrophoretic

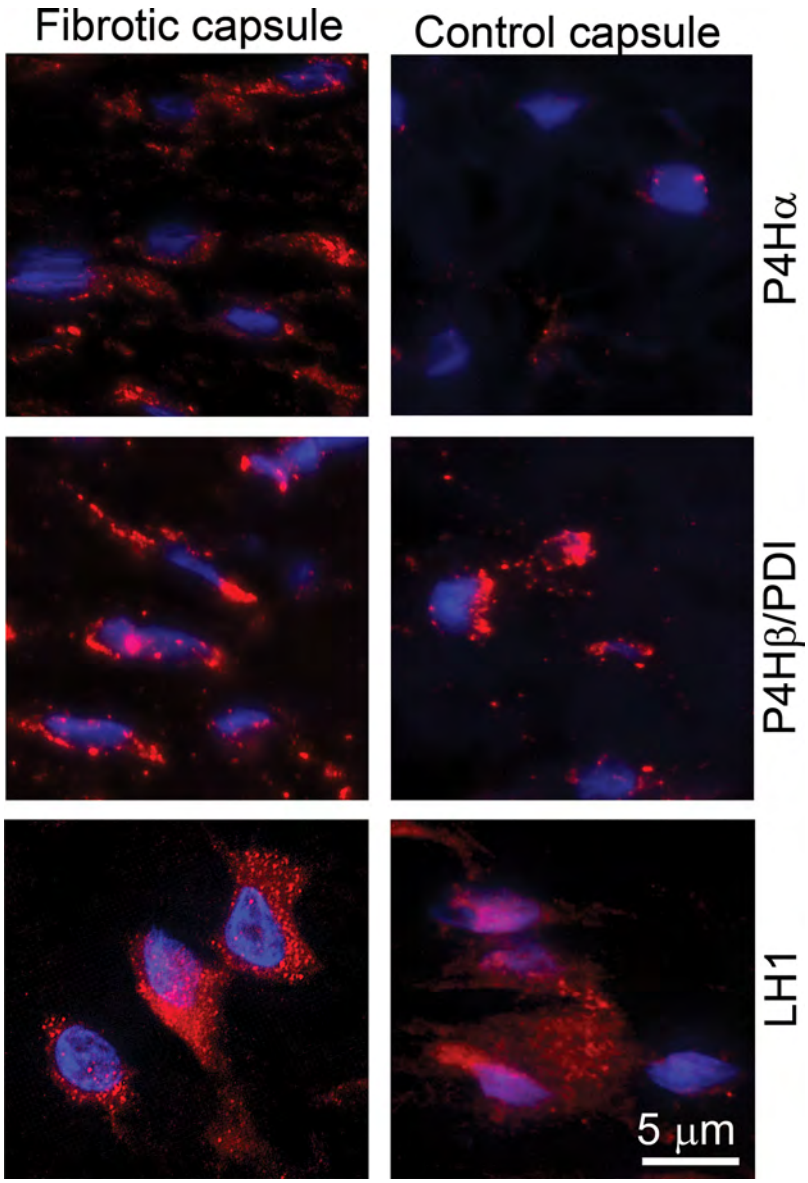

Figure 7. Immunostaining of cross-sections of fibrotic and control PCs for P4Hα, P4Hβ/PDI, and LH1.

measurements of the cross-linked versus non-cross-linked collagen chains, we determined that the relative amounts of the cross-linked fractions in the injured and healthy capsules were similar. As in our assays, we employed the pepsin-soluble fraction of the collagen pool, we cannot exclude the possibility of changes in the quality and the quantity of cross-links present in the non-soluble fraction. Akeson et al. have demonstrated an increase in the quantity of cross-links in collagen isolated from periarticular tissues isolated from immobilized rabbits' knees. Unlike our studies in which we specifically isolated the PCs of affected joints, Akeson et al. isolated periarticular tissues that included fascia, ligaments, and capsule. Employing these tissues, the authors demonstrated that the major cross-links that increased are hydroxylysinonorleucine, dihydroxylysinonorleucine, and histidinohydroxymerodesmosine types.[48]

Our microscopic assays revealed alterations of fibril organization seen in longitudinal sections of the injured joint capsules. Specifically, we demonstrated that the dominant fishbone-like pattern of organization of the fibrils seen in control capsules changes to a random distribution of fibrils synthesized during fibrosis. Such a random orientation of the fibrils could result from prolonged inactivity of the injured joints and ongoing tissue remodeling that includes degeneration of collagen fibrils. The importance of the mechanical forces for the tissue-specific alignment of fibrils is a well-recognized phenomenon. In 1951, MacConaill concluded that "as iron filings are to a magnetic field so are collagen fibrils to a tension field."[49] Since then, the role of mechanical forces in fibril organization was demonstrated in connective tissues such as meniscus, tendon, ligament, and others.[50,51] Researchers have demonstrated that the force-fibril orientation relation-

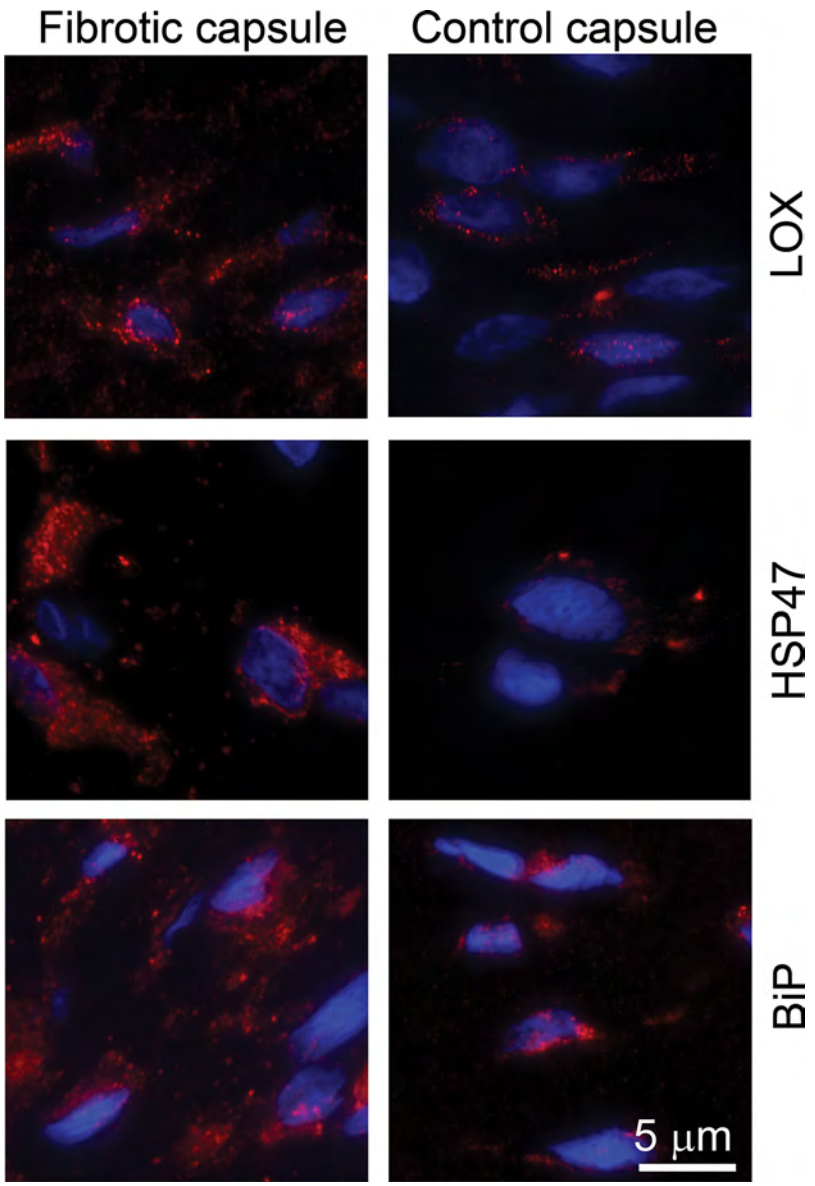

Figure 8. Immunostaining of cross-sections of fibrotic and control PCs for LOX, HSP47, and BiP.

ship is a key parameter that defines micro-structural properties in all of those tissues. Based on these considerations, we believe that abnormal fibril orientation rather than excessive cross-link formation contributes to altered mechanical properties of injured capsules. In support of this postulation is a recent study of muscle fibrosis reported by Chapman et al. In this study, researchers have demonstrated that the stiffness of skeletal muscles of experimental mice could not be explained by increased collagen cross-linking. Indeed, the authors suggested changes in collagen fibril orientation as a possible decisive factor in developing the muscle stiffness.[52] Similar suggestions on the potential role of aberrations of the micro-architecture of collagen fibrils in joint contracture were made in early studies carried out with the use of a rabbit-based model.[25]

To further elucidate the mechanisms that facilitate the excessive deposition of collagen-rich matrix in PCs, we analyzed protein chaperones that play a critical role in the intracellular processes of the biosynthesis of collagen molecules. Among the chaperones analyzed (PDI, BiP, and HSP47), the expression of HSP47 increased most significantly.

Our demonstration of the increased production of HSP47, a key collagen-specific chaperone, indicates that this protein plays a critical role in maintaining the proper folding of collagen molecules in the fibrotic PC. Numerous reports of increased HSP47 production in fibrotic tissues that include skin, cornea, liver, and tendon adhesions further highlight the critical role of this chaperone in maintaining the fibrotic process.[53] Thus, the increased production of HSP47 and, to a lesser extent, other chaperone proteins seen in our study may represent a common defense mechanism protecting fibrotic cells from ER stress-associated apoptosis. Indeed, experimental deletion of HSP47 in hepatic stellate cells causes excessive intracellular

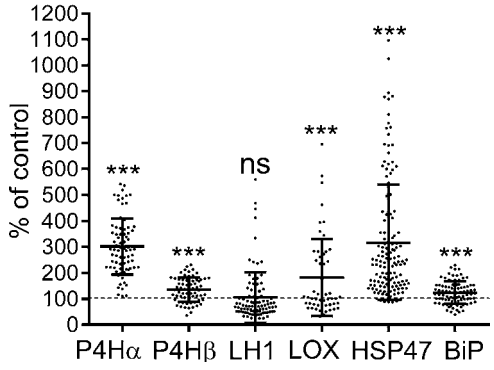

Figure 9. Graphic representation of relative intracellular content of P4Hα, P4Hβ/PDI, LH1, LOX, HSP47, and BiP. The mean values (± SD) seen in scatter plots represent changes in indicated proteins present in cells seen in the injured PCs. Each point in the plot represents the mean value calculated for the group of cells seen in the particular viewing area of analyzed specimens. The dotted line, set at 100%, represents the corresponding values calculated for control cells observed in non-injured PCs (***$p < 0.001$, ns; not significant).

accumulation of misfolded collagen molecules which leads to ER stress and cell death.[54]

The processing of the N-terminal and the C-terminal propeptides is prerequisite for collagen fibril formation. Studies in induced liver fibrosis demonstrated that the activity of PCP increases due to upregulation of the expression of procollagen C–proteinase enhancer protein (PCPE).[55] Similarly, Hultström et al. demonstrated a significant increase in the expression of PNP in a rat model of renal fibrosis and clearly associated this increase with excessive accumulation of collagen-rich deposits.[56] These data suggest that upregulation of PNP and PCP is needed in fibrosis to ensure effective conversion of procollagen into fibril-forming collagen molecules. Although detailed assays of procollagen processing are beyond the scope of this study, it is worth noting the potential role of the mast cells chymase in the removal of procollagen propeptides. As chymase processes both procollagen propeptides in a way that enables collagen molecules to assemble into proper fibrils, we cannot exclude the possibility that this enzyme may contribute to excessive production of fibrotic deposits seen in PCs of contracted joints.[19]

Due to inherent limitations of our animal-based model of joint contracture, such as anatomical differences and specific injury type, results of our study may not fully represent human pathology associated with joint contracture. By following the fundamental steps in the path of fibrillar collagens, however, our study sheds new light on the fundamental mechanisms that control excessive production of fibrotic deposits. Specifically, our data indicate that increased production of the P4H subunits and upregulation of the biosynthesis of HSP47 are critical for the intracellular processing of excessively produced collagen molecules. Moreover, the data emphasize a potential role of mast cells in extracellular processing of procollagens, shedding new light on a possible role of these cells in propagating fibrosis. In addition, detailed assays of newly formed collagen fibrils in injured joint capsules indicate that their altered organization, rather than atypical crosslinks, is a potentially critical contributor to the observed changes in the flexion contracture. Taken together, our study extends knowledge on the pathomechanisms of post-traumatic joint contracture, thereby contributing to developing new concepts for potential therapy approaches.

AUTHORS' CONTRIBUTIONS

A. Steplewski and J. Fertala: Substantial contribution to the acquisition, analysis, and interpretation of data. Contributed to drafting the manuscript. A. Fertala, P. Beredjiklian, J. Abboud, and J. Barlow: Substantial contribution to research design and execution of key experiments. M. Wang, S. Namdari, M. Rivlin, and W. Arnold: Substantial contribution to the acquisition and interpretation of data form an animal model. J. Kostas and C. Hou: Substantial contribution to the acquisition and interpretation of data. All authors have read and approved the final submitted manuscript

ACKNOWLEDGMENTS

This research was supported by a grant from Department of Defense (W81XWH-13-1-0393) awarded to A.F., P.B., and J.A. The authors are grateful to veterinarians and animal health staff for an excellent veterinary assistance. The authors also thank Jennifer Fisher Wilson for revising the article.

REFERENCES

1. Fergusson D, Hutton B, Drodge A. 2007. The epidemiology of major joint contractures: a systematic review of the literature. Clin Orthop Relat Res 456:22–29.
2. Abdel MP, Morrey ME, Barlow JD, et al. 2012. Myofibroblast cells are preferentially expressed early in a rabbit model of joint contracture. J Orthop Res 30:713–719.
3. Hagiwara Y, Chimoto E, Takahashi I, et al. 2008. Expression of transforming growth factor-beta1 and connective tissue growth factor in the capsule in a rat immobilized knee model. Ups J Med Sci 113:221–234.
4. Prockop DJ, Kivirikko KI. 1995. Collagens: molecular biology, diseases, and potentials for therapy. Annu Rev Biochem 64:403–434.
5. Cohen MS, Hastings H 2nd. 1998. Post-traumatic contracture of the elbow. Operative release using a lateral collateral ligament sparing approach. J Bone Joint Surg 80:805–812.
6. Hildebrand KA, Sutherland C, Zhang M. 2004. Rabbit knee model of post-traumatic joint contractures: the long-term natural history of motion loss and myofibroblasts. J Orthop Res 22:313–320.
7. Hildebrand KA, Zhang M, Salo PT, et al. 2008. Joint capsule mast cells and neuropeptides are increased within four weeks of injury and remain elevated in chronic stages of posttraumatic contractures. J Orthop Res 26:1313–1319.
8. Lindenhovius AL, Jupiter JB. 2007. The posttraumatic stiff elbow: a review of the literature. J Hand Surg 32:1605–1623.
9. Prockop DJ, Berg RA, Kivirikko KI, et al. 1976. Intracellular steps in the biosynthesis of collagen. In: Ramachandran GN, Reddi AH, editors. Biochemistry of collagen. New York: Plenum. p 163–237.
10. Bottomley MJ, Batten MR, Lumb RA, et al. 2001. Quality control in the endoplasmic reticulum: PDI mediates the ER

retention of unassembled procollagen C-propeptides. Curr Biol 11:1114–1118.
11. Fietzek PP, Rexrodt FW, Wendt P, et al. 1972. The covalent structure of collagen. Amino-acid sequence of peptide 1-CB6-C2. Eur J Biochem 30:163–168.
12. Morello R, Bertin TK, Chen Y, et al. 2006. CRTAP is required for prolyl 3- hydroxylation and mutations cause recessive osteogenesis imperfecta. Cell 127:291–304.
13. Engel J, Prockop DJ. 1991. The zipper-like folding of collagen triple helices and the effects of mutations that disrupt the zipper. Annu Rev Biophys Biophys Chem 20:137–152.
14. Lamande SR, Bateman JF. 1999. Procollagen folding and assembly: the role of endoplasmic reticulum enzymes and molecular chaperones. Semin Cell Dev Biol 10:455–464.
15. Kadler KE, Hojima Y, Prockop DJ. 1987. Assembly of collagen fibrils de novo by cleavage of the type I pC-collagen with procollagen C-proteinase. Assay of critical concentration demonstrates that collagen self-assembly is a classical example of an entropy-driven process. J Biol Chem 262:15696–15701.
16. Colige A, Vandenberghe I, Thiry M, et al. 2002. Cloning and characterization of ADAMTS-14, a novel ADAMTS displaying high homology with ADAMTS-2 and ADAMTS-3. J Biol Chem 277:5756–5766.
17. Li SW, Sieron AL, Fertala A, et al. 1996. The C-proteinase that processes procollagens to fibrillar collagens is identical to the protein previously identified as bone morphogenic protein-1. Proc Natl Acad Sci USA 93:5127–5130.
18. Broder C, Becker-Pauly C. 2013. The metalloproteases meprin alpha and meprin beta: unique enzymes in inflammation, neurodegeneration, cancer and fibrosis. Biochem J 450:253–264.
19. Kofford MW, Schwartz LB, Schechter NM, et al. 1997. Cleavage of type I procollagen by human mast cell chymase initiates collagen fibril formation and generates a unique carboxyl-terminal propeptide. J Biol Chem 272:7127–7131.
20. Prockop DJ, Fertala A. 1998. The collagen fibril: the almost crystalline structure. J Struct Biol 122:111–118.
21. Romanic AM, Adachi E, Kadler KE, et al. 1991. Copolymerization of pNcollagen III and collagen I. pNcollagen III decreases the rate of incorporation of collagen I into fibrils, the amount of collagen I incorporated, and the diameter of the fibrils formed. J Biol Chem 266:12703–12709.
22. Brinckmann J, Notbohm H, Tronnier M, et al. 1999. Overhydroxylation of lysyl residues is the initial step for altered collagen cross-links and fibril architecture in fibrotic skin. J Invest Dermatol 113:617–621.
23. Pingel J, Lu Y, Starborg T, et al. 2014. 3-D ultrastructure and collagen composition of healthy and overloaded human tendon: evidence of tenocyte and matrix buckling. J Anat 224:548–555.
24. Akeson WH, Amiel D, Woo SL. 1980. Immobility effects on synovial joints the pathomechanics of joint contracture. Biorheology 17:95–110.
25. Woo SL, Matthews JV, Akeson WH, et al. 1975. Connective tissue response to immobility. Correlative study of biomechanical and biochemical measurements of normal and immobilized rabbit knees. Arthritis Rheum 18:257–264.
26. Nesterenko S, Morrey ME, Abdel MP, et al. 2009. New rabbit knee model of posttraumatic joint contracture: indirect capsular damage induces a severe contracture. J Orthop Res 27:1028–1032.
27. Hildebrand KA, Holmberg M, Shrive N. 2003. A new method to measure post-traumatic joint contractures in the rabbit knee. J Biomech Eng 125:887–892.
28. Hildebrand KA, Holmberg M, Sutherland C, et al. 2002. Posttraumaticjoint contractures: development of rabbit model. Annual Meeting of the Orthopaedic Research Society. Dallas, TX; p. 0068.
29. Hildebrand KA, Zhang M, Germscheid NM, et al. 2008. Cellular, matrix, and growth factor components of the joint capsule are modified early in the process of posttraumatic contracture formation in a rabbit model. Acta Orthop 79:116–125.
30. Monument MJ, Hart DA, Befus AD, et al. 2012. The mast cell stabilizer ketotifen reduces joint capsule fibrosis in a rabbit model of post-traumatic joint contractures. Inflamm Res 61:285–292.
31. Abdel MP, Morrey ME, Barlow JD, et al. 2014. Intra-articular decorin influences the fibrosis genetic expression profile in a rabbit model of joint contracture. Bone Joint Res 3:82–88.
32. Hildebrand KA, Zhang M, Hart DA. 2006. Joint capsule matrix turnover in a rabbit model of chronic joint contractures: correlation with human contractures. J Orthop Res 24:1036–1043.
33. Crum JA, LaPrade RF, Wentorf FA. 2003. The anatomy of the posterolateral aspect of the rabbit knee. J Orthop Res 21:723–729.
34. Woessner JF. 1961. The determination of hydroxyproline in tisue and protein samples containing small proportions of this imino acid. Archiv Biochem Biophys 93:440–447.
35. Sykes B, Puddle B, Francis M, et al. 1976. The estimation of two collagens from human dermis by interrupted gel electrophoresis. Biochem Biophys Res Commun 72:1472–1480.
36. Junqueira LC, Bignolas G, Brentani RR. 1979. Picrosirius staining plus polarization microscopy, a specific method for collagen detection in tissue sections. Histochem J 11:447–455.
37. Hiss J, Hirshberg A, Dayan DF, et al. 1988. Aging of wound healing in an experimental model in mice. Am J Forensic Med Pathol 9:310–312.
38. Perez-Tamayo R, Montfort I. 1980. The susceptibility of hepatic collagen to homologous collagenase in human and experimental cirrhosis of the liver. Am J Pathol 100:427–442.
39. Whittaker P, Kloner RA, Boughner DR, et al. 1994. Quantitative assessment of myocardial collagen with picrosirius red staining and circularly polarized light. Basic Res Cardiol 89:397–410.
40. Boudaoud A, Burian A, Borowska-Wykret D, et al. 2014. FibrilTool, an ImageJ plug-in to quantify fibrillar structures in raw microscopy images. Nat Protoc 9:457–463.
41. Schneider CA, Rasband WS, Eliceiri KW. 2012. NIH Image to ImageJ: 25 years of image analysis. Nat Methods 9:671–675.
42. Waters JC. 2009. Accuracy and precision in quantitative fluorescence microscopy. J Cell Biol 185:1135–1148.
43. Freeman TA, Parvizi J, Dela Valle CJ, et al. 2010. Mast cells and hypoxia drive tissue metaplasia and heterotopic ossification in idiopathic arthrofibrosis after total knee arthroplasty. Fibrogenesis Tissue Repair 3:17.
44. Hildebrand KA, Zhang M, Hart DA. 2007. Myofibroblast upregulators are elevated in joint capsules in posttraumatic contractures. Clin Orthop Relat Res 456:85–91.
45. Vuorela A, Myllyharju J, Nissi R, et al. 1997. Assembly of human prolyl 4-hydroxylase and type III collagen in the yeast pichia pastoris: formation of a stable enzyme tetramer requires coexpression with collagen and assembly of a stable collagen requires coexpression with prolyl 4-hydroxylase. EMBO J 16:6702–6712.
46. van der Slot AJ, Zuurmond AM, van den Bogaerdt AJ, et al. 2004. Increased formation of pyridinoline cross-links due to

higher telopeptide lysyl hydroxylase levels is a general fibrotic phenomenon. Matrix Biol 23:251–257.
47. Eyre DR, Paz MA, Gallop PM. 1984. Cross-linking in collagen and elastin. Annu Rev Biochem 53:717–748.
48. Akeson WH, Amiel D, Mechanic GL, et al. 1977. Collagen cross-linking alterations in joint contractures: changes in the reducible cross-links in periarticular connective tissue collagen after nine weeks of immobilization. Connect Tissue Res 5:15–19.
49. Macconaill MA. 1951. The movements of bones and joints. IV. The mechanical structure of articulate cartilage. J Bone Joint Surg 33-B:251–257.
50. Parry DA. 1988. The molecular and fibrillar structure of collagen and its relationship to the mechanical properties of connective tissue. Biophys Chem 29:195–209.
51. Provenzano PP, Vanderby R Jr. 2006. Collagen fibril morphology and organization: implications for force transmission in ligament and tendon. Matrix Biol 25:71–84.
52. Chapman MA, Pichika R, Lieber RL. 2015. Collagen cross-linking does not dictate stiffness in a transgenic mouse model of skeletal muscle fibrosis. J Biomech 48:375–378.
53. Taguchi T, Razzaque MS. 2007. The collagen-specific molecular chaperone HSP47: is there a role in fibrosis? Trends Mol Med 13:45–53.
54. Kawasaki K, Ushioda R, Ito S, et al. 2015. Deletion of the collagen-specific molecular chaperone Hsp47 causes endoplasmic reticulum stress-mediated apoptosis of hepatic stellate cells. J Biol Chem 290:3639–3646.
55. Ogata I, Auster AS, Matsui A, et al. 1997. Up-regulation of type I procollagen C-proteinase enhancer protein messenger RNA in rats with CCl4-induced liver fibrosis. Hepatology 26:611–617.
56. Hultstrom M, Leh S, Skogstrand T, et al. 2008. Upregulation of tissue inhibitor of metalloproteases-1 (TIMP-1) and procollagen-N-peptidase in hypertension-induced renal damage. Nephrol Dial Transplant 23:896–903.

Blocking Collagen Fibril Formation in Injured Knees Reduces Flexion Contracture in a Rabbit Model

Andrzej Steplewski,[1] Jolanta Fertala,[1] Pedro K. Beredjiklian,[1,2] Joseph A. Abboud,[1,2] Mark L.Y. Wang,[1,2] Surena Namdari,[1,2] Jonathan Barlow,[1,2] Michael Rivlin,[1,2] William V. Arnold,[1,2] James Kostas,[1] Cheryl Hou,[1] Andrzej Fertala[1]

[1]Department of Orthopaedic Surgery, Sidney Kimmel Medical College, Thomas Jefferson University, Curtis Building, 1015 Walnut Street, Philadelphia, Pennsylvania 19107 , [2]Rothman Institute of Orthopaedics, Thomas Jefferson University Hospital, Philadelphia, Pennsylvania 19107

Received 25 March 2016; accepted 13 July 2016
Published online in Wiley Online Library (wileyonlinelibrary.com). DOI 10.1002/jor.23369

ABSTRACT: Post-traumatic joint contracture is a frequent orthopaedic complication that limits the movement of injured joints, thereby severely impairing affected patients. Non-surgical and surgical treatments for joint contracture often fail to improve the range of motion. In this study, we tested a hypothesis that limiting the formation of collagen-rich tissue in the capsules of injured joints would reduce the consequences of the fibrotic response and improve joint mobility. We targeted the formation of collagen fibrils, the main component of fibrotic deposits formed within the tissues of injured joints, by employing a relevant rabbit model to test the utility of a custom-engineered antibody. The antibody was delivered directly to the cavities of injured knees in order to block the formation of collagen fibrils produced in response to injury. In comparison to the non-treated control, mechanical tests of the antibody-treated knees demonstrated a significant reduction of flexion contracture. Detailed microscopic and biochemical studies verified that this reduction resulted from the antibody-mediated blocking of the assembly of collagen fibrils. These findings indicate that extracellular processes associated with excessive formation of fibrotic tissue represent a valid target for limiting post-traumatic joint stiffness. © 2016 Orthopaedic Research Society. Published by Wiley Periodicals, Inc. J Orthop Res

Keywords: joint contracture; posterior capsule collagen; collagen fibrils; arthrofibrosis; antibody

The fibrotic deposits in stiff joints consist mainly of fibril-forming collagen I and collagen III.[1,2] The formation of these collagen fibrils is needed for proper wound healing in response to joint injury, but excessive fibrillogenesis causes unwanted fibrosis and results in post-traumatic joint contracture.[3] Non-surgical treatments to improve range of motion (ROM), including physical therapy, continuous passive motion, splinting or casting, as well as anti-inflammatory drugs, often fail to improve joint mobility. In cases where conservative management fails, surgical intervention can be attempted to correct joint function. Procedures used to improve ROM include manipulation under anesthesia, open or arthroscopic debridement, capsular release, lysis of adhesions, and tenolysis.

The biologic prevention or treatment of arthrofibrosis may provide alternative therapies to improve ROM. Experimental approaches to limit the formation of fibrotic tissue in injured joints have included blocking the profibrotic activity of tissue growth factor β1 (TGF-β1) with neutralizing antibodies or decorin, inhibiting vascular endothelial growth factor and fibroblast growth factor 2, and applying ketotifen to reduce profibrotic processes in mast cells that invade the injured joint tissues.[4–9]

In this study, we tested the feasibility of limiting post-traumatic joint contracture by reducing the formation of collagen-rich deposits in the capsules of injured knee joints in rabbits. We aimed to directly interfere with the extracellular process of collagen fibril formation by blocking the critical collagen–collagen interaction mediated by the C-terminal telopeptide region of collagen I molecules.[10] Prior studies have shown that this strategy reduces collagen fibril formation in vitro, in ex vivo cell culture systems, and in organotypic tissue constructs.[11–13] Here, employing a rabbit model of post-traumatic joint contracture, we tested the utility of a recombinant antibody that targets the C-terminal telopeptide of the α2 chain of collagen I (α2Ct) to reduce the formation of fibrotic tissue. We hypothesized that, with the intraarticular utilization of the recombinant antibody, we would see improved biomechanical characteristics in the form of decreased severity of flexion contracture compared to control, as well as a beneficial pattern of collagen organization and morphology compared to controls. To determine the effectiveness of the proposed strategy, we conducted mechanical measurements of the flexion contracture that developed in injured rabbit knee joints in the presence or absence of the therapeutic antibodies. We also performed microscopic and biochemical analyses of collagen deposits and examined the organization and morphology of collagen fibrils formed in the posterior capsules of these two groups of rabbits.

MATERIALS AND METHODS

Antibodies

We employed two recombinant antibody variants of IgG type: (i) non-modified anti-α2Ct antibody (ACA) and (ii) PEGylated ACA (P-ACA).[13] The PEGylated variant was generated by binding a 12-mer polyethylene glycol chains

Current address for Jonathan Barlow is Department of Orthopaedics, Ohio State University, Columbus, Ohio.
Conflicts of interest: The authors have declared that no competing interest exists. AF and AS have applied for the protection of the sequence of the antibody used in this study.
Grant sponsor: Department of Defense; Grant numbers: W81XWH-13-1-0393, W81XWH-13-1-0395, W81XWH-13-1-0394.
Correspondence to: Andrzej Fertala (T: +215-503-0113; F: +215-955-9159; E-mail: andrzej.fertala@jefferson.edu)

(PEG; ThermoFisher Sci., Rockford, IL) to random lysine residues present in the ACA. Since binding the PEG molecules increases the mass of the ACA chains, we monitored the outcomes of the PEGylation by gel electrophoresis (Supplementary Material).

Binding Characteristics of the P-ACA

We have described the specificity and the affinity of the ACA-collagen I binding elsewhere.[13] Here, we analyzed the binding characteristics of the P-ACA (Supplementary Material).

Stability of Antibodies

Prior to employing the antibodies for their pump-controlled delivery into the injured knees, we analyzed whether their stability, solubility, and the binding characteristics remained unchanged despite the antibody-filled pumps being kept constantly under the skin of the rabbits (Supplementary Material).

Animals

We employed female New Zealand White rabbits, 8- to 12-months old (Covance, Inc., Princeton, NJ). All animal studies were approved by the TJU Institutional Animal Care and Use Committee. The following attributes make rabbits a relevant model to study post-traumatic joint contracture: (i) the critical α2Ct epitope recognized by the ACA in rabbits is identical with its human counterpart and (ii) the rabbit model employed here adequately represents clinical features associated with post-traumatic joint contractures in human patients.[2,14–16]

Experimental Groups

We created the following experimental groups: (i) 2- and 16-week recovery control groups treated in the injured knees with phosphate buffered saline (PBS) only (PBS-2, PBS-16); (ii) 2- and 16-week recovery groups treated in the injured knees with a 2-mg/ml solution of the ACA (ACA-2, ACA-16); and (iii) 2- and 16-week recovery groups treated in the injured knees with a 2-mg/ml solution of the P-ACA (P-ACA-2, P-ACA-16). In these groups, the PBS and antibodies were delivered continuously for 8 weeks.

Surgical Procedures

We employed an established rabbit model of post-traumatic joint contracture.[2,15–17] In brief, knee injury is caused by intra-articular fracture and mechanical disruption of the posterior capsule (PC). The injured knees are maintained in a flexed position for 8 weeks with the use of Kirschner (K)-wires. The unoperated contralateral leg serves as control. Following 8 weeks of immobilization, the K-wires are removed and the rabbits are allowed free cage activity for 2 or 16 weeks. Specific modification to this model, namely installation of a peristaltic pump for direct antibody delivery into articular cavity, is described in Supplementary Material (Figs. S1 and S2). This modification is based on earlier studies utilizing pumps for direct drug delivery into joints of model rabbits.[6,8,18]

Antibody Delivery

The delivery of the ACA and P-ACA started immediately after surgery and continued for 8 weeks at 1 μl/h. This 8-week time frame is referred to as the treatment period. At the mid-point of this period, that is, 4 weeks after surgery, the pumps' reservoirs were refilled through a subdermal port (Fig. S2).

We randomly selected a group of rabbits to confirm a correct flow path at the end of the treatment period. In those tests we utilized a contrast agent (Hexabrix, donated by Mallinckrodt Inc., St. Louis, MO) and X-ray imaging. Moreover, immunostaining was employed to analyze the presence of the ACA and P-ACA within the PCs collected from rabbits that had to be sacrificed within the initial 8-week treatment period (Table 1).

Joint Angle Measurements

Following euthanasia, flexion contracture was measured using a custom-made instrument (Test Resources, Inc., Shakopee, MN), as described (Fig. S3).[2] Flexion contracture was defined as the difference between the angles recorded at 0.2 Nm torque for the control limb and for the injured limb.[2,17] Accordingly, a larger difference between the maximum extension angles of control and operated limbs indicates a more severe joint contracture (Supplementary Material).

Tissue Collection

Since the PC is the main contributor to the knee contracture in the rabbit model employed here, the PCs were dissected from the limbs, as described (Fig. S4).[1,2] While one part of the PC was processed for histology, another part was processed for assays of collagen content and composition.

Quantitative Microscopy of Collagen Fibrils

Three-micrometer-thick cross-sections and longitudinal sections of the PCs were stained with collagen-specific picrosirius red to visualize collagen fibrils (Polysciences, Inc., Warrington, PA).[2] Polarized-light microscopy of the fibrils made it possible to describe their thickness and the organization.[2,19] As the thickness of fibers increases, their birefringence color changes from green to yellow to orange to red, that is, from shorter to longer wavelengths.[19] Employing a polarizing microscope (Eclipse LV100POL, Nikon Inc., Melville, NY) and the NIS Elements software (Nikon Inc.), the following groups of colors were defined: (i) green, (ii) yellow, and (iii) orange-red.[2,20] Utilizing the NIS Elements software, we collected data from the entire image, and then we calculated the surface areas occupied by pixels corresponding to the defined colors. Considering the sum of all pixels to be 100%, the percentage of each color group in the analyzed images was determined. Subsequently, we calculated changes in the injured PC, within each color category, as the injured-PC/uninjured-PC ratios. A minimum of three histological sections for each PC sample was examined per each analyzed rabbit. Employing the longitudinal sections of the PCs, the organization of collagen fibrils, expressed as theoretical anisotropy score, was evaluated by ImageJ software that included the FibrilTool plug-in, as described.[2,21,22]

Relative Collagen Content

The PC samples were frozen in liquid nitrogen and then pulverized; each sample was then divided for assays of total collagen content and for extraction of fibrillar collagens. Following fat removal, the samples used for total collagen assays were lyophilized and weighed. Finally, a hydroxyproline assay was employed to determine the collagen content per unit of dry mass.[2,23]

Table 1. Surgery Outcomes

	Number of rabbits in specific groups					
Status	PBS-2	ACA-2	P-ACA-2	PBS-16	ACA-16	P-ACA-16
[a]A	13	14	7	6	6	6
B	2	1	0	0	0	0
C	2	0	0	0	0	0
D	0	0	1/3 wks 1/6 wks 1/7 wks	0	1/4 wks	0
E	0	0	1/4 wks	0	0	0
F	2/2 h 1/5 wks	0	0	0	0	0
G	0	0	0	0	1	1
H	0	0	0	0	1/4 days	0
I	0	1/4 wks	0	0	0	1/3 wks

[a]A, a number of rabbits that reached the end of study; all rabbits were used in described assays. B, intraoperative tibia fracture due to drilling during initial surgery. C, intraoperative femur fracture during initial surgery. D, post-operative tibia fracture/weeks after initial surgery; fracture occurred during normal cage activities. E, post-operative tibia fracture/weeks after initial surgery; fracture occurred at K-wire entry during handling of rabbit during pump refill. F, peri- and post-operative failure of a k-wire/time after k-wire installation. G, stopped breathing during preparation for the second surgery. H, autopsy revealed pre-existing congenital heart problems. Significant findings included chronic active myocardial degeneration with fibrosis of older lesions, inflammatory infiltrates associated with degenerated myocytes, and acute injury with swelling and hyalinization of myocytes. Multifocal hepatic centrilobular necrosis and congestion was observed and these lesions can be associated with impaired heart function. Moderate pulmonary edema was also observed which also is suggestive of impaired cardiac function. I, euthanized due to complications associated with self-mutilation/weeks after initial surgery; chewing/biting of toes.

Collagen III:Collagen I Ratio

Collagen was extracted from the PC samples with the use of 0.5 M acetic acid containing pepsin added at 0.1 mg/1 mg of wet tissue. The extraction was done by placing the samples in a shaker for 48 h at 4°C. Following extraction, the samples were centrifuged and then filtered to remove insoluble debris. Finally, the concentration of pepsin-soluble collagen was determined by a hydroxyproline assay. Employing an interrupted electrophoresis in 6% polyacrylamide gels, we separated the monomeric, that is, not cross-linked collagen I chains, from monomeric forms of collagen III chains.[2] Subsequently, protein bands were stained with Coomassie blue and then pixel intensities of protein bands corresponding to the monomeric collagen I and collagen III α-chains were measured by densitometry (EZQuant Ltd., Tel-Aviv, Israel). Then, the relative amounts of collagen III in injured PC and in uninjured PC were expressed as the collagen III:collagen I ratio. Finally, the proportion of the collagen III:collagen I ratios calculated for the injured PC and the uninjured PC was determined for each rabbit.[2]

Collagen Cross-Linking

Using electrophoresis, the relative amount of the cross-linked collagen chains that persisted after limited pepsin extraction in the pool of collagen molecules was analyzed for each PC. In brief, following electrophoretic separation in reducing conditions, the relative content of the cross-linked α-chains forming the β and the γ oligomers was calculated by comparing their amount to the amount of the monomeric α-chains.[2] Based on these measurements the relative amount of cross-linked chains was expressed as the cross-linked chains:non-cross-linked chains ratio. Finally, the proportion of these ratios calculated for injured PC and uninjured PC was determined for each rabbit.

Statistical Analyses

Upon arrival, the rabbits were randomly divided to specific groups. We analyzed each outcome in a context of measurements obtained for the injured side versus the measurement obtained for the healthy side, in effect, using each animal as its own control. Consequently, ratio = 1 indicates no change in injured PC versus uninjured PC, ratio > 1 indicates increase in a measured parameter, and ratio < 1 indicates decrease in the measured parameter. The main comparisons of the means were done between the PBS and the ACA groups and between the PBS and the P-ACA groups. The Student's *t*-test was employed to determine the statistical significance of differences between the control group mean and the experimental group mean (GraphPad Prism v. 5.03, GraphPad Software, Inc., La Jolla, CA).

Considering the number of rabbits needed for each group, we focused on a parameter directly influenced by the ACA (i.e., the amount of collagen fibrils formed de novo). Employing quantitative microscopic techniques, we calculated the change in the amount of new fibrils formed in response to injury as the function of the presence or the absence of a tested agent.[2] Considering a 1.5-fold increase in newly formed fibrils in the PBS-2 weeks group, a 1.14-fold increase in the ACA-2 weeks group, and the standard deviation (SD) of about 0.2, we estimated we will need approximately six animals per group to have 80% power to detect such a difference using a two-sided *t*-test, with an alpha of 0.05 (StatMate 2, GraphPad Software, Inc.). Specific numbers (n) of animals analyzed in each group are indicated in Table 1.

RESULTS

Antibody Variants

Although the presence of PEG molecules on the surface of the P-ACA variant caused some steric hindrance, assays indicated that this antibody variant

retains its binding specificity (Fig. S5). Biosensor-based binding assays demonstrated that the affinity for the P-ACA-collagen I binding compares to that of the ACA (data not shown).[13]

Stability of Antibodies

Assays of antibodies stored at 37°C in an incubator and those recovered from pumps implanted for 8 weeks in the rabbits indicated that long-term incubation changed neither their structural integrity nor their binding specificity nor their binding affinity (not shown). Analysis of the size exclusion chromatography (SEC) elution profiles of the antibody variants did not show formation of antibody aggregates (not shown).

Surgery Outcomes

We processed 70 rabbits divided into experimental and control groups (Table 1). While 52 rabbits (74%, Table 1, group A) reached the experimental end point, 18 rabbits (26%) had to be eliminated from the study (Table 1). The most notable single problem (5.7%) was post-operative fracture of tibia (Table 1, group D). In this group, all tibia fractures occurred at the point of entry of K-wires during normal cage activities 3–7 weeks post-surgery. The majority of the losses of rabbits in categories B (4.3%), C (2.9%), and F (4.3%) were associated with perioperative bone fractures and K-wire failures. Losses in groups E (1.4%), G (2.9%), H (1.4%), and I (2.9%) occurred due to tibia fracture during handling a rabbit to refill a pump, complications due to anesthesia, other non-orthopaedic medical problems, and complications associated with self-mutilation, respectively.

Antibody Delivery

Examinations of the rabbits during the K-wire removal surgery showed neither infection nor inflammation reactions to the 8-week presence of the pumps. All the pumps operated, as programmed, and no tubes failed or became dislodged from the articular cavities of the operated knee joints (Figs. S2 and S4). We demonstrated an unobstructed flow path from the pump to the injured knee at the end of the 8-week treatment period (Fig. 1). Moreover, immunohistological assays done on the PCs of rabbits that had to be sacrificed during the treatment period (Table 1) have shown ACA- and P-ACA-positive staining in antibody-treated knees. In contrast, the antibody-specific staining was not seen in PCs isolated from untreated healthy joints (Fig. S6).

Effects of ACA and P-ACA on Joint Contracture

Compared to the PBS-2 group, the flexion contracture was significantly reduced in the ACA-2 group ($p = 0.05$) and P-ACA-2 group ($p = 0.003$) (Fig. 2 and Table S1). Rabbits treated with the P-ACA showed a trend toward greater reduction of the flexion contracture compared to those treated with the ACA-2 ($p = 0.1$). The flexion contractures for the PBS-16 and ACA-16 groups were similar ($p = 0.7$). In comparison to the PBS-16 or ACA-16 groups, the flexion contracture of the P-ACA-treated rabbits trended toward lower values ($p = 0.2$ and 0.1, respectively).

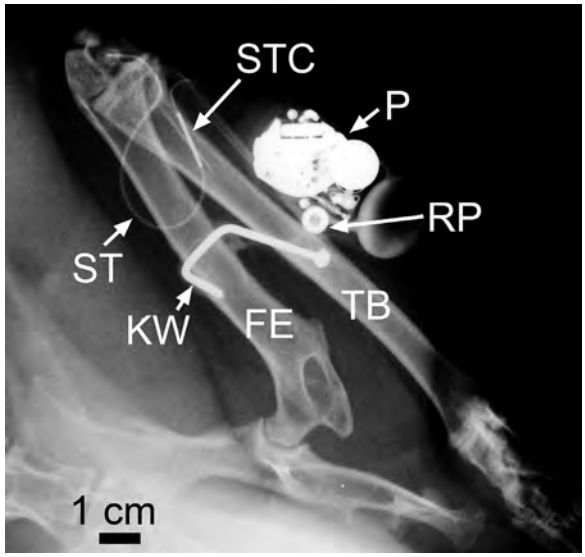

Figure 1. An X-ray depicting an uninterrupted flow path of a contrast agent from a pump to the knee cavity at the end of the 8-week delivery period. STC—stainless steel connector; P—pump; RP—refill port; TB—tibia; FE—femur; KW—K-wire; ST—silicone tube.

Comparing the flexion contractures between corresponding groups of rabbits from the 2- and 16-week recovery groups (i.e., PBS-2 vs. PBS-16, ACA-2 vs. ACA-16, and P-ACA-2 vs. P-ACA-16), we observed a statistically significant reduction of the flexion contracture had occurred in the PBS-16 group ($p = 0.005$).

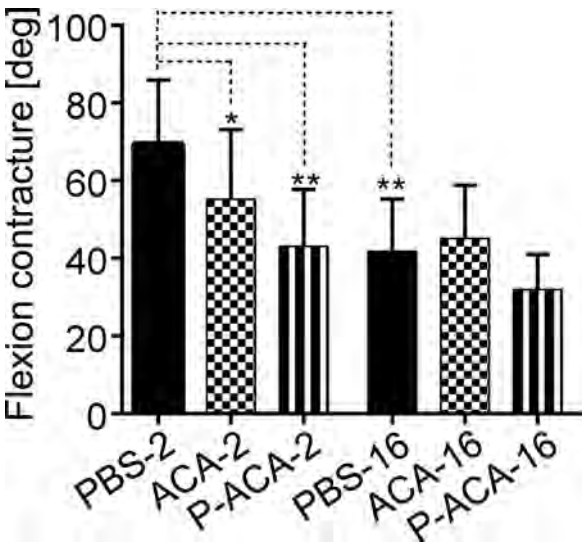

Figure 2. A graphic representation of the measurements of the flexion contracture of the injured knees. The flexion contracture was calculated as the difference between the flexion contracture of the non-injured leg and the flexion contracture of the injured leg. Note that a larger difference between the maximum extension angles of control and operated limbs indicates a more severe joint contracture. Asterisks indicate statistically significant differences between analyzed groups: $^{*}p < 0.05$, $^{**}p < 0.01$.

Although the flexion contractures trended toward lower values in the ACA-16 and P-ACA-16 groups compared to the 2-week recovery counterparts, these changes were not statistically significant ($p = 0.2$ and 0.1, respectively).

Subpopulations of Collagen Fibrils

Consistent with earlier observations, the relative content of green-colored thin fibrils in the PBS-2 group increased in the injured knees (Fig. 3A).[2] Compared to the PBS-2 group, the increase in the relative content of thin fibrils was significantly smaller in the ACA-2 group ($p = 0.01$) and P-ACA-2 groups ($p = 0.04$) (Fig. 3).

A similar trend was observed in the 16-week recovery groups, but the differences were not statistically significant between the PBS-16 and ACA-16 groups ($p = 0.3$) and between the PBS-16 and P-ACA-16 groups ($p = 0.4$) (Fig. 3B). Figure 4 depicts representative images of collagen fibrils seen in cross sections of analyzed in the PCs.

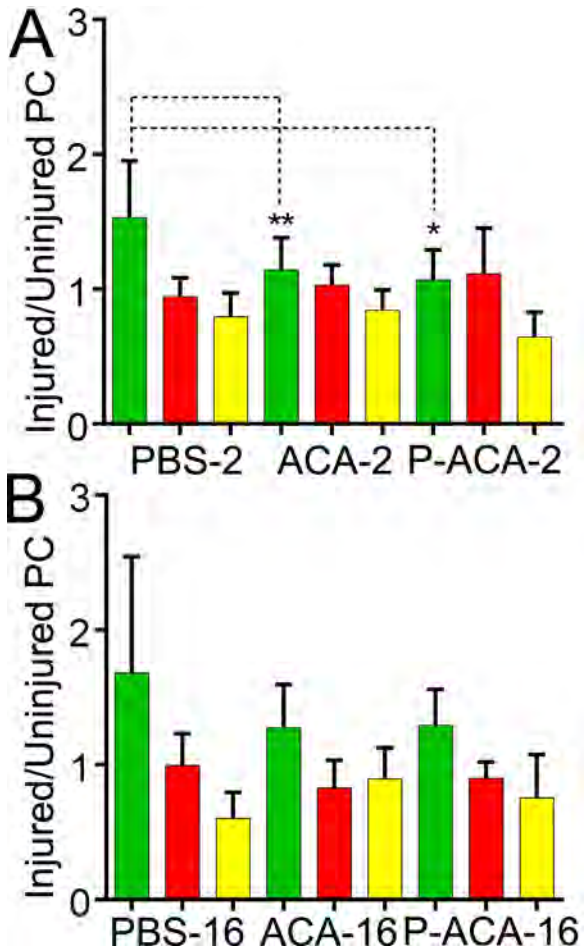

Figure 3. Graphic representations of results from quantitative microscopic assays of changes in subpopulations of collagen fibrils present in the PCs from injured versus uninjured knees: (A) 2-week recovery group; (B) 16-week recovery group. Bars represent the ratios of percent areas occupied by corresponding birefringence colors seen in injured and uninjured PCs. Asterisks indicate statistically significant differences between analyzed groups: $^{*}p < 0.05$, $^{**}p < 0.01$.

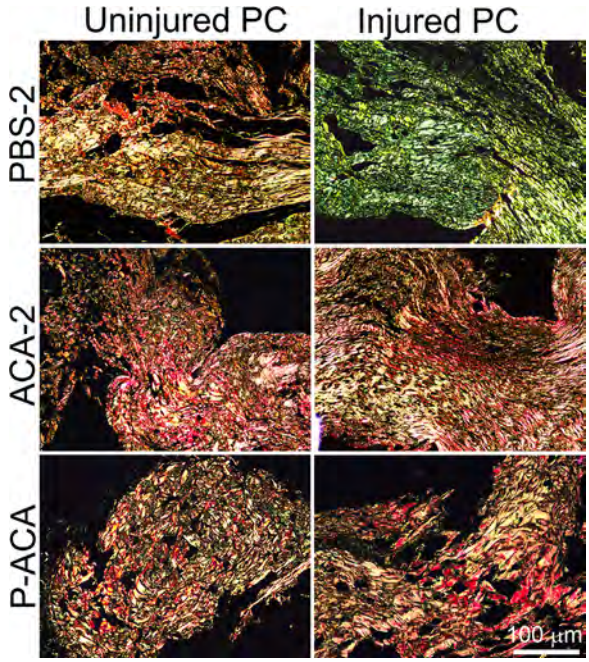

Figure 4. Representative images of collagen fibrils observed in the PCs with the use of a polarizing microscope.

Fibril Organization

While the anisotropy score was relatively high in the uninjured knees of all groups, thus indicating the preferred orientation of fibrils (Fig. 5), it was relatively low in the injured knees of the PBS-2 group. This low anisotropy score suggests non-preferential or more random organization of the fibrillar structures seen in the longitudinal sections of the injured PCs. Antibody-treated injured PCs in the 2-week groups showed similar anisotropy scores to those of their uninjured counterparts. As represented by the PBS-16 group, the anisotropy score values were comparable in the injured and uninjured PCs from the 16-week recovery groups (Fig. 5).

Relative Collagen Content

Assays indicated a relatively high content of collagenous proteins per unit of dry mass of the PCs isolated from the healthy and contracted knees (Fig. 6). When we compared the relative collagen content in uninjured PCs and injured PCs within the PBS-2, ACA-2, and P-ACA-2 groups, the findings indicated a statistically significant decrease of the collagen content in the injured PCs of the P-ACA-treated capsules ($p = 0.04$). There were no statistically significant differences between the collagen content in the PCs from the injured and uninjured knees from the 16-week recovery groups.

Collagen III Content

When we compared the relative contents of collagen III (Fig. 7A and B) in the uninjured and injured PCs, we found a 1.35-fold (± 0.4 SD) increase in the PBS-2 group. The relative content of collagen III in injured

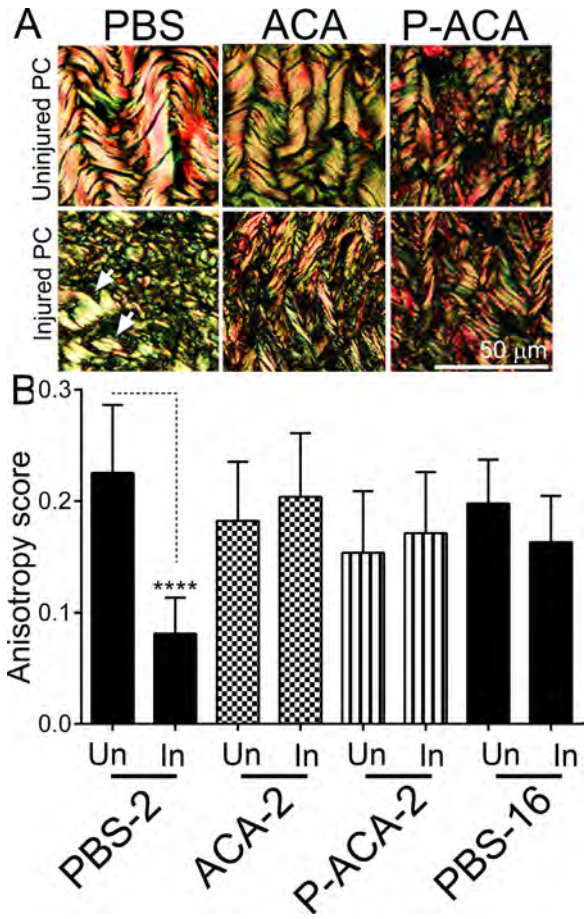

Figure 5. Analysis of the organization of collagen fibrils in the longitudinal sections of the uninjured (Un) and injured (In) PCs. (A) Representative images of collagen fibrils seen in selected PCs. Arrows indicates where the alignment of the fibrils in an injured PC resembles its uninjured counterpart. (B) A graphic representation of measurements of the anisotropy scores. Asterisks indicate statistically significant differences between analyzed groups: $^{****}p < 0.0001$.

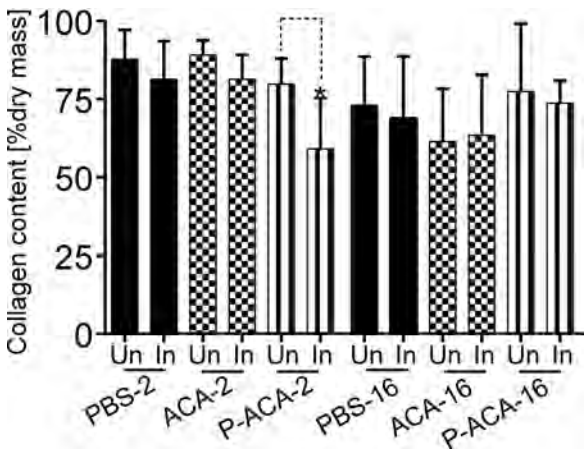

Figure 6. A graphic representation of the collagen content in the uninjured (Un) and injured (In) PCs. Asterisk indicates statistically significant differences between analyzed groups: $^{*}p < 0.05$.

PCs increased 1.06-fold (±0.2 SD) in the ACA-2 group and 1.10-fold (±0.3 SD) in the P-ACA-2 group. The relative content of collagen III in the uninjured and injured PCs indicated a 1.12-fold (±0.3 SD) increase in the PBS-16 group. The relative content of collagen III in injured PCs changed 0.91-fold (±0.2 SD) in the ACA-16 and 0.96-fold (±0.3 SD) in the P-ACA-16 groups (Fig. 7B).

Relative Amount of Cross-Linked Collagen Chains

When we analyzed the relative content of the cross-linked collagen chains in the uninjured PCs and in injured PCs, we discovered no changes across all analyzed groups (Fig. 7C).

DISCUSSION

Based on our earlier studies demonstrating that ACA inhibits collagen fibril formation in various experimental models of collagen fibril formation, we analyzed the feasibility of applying this antibody after knee injury to reduce post-traumatic joint contracture.[11–13] Mechanical tests carried out at the end of recovery periods demonstrated that the flexion contractures in the ACA-2 and P-ACA-2 groups were significantly reduced compared to the PBS-2 control. Although the flexion contractures decreased further in the ACA-16 and P-ACA-16 rabbits compared to the corresponding 2-week recovery groups, this decrease was not statistically significant. In contrast, the decrease in the flexion contracture in the PBS-16 group compared to the PBS-2 group was statistically significant. A spontaneous reduction of the flexion contracture during the 16-week recovery period in the non-treated PBS-16 group is consistent with results presented by Hildebrand et al.[24] The authors reported that, due to constant tissue remodeling and movement of joints, the flexion contracture of the rabbits' knees had decreased 10% at 8 weeks after K-wire removal. Then, 8 week later, that is, 16 weeks after removing K-wires, the flexion contracture had decreased to about 50% of value measured soon after K-wire removal. Measurements of the flexion contractures 16 weeks later, that is, 32 weeks after removing K-wires, did not show any additional reduction, thus indicating a plateau of spontaneous recovery.

Just 2 weeks following K-wire removal, we measured a 20% difference in the flexion contracture in the ACA-treated group and a 40% difference in the P-ACA-treated group compared to the control group. We propose that this reduction most likely resulted from limiting the development of full fibrotic change rather than accelerating spontaneous recovery.

Since earlier rabbit-based studies demonstrated that applying non-specific IgGs to the cavities of injured knees does not change the flexion contracture of the injured joints, we propose that the changes observed in the ACA-2 and P-ACA-2 groups are antibody-specific.[4] We analyzed the PCs to learn what caused the reduced flexion contracture in the

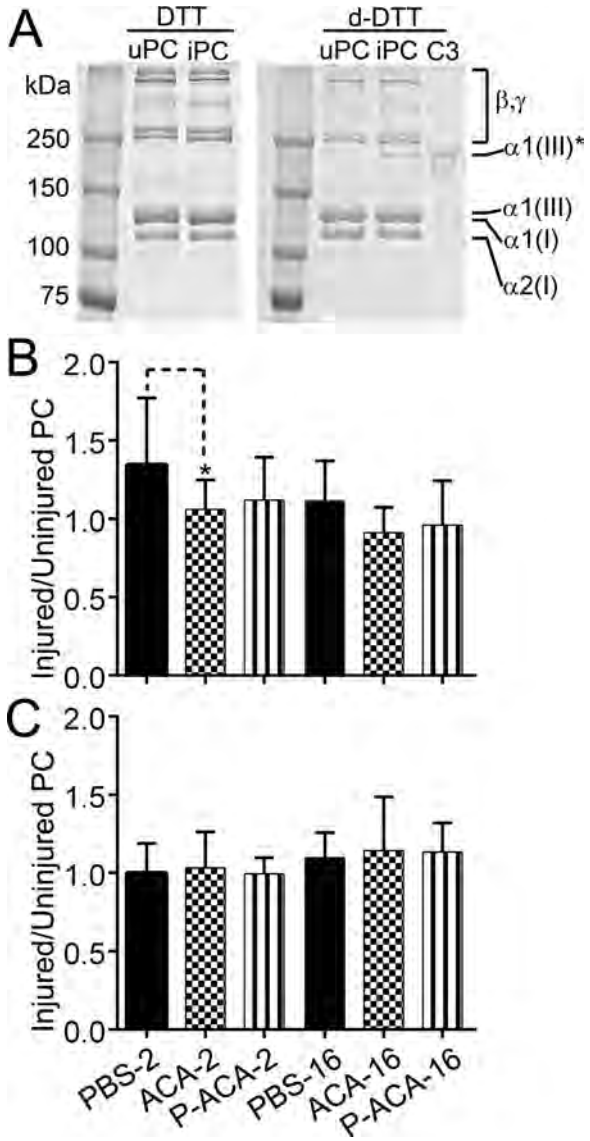

Figure 7. A graphic representation of the results from electrophoretic assays of collagens extracted from the PCs. (A) Patterns of migration of collagen I and collagen III chains separated in standard reducing conditions (DTT) and in delayed-reduction conditions (d-DTT) of electrophoresis. (B) A graphic representation of the proportions of the collagen III:collagen I ratios calculated for the injured and uninjured PCs ($^*p < 0.05$). (C) A graphic depiction of the results of measurements of the proportions of the βγ:α ratios; no statistically significant difference was observed. uPC, iPC—uninjured and injured PC; C3—collagen III marker; α1(I), α2(I), α1(III)—specific chains of collagen I and collagen III, respectively; α1(III)*—collagen III chains separated with the use of delayed-reduction conditions; β, γ—β and the γ oligomers consisting of cross-linked collagen α chains.

ACA-treated or P-ACA-treated groups. Since collagen fibril formation is the main target of the ACA and P-ACA, we first studied the fibrillar architecture of the treated PCs. In earlier studies, we had determined that an increase in green-birefringence thin collagen fibrils reflects an active process of collagen fibrillogenesis in injured PCs in response to injury.[2] Based on the reduced amount of green-birefringence fibrils in the injured PCs, we postulate that the ACA and P-ACA inhibited the collagen fibril formation process.

The anisotropy scores in the injured and uninjured PCs from the antibody-treated groups also indicate that the ACA and P-ACA may have reduced the formation of new fibrils. We propose that the relatively high anisotropy scores measured in the injured PCs reflect the organization of mature fibrils that existed before joint injury rather that improved organization of new fibrils formed de novo in response to joint trauma. In the injured PCs from the PBS-2 group, however, the general pattern of organization of the original fibrils is markedly disrupted by newly formed fibrillar assemblies.

To further elucidate the mechanisms that reduced flexion contracture in the ACA-treated and the P-ACA-treated groups, we analyzed the relative collagen content in the PCs. Although we were able to determine the relative content of collagen per unit of dry mass of the PCs, it is impossible to determine the total mass of a capsule or the total amount of collagen. Consequently, similar values for the relative collagen content per unit mass in the injured and uninjured PCs do not necessary indicate that the overall total masses of these capsules are identical. Thus, our collagen assays are not able to predict changes in the mass of fibrotic PCs as the function of the presence or the absence of the antibodies. These assays, however, provide useful information for antibody-dependent changes in collagen content relative to other macromolecules produced in the PCs.

We propose that the approximately 20% reduction of the collagen content in the injured PCs from the P-ACA-2 group resulted from substantially blocked incorporation of newly produced collagen molecules into fibrils and their degradation. Studies by Leikina et al. support this notion.[25] Specifically, the authors demonstrated that the triple-helical structure of individual collagen molecules, that is, not incorporated into a fibril, is quite unstable at body temperature, allowing their degradation by proteolytic enzymes. In contrast, the stability of collagen molecules increases upon their incorporation into fibrils, thereby rendering them more resistant to enzymatic degradation.

We have also analyzed potential effects of applied treatments on the collagen III:collagen I ratio in the injured PCs and on the relative amount of cross-links present in the pepsin-extracted fraction of collagenous proteins. Consistent with our earlier studies, the relative amount of collagen III increased in the injured PCs from the PBS-2 group[2]. Although the collagen III:collagen I ratio trended lower in the antibody-treated groups, a statistically significant difference was observed only between the PBS-2 and ACA-2 groups.

We determined that the relative amounts of the cross-linked fractions of pepsin-extracted collagen in the injured and healthy capsules were similar in all analyzed groups. Since we employed the pepsin-soluble fraction in which a portion of cross-linked chains is converted to monomers, we cannot exclude the possibility of changes in the quality and quantity of cross-links present in the initial collagen pool.

Considering the similar quantities of the cross-linked collagen chains present in the pepsin-extracted collagen pool, we postulate that the aberrant architectural arrangement of the collagen fibrils, formed de novo in response to injury, mostly likely contributed to joint stiffness. In a study of muscle fibrosis that supports this postulation, Chapman et al. suggested that a change in collagen fibril orientation, rather than increased cross-linking, was a decisive factor in developing muscle stiffness.[26] Similarly, studies have also indicated that aberrations in the microarchitecture of collagen fibrils contribute to the mechanism of joint contracture in a rabbit-based model.[27]

Our results showed that the P-ACA causes stronger effects compared to the ACA. We speculate that these stronger effects were likely due to greater stability of the PEG-modified antibody and perhaps to its prolonged residence in the injury sites. These qualities of PEG-modified molecules are well documented in studies where PEGylated peptides are utilized as therapeutic compounds.[28,29] Still, we cannot exclude the possibility that the stronger inhibitory effects were, in part, a consequence of a greater steric hindrance imposed by the bulkier architecture of the P-AFA which resulted from the presence of the PEG molecules on the surface of the AFA.

As rapid recovery of joint motion improves the quality of life of affected patients including reduction of chronic pain, early return to work, less need for physiotherapy, less need for surgery, we suggest that collagen fibril formation could be considered a valid target to reduce post-traumatic joint contracture. Unlike anti-fibrotic approaches that target broad intracellular processes associated with inflammation and cell proliferation, the anti-fibrotic approach tested here targets a well-defined extracellular process, thereby potentially reducing the chance for unwanted side effects. In this sense, our experimental approach is similar to targeting extracellular lysyl oxidase, or αvβ6 integrin that activates pro-fibrotic TGF-β1.[30,31]

Since we still observed flexion contracture despite the antibody treatment, our model approach was not able to fully prevent development of joint stiffness. We propose the following key reasons to explain this limitation: (i) antibodies do not reach fully effective concentration; (ii) antibodies are not able to access all sites of fibrosis; and (iii) antibodies do not target the formation of non-collagenous elements of fibrotic tissue.

In view of these limitations, we propose that future efforts to target extracellular processes of fibrotic tissue formation should include optimization of antibody concentration, employing more effective antibody delivery systems, and designing small molecular mass inhibitors able to penetrate fibrotic tissues more effectively than antibodies.

AUTHORS' CONTRIBUTIONS

A. Steplewski and J. Fertala: Substantial contribution to the acquisition, analysis, and interpretation of data. Contributed to drafting the manuscript. A. Fertala, P. Beredjiklian, and J. Abboud, J. Barlow: Substantial contribution to research design and execution of key experiments. M. Wang, S. Namdari, M. Rivlin, and W. Arnold: Substantial contribution to the acquisition and interpretation of data form an animal model. J. Kostas and C. Hou: Substantial contribution to the acquisition and interpretation of data. All authors have read and approved the final submitted manuscript.

ACKNOWLEDGMENTS

This research was supported by grants from Department of Defense: W81XWH-13-1-0393 awarded to AF, W81XWH-13-1-0395 to PB, and W81XWH-13-1-0394 to JA. The authors are grateful to veterinarians and animal health staff for an excellent veterinary assistance. The authors also thank Jennifer Fisher Wilson for revising the article.

REFERENCES

1. Hildebrand KA, Zhang M, Germscheid NM, et al. 2008. Cellular, matrix, and growth factor components of the joint capsule are modified early in the process of posttraumatic contracture formation in a rabbit model. Acta Orthop 79:116–125.
2. Steplewski A, Fertala J, Beredjiklian PK, et al. 2015. Auxiliary proteins that facilitate formation of collagen-rich deposits in the posterior knee capsule in a rabbit-based joint contracture model. J Orthop Res 34:489–501.
3. Fergusson D, Hutton B, Drodge A. 2007. The epidemiology of major joint contractures: a systematic review of the literature. Clin Orthop Relat Res 456:22–29.
4. Fukui N, Tashiro T, Hiraoka H, et al. 2000. Adhesion formation can be reduced by the suppression of transforming growth factor-beta1 activity. J Orthop Res 18:212–219.
5. Abdel MP, Morrey ME, Barlow JD, et al. 2014. Intra-articular decorin influences the fibrosis genetic expression profile in a rabbit model of joint contracture. Bone Joint Res 3:82–88.
6. Fukui N, Fukuda A, Kojima K, et al. 2001. Suppression of fibrous adhesion by proteoglycan decorin. J Orthop Res 19:456–462.
7. Emami MJ, Jaberi FM, Azarpira N, et al. 2012. Prevention of arthrofibrosis by monoclonal antibody against vascular endothelial growth factor: a novel use of bevacizumab in rabbits. Orthop Traumatol Surg Res 98:759–764.
8. Fukui N, Nakajima K, Tashiro T, et al. 2001. Neutralization of fibroblast growth factor-2 reduces intraarticular adhesions. Clin Orthop Relat Res 383:250–258.
9. Monument MJ, Hart DA, Befus AD, et al. 2012. The mast cell stabilizer ketotifen reduces joint capsule fibrosis in a rabbit model of post-traumatic joint contractures. Inflamm Res 61:285–292.
10. Prockop DJ, Fertala A. 1998. Inhibition of the self-assembly of collagen I into fibrils with synthetic peptides. Demonstration that assembly is driven by specific binding sites on the monomers. J Biol Chem 273:15598–15604.
11. Chung HJ, Steplewski A, Chung KY, et al. 2008. Collagen fibril formation. A new target to limit fibrosis. J Biol Chem 283:25879–25886.
12. Fertala J, Kostas J, Hou C, et al. 2014. Testing the anti-fibrotic potential of the single-chain Fv antibody against the alpha2 C-terminal telopeptide of collagen I. Connect Tissue Res 55:115–122.
13. Fertala J, Steplewski A, Kostas J, et al. 2013. Engineering and characterization of the chimeric antibody that targets the C-terminal telopeptide of the alpha2 chain of human

collagen I: a next step in the quest to reduce localized fibrosis. Connect Tissue Res 54:187–196.
14. Akeson WH, Amiel D, Woo SL. 1980. Immobility effects on synovial joints the pathomechanics of joint contracture. Biorheology 17:95–110.
15. Nesterenko S, Morrey ME, Abdel MP, et al. 2009. New rabbit knee model of posttraumatic joint contracture: indirect capsular damage induces a severe contracture. J Orthop Res 27:1028–1032.
16. Barlow JD, Hartzler RU, Abdel MP, et al. 2013. Surgical capsular release reduces flexion contracture in a rabbit model of arthrofibrosis. J Orthop Res 31:1529–1532.
17. Hildebrand KA, Holmberg M, Shrive N. 2003. A new method to measure post-traumatic joint contractures in the rabbit knee. J Biomechan Eng 125:887–892.
18. Badlani N, Inoue A, Healey R, et al. 2008. The protective effect of OP-1 on articular cartilage in the development of osteoarthritis. Osteoarthritis Cartilage 16:600–606.
19. Junqueira LC, Bignolas G, Brentani RR. 1979. Picrosirius staining plus polarization microscopy, a specific method for collagen detection in tissue sections. Histochem J 11:447–455.
20. Whittaker P, Kloner RA, Boughner DR, et al. 1994. Quantitative assessment of myocardial collagen with picrosirius red staining and circularly polarized light. Basic Res Cardiol 89:397–410.
21. Boudaoud A, Burian A, Borowska-Wykret D, et al. 2014. FibrilTool, an ImageJ plug-in to quantify fibrillar structures in raw microscopy images. Nat Protoc 9:457–463.
22. Schneider CA, Rasband WS, Eliceiri KW. 2012. NIH Image to ImageJ: 25 years of image analysis. Nat Methods 9:671–675.
23. Woessner JF. 1961. The determination of hydroxyproline in tisue and protein samples containing small proportions of this imino acid. Arch Biochem Biophys 93:440–447.
24. Hildebrand KA, Sutherland C, Zhang M. 2004. Rabbit knee model of post-traumatic joint contractures: the long-term natural history of motion loss and myofibroblasts. J Orthop Res 22:313–320.
25. Leikina E, Mertts MV, Kuznetsova N, et al. 2002. Type I collagen is thermally unstable at body temperature. Proc Natl Acad Sci USA 99:1314–1318.
26. Chapman MA, Pichika R, Lieber RL. 2015. Collagen crosslinking does not dictate stiffness in a transgenic mouse model of skelmuscle fibrosis. J Biomech 48:375–378.
27. Woo SL, Matthews JV, Akeson WH, et al. 1975. Connective tissue response to immobility. Correlative study of biomechanical and biochemical measurements of normal and immobilized rabbit knees. Arthritis Rheum 18:257–264.
28. Pasut G. 2014. Pegylation of biological molecules and potential benefits: pharmacological properties of certolizumab pegol. BioDrugs 28:15–23.
29. Koussoroplis SJ, Paulissen G, Tyteca D, et al. 2014. PEGylation of antibody fragments greatly increases their local residence time following delivery to the respiratory tract. J Control Release 187:91–100.
30. Katsumoto TR, Violette SM, Sheppard D. 2011. Blocking TGFbeta via inhibition of the alphavbeta6 integrin: a possible therapy for systemic sclerosis interstitial lung disease. Int J Rheumatol 2011:208219.
31. Rodriguez HM, Vaysberg M, Mikels A, et al. 2010. Modulation of lysyl oxidase-like 2 enzymatic activity by an allosteric antibody inhibitor. J Biol Chem 285:20964–20974.

SUPPORTING INFORMATION

Additional supporting information may be found in the online version of this article.

SYNOPSIS OF "OVERALL PROJECT SUMMARY" VS. APPROVED SOW

STATEMENT OF WORK – July/09/2013
PROPOSED START DATE September/01/2013

Site 1: Department of Orthopaedic Surgery, Thomas Jefferson University, Curtis Building
1015 Walnut Str. Philadelphia, PA 19107
PI: Dr. Andrzej Fertala

Site 2: The Rothman Institute, 925 Chestnut Street, Philadelphia, PA

The Rothman Institute, 925 Chestnut Street, Philadelphia, PA
Partnering PIs: Drs. Joseph Abboud and Pedro Beredjiklian

APPROVED SOW	OUTCOMES
Specific Aim 1"To block the fibrotic process after joint injury in a rabbit-based model"	
Major Task 1 **Production and purification of therapeutic antibodies** In this task performed on a continuous basis for both specific aims, we will employ CHO cells that produce the monoclonal antibody (chIgG), which will be applied to reduce the fibrotic response of the injured knees of experimental rabbits. As a result, the critical chIgG variant will be available throughout the entire study.	-This task has been successfully accomplished. -No major changes were introduced to this task. -No major technical problems were encountered. The monoclonal antibody (chIgG) has been produced in cultures of CHO cells maintained in the BioFlo/CelliGen 115 bioreactor. Seeding CHO cells into the bioreactor required selecting a cell sub-population able to grow in suspension in serum-free conditions. This was achieved by passaging the cells in spinner flasks until the sub-population with required characteristics was selected. Following seeding the bioreactor, cell cultures were maintained constantly for up to 8 weeks. During this time the chIgG was purified from batches of conditioned media.
Subtask 1 **High-density cell culture to produce preparative-scale amounts of therapeutic chIgG** -In this subtask, cell cultures will be carried out in a laboratory-scale bioreactor.	We developed a technology to initiate and maintain high-density cultures of CHO cells that produce the chIgG. Detailed protocols for seeding the bioreactor were developed. Moreover, we established a set of key parameters defining proper conditions for seeded CHO cells. These parameters included oxygen tension, glucose consumption, lactate production, optimal pH, and composition of cell culture media.
Subtask 2 **Purification of the chIgG** - chIgG secreted by CHO cells will be purified by salt precipitation and	We successfully developed a protocol for purification of chIgG. This protocol includes the following key steps: (i) collection of conditioned

chromatography. If necessary, variable fragments of the chIgG, F(ab')2, will be prepared by pepsin digestion.	media from the bioreactor; (ii) filtration of cell culture media; (iii) binding of the chIgG to an affinity column; (iii) elution of bound chIgG from the column. Although we developed methods to generate and purify variable fragments of the chIgG, F(ab')2, their use was unnecessary. Specifically, we determined that the full-length version of the chIgG did not cause any side effects *in vivo*.
Subtask 3 **Quality control of purify chIgG** - The structural integrity and purity of purified chIgG will be monitored by polyacrylamide gel electrophoresis done in reducing and non-reducing conditions. The specific activity of the chIgG will be monitored by its ability to interact with the targeted epitope.	We developed a set of assays to ensure the proper quality of the chIgG. These assays include: (i) electrophoresis to determine the structural integrity of the chIgG; (ii) biosensor-based binding assays to determine the binding affinity of purified chIgG; (iii) size exclusion chromatography (SEC) to ensure the monomeric state of the chIgG after concentrating it. We have also developed a method to stabilize the chIgG and, possibly, prolong its activity *in vivo*. Specifically, we modified the chIgG by binding polyethylene glycol (PEG) to its surface. The PEGylated version of the chIgG was thoroughly tested for its stability and activity
Milestone(s) Achieved: Establishing conditions for the preparative-scale production of a functional, high-purity therapeutic antibody for animal-based tests.	We developed a robust methodology for production of chIgG suitable for tests in animal-based models.
Local IRB/IACUC Approval; Already approved Milestone Achieved: HRPO/ACURO Approval; The ACURO approval has been granted.	All animal protocols and their amendments were approved by IACUC and ACURO.
Major Task 2 **Testing procedures for generating a rabbit-based model of joint stiffness.** In the initial phase of the proposed study, participating clinical PIs, together with supporting personnel, will prepare a pilot group of animals to test procedures needed to create the required animal model. As a result, not only will surgical methods and procedures be perfected, but a pilot set of data will also be obtained. This data set will be critical for generating the animal groups needed for Specific Aim 2.	This task has been successfully accomplished. -No major changes were introduced to this task. -No major technical problems were encountered. We developed effective surgical procedures needed to create a rabbit-based model of posttraumatic joint stiffness.
Subtask 1 **Performing surgeries and immobilization of joints-** The participating surgeons will establish detailed procedures for the critical joint-contracture model.	The participating surgeons have established detailed protocols for creating a joint contracture model in rabbits. One minor unexpected problem was that some operated rabbits had a tendency to self-mutilate. The veterinary team has developed post-surgery

	procedures to minimize consequences of this habit.
Subtask 2 **Establishing the effective range of chIgG concentrations for limiting the post-traumatic fibrotic response of injured joint -** Groups of rabbits will be treated with various concentrations of the inhibitory chIgG. As a result, effective and safe ranges of concentration of therapeutic chIgG will be established.	Our initial concern was that applying the chIgG may have some negative side effects. Early tests with varying concentrations of the chIgG did not show any adverse effects. Thus, in the following experiments we applied the highest tested concentration of the chIgG as potentially most effective in our experimental system.
Subtask 3 **Microscopic, biochemical and biomechanical tests of the pilot group of animals** - A pilot group of rabbits will be sacrificed and knee joints from treated and control groups will be analyzed. Specifically, light and electron microscopy will be employed to analyze changes in the content of bundles of collagen fibrils present in the joints' tendons and capsules. Changes in the total collagen content in the analyzed elements of injured knee joints will be analyzed by measuring hydroxyproline, a residue prevalent in collagenous proteins. The relevant content of collagen cross-links, an important indicator of fibrotic changes, will be determined by gel electrophoresis. A mechanical test of the analyzed joints will finally establish the efficacy of the applied inhibitory chIgG to sustain the mobility of joints after traumatic injury.	We have developed and successfully applied microscopic, biochemical, and biomechanical assays to test the efficacy of the chIgG to limit posttraumatic joint stiffness. The most informative and relevant microscopic assay of collagen fibrils formed in response to injury in the presence or the absence of the chIgG was that of Sirius red-stained samples. This collagen fibril-specific staining allowed us to determine the composition of newly-formed collagen-rich matrices and calculate the anisotropy score that describes the orientation of collagen fibrils. In contrast, electron microscopy assays of pilot samples did not provide any useful information, thus we did not apply these assays beyond the pilot experiments. We also applied Fourier Transformation Infrared spectroscopy to analyze the effects of the chIgG on reducing the formation of collagen fibrils that contribute to posttraumatic joint stiffness.
Milestone(s) Achieved: Establishing key experimental parameters and procedures needed for complex animal-based studies.	We successfully developed all methods needed to analyze the efficacy of the chIgG to reduce posttraumatic joint contracture.
Specific Aim 2 **"To analyze long-term effects of the antibody-based inhibitor of fibrosis at the biochemical, cellular, and biomechanical levels"**	
Major Task 3 **Creating an animal model for joint-contracture -** A model representing posttraumatic joint contracture will be created. This model will be used to test the central hypothesis that by blocking post-traumatic fibrosis, it is possible to prevent or significantly reduce joint stiffness.	-This task has been successfully accomplished. -No major changes were introduced to this task. -No major technical problems were encountered.
Subtask 1 **Preparing critical animal groups -** Animal groups will include the following: (i) a control group in which the injured knee joint will be treated with an anti-	We established critical animal groups needed to study the efficacy of the chIgG to limit posttraumatic joint stiffness. Although we initially contemplated creating a group treated with control human IgG, we

inflammatory agent, (ii) a chIgG-treated group in which the injured knee joint will be treated with the therapeutic chIgG variant, (iii) a control IgG-treated group in which the injured knee joint will be treated with an inactive IgG variant, and (iv) a non-treated control group in which the injured knee joint will not be treated with any therapeutic agents.	ultimately decided to create a group treated with solvent (PBS) only. The following reasons dictated this decision: (i) according to literature non-specific IgG injected into a rabbit's knee, like PBS, does not have any effects; (ii) we were concerned, however, that commercially-available batches of human IgG may vary, thus not offering a stable and well-defined control.
Subtask 2 **Applying inhibitory chIgG and control agents into injured joints** - Animals from the groups identified in Subtask 1 (see above) will receive the inhibitory chIgG and control agents. Techniques that ensure stability of antibodies will be applied according to the suggestions of Dr. Shoyele, an expert in the field of therapeutic biologics (see letter of support in original application)	We successfully established a method for delivery of the chIgG into injured joints. Specific tests confirmed the presence of the chIgG in target sites.
Milestone(s) Achieved: Manuscript describing results on the behavior of antibody-based therapeutic agents administered to the joint cavity. Presentation of preliminary results on the rabbit-based experimental system for inhibiting post-traumatic joint stiffness at a professional scientific meeting.	Following the initial stages of our project, we submitted an abstract for a conference organized by the Orthopaedic Research Society. Moreover, we submitted a manuscript to the Journal of Orthopaedic Research.
Major Task 4 **Evaluating the efficacy of inhibitory chIgG to reduce the consequences of traumatic joint injury** - In this task microscopic, biochemical, and biomechanical assays will be employed to determine the efficacy of the proposed treatment of injured joints. These tests (see below) will provide the ultimate evidence to determine to what extent inhibiting excessive formation of collagen-rich deposits by blocking collagen fibril formation reduces the post-traumatic contractures of affected joints. At the same time, these tests will demonstrate how our novel approach differs in its effectiveness when compared to methods currently applied (application of steroids) in joint contractures.	-This task has been successfully accomplished. -No major changes were introduced to this task. -No major technical problems were encountered. We successfully applied protocols and methods to determine the utility of the chIgG to limit posttraumatic joint contracture.
Subtask 1 **Microscopic testing of analyzed joints** - Electron and light microscopy techniques such as polarized-light microscopy will be employed to analyze the morphology and quantity of fibrous deposits. Electron microscopy will be performed in a specialized facility available for us on the TJU campus. Light	Employing microscopic techniques we identified novel mechanisms that contribute to the fibrotic process taking place due to joint injury. Our results demonstrated the increased expression of auxiliary proteins needed to produce collagen-rich fibrotic deposits. We also determined the production of thin

microscopy will be done in Dr. Fertala's laboratory equipped with state-of-the art imaging hardware and software.	disorganized collagen fibrils in posterior joint capsules of injured knees.
Subtask 2 **Biochemical assays of the content of fibrotic tissue** - Biochemical assays of the content of collagenous deposits will be done by assaying the content of hydroxyproline residues. Analyses of collagen cross-links, an indicator of the degree of fibrosis, will be done electrophoretically.	We successfully analyzed the content of total collagen in injured joint capsules. Moreover, we analyzed the specific content of collagen I and collagen III. The cross-linking of collagen molecules that form fibrotic deposits was also analyzed in joint capsules.
Subtask 3 **Biomechanical assays** - Biomechanical measurements of joint stiffness will be done by measuring a defined set of biomechanical parameters. These assays directed by Dr. J. Abboud will be done with the assistance of Dr. Soslowsky, an expert in the field (see letter of support).	The mechanical characteristics of injured and uninjured contralateral knee joints were analyzed using a custom-made tester.
Milestone(s) Achieved: Manuscript describing biochemical analyses of fibrotic tissue formed in the presence of inhibitory antibody vs. controls. Presentation of ongoing studies at a professional orthopaedic meeting.	A manuscript describing the biochemical analyses of fibrotic posterior capsules of injured knee joints has been published in the Journal of Orthopaedic Research. Moreover, a poster was presented at the Orthopaedic Research Society conference.
Major Task 5 **Task 4. Data analysis and statistical evaluation of results**-	-This task has been successfully accomplished. -No major changes were introduced to this task. -No major technical problems were encountered
Subtask 1 **Continuous data collection and analysis** - Data will be collected throughout the duration of animal-based experiments. Critical analysis of data will be done with the assistance of Biostatistics Shared Resources available at TJU.	We effectively collected tissue samples and analyzed them according to methods we developed for this study.
Milestone(s) Achieved: Manuscripts describing results of biological and biomechanical tests done on traumatic joints healed in the presence of therapeutic antibodies. Presentation of the entire study at a professional conference. Establishing a research enterprise consisting of basic research and clinical components.	We published a second paper in the Journal of Orthopaedic Research describing that the chIgG is effective in reducing the posttraumatic joint stiffness. Moreover, our findings were presented at the "Fibrosis: From Basic Mechanisms to Target Therapies" Keystone Symposium and at the Orthopaedic Research Society conference. The original project was funded through the Translational Research Partnership Award. This mechanism required research teams to conduct translational studies that would accelerate the movement of promising ideas in orthopaedic research into clinical applications to benefit soldiers with combat-relevant traumatic orthopaedic injuries.

	Moreover, this award mechanism required the formation of the multi-institutional and multi-disciplinary research partnership among orthopaedic surgeons and basic researchers. Our group has fulfilled both of these requirements. Specifically, our group has been extremely successful in establishing a well-integrated partnership among orthopaedic surgeons and basic researchers focusing on research associated with post-traumatic joint stiffness. This team has grown from a group of three initial Principal Investigators into the Scientific Consortium for Arthrofibrotic Research (SCAR). At present, the scientists that form SCAR focus on the scarring of elements of the musculoskeletal system, including tendons, joint capsules, peripheral nerves, and others. Moreover, the integration of our group is strengthened by the university-wide initiative entitled: “The Link between Wound Repair, Inflammation, Fibrosis and Cancer”.